Synthesis and characterization of Ru(II) phenyl-3-indenylidene olefin metathesis type complexes

YALEZO Ntsikelelo

Department of Chemistry

Faculty of Science and Agriculture

University of Fort Hare

Together in Excellence

January 2015

Synthesis and characterization of Ru(II) phenyl-3-indenylidene olefin metathesis type complexes

By

YALEZO Ntsikelelo (200909297)

B. Sc., B. Sc. (Honours) Chemistry (UFH)

Being a dissertation submitted to the Faculty of Science and Agriculture in fulfilment of the requirements for the award of the degree of

Master of Science in Chemistry

of the

University of Fort Hare

Supervisor: Professor P. A. Ajibade

January 2015

DECLARATION BY CANDIDATE

"I hereby declare that this dissertation submitted for MSc degree in Chemistry, at the University of Fort Hare, is my own original work and has not previously submitted to any other institution of higher learning. I further declare that all sources cited or quoted are indicated and acknowledged by means of a comprehensive list of references".

_____ _____

Date Yalezo Ntsikelelo

CERTIFICATION

This is to certify that this research is a record of original work carried out by Yalezo Ntsikelelo under my supervision in the Inorganic Materials Research laboratory of the Department of Chemistry, University of Fort Hare in fulfilments of the requirements for the award of Master of Science degree in Chemistry.

_____ _____

Date Supervisor

P. A. Ajibade
Professor of Inorganic Materials Chemistry
B. Sc (Hons), MSc (Ibadan);
PhD (UniZul); MRSC (London)

DEDICATION

This dissertation is dedicated to my mother, Buyiswa Cynthia Yalezo and my two siblings, Vuyo Yalezo and Sabelo Yalezo.

ACKNOWLEDGEMENTS

First and foremost, I would like to thank the God almighty for strength, wisdom and the grace he has blessed me with during the course of this study, without him would not have made it. Huge appreciation to my supervisor: Professor P. A. Ajibade, a mentor and a father for his guidance, life lessons, and motivations he has played the huge role both personal and academically. One of the most common themes says '*a child is built by the whole village'* and many people have contributed towards this success and I am very humbled by the supports I have received from my family: mother and my two siblings, their efforts are what kept me going for greater things.

It is of great importance for me to also thank the Vice Chancellor of Fort Hare Dr. Mvuyo Tom and Mr Xoseka (Vice Chancellor`s personal assistant) for their belief in me after finishing my matric by offering me a scholarship to study at University of Fort Hare. I would also like to acknowledge my fellow laboratory researchers: The late Casa, Peter, Shadrack, Odularu, Jejenija, Thobani, Tshefu, Andile, Ntuku, Nandi, Mathato etc. I had very nice time with them over the two years. Last but not least would like to thank Sasol Inzalo Foundation/ Nation Research Foundation and GMRDC for Financial assistance.

TABLE OF CONTENT

DECLARATION BY CANDIDATE i

CERTIFICATION ii

DEDICATION iii

ACKNOWLEDGEMENTS iv

TABLE OF CONTENT v

LIST OF FIGURES x

LIST OF SCHEMES xii

LIST OF TABLES xiv

ABBRIVATIONS AND SYMBOLS xv

ABSTRACT xviii

CHAPTER ONE 1

INTRODUCTION AND LITERATURE REVIEW 1

1.1 Olefin metathesis 1

1.2 Types of olefin metathesis transformation 2

1.3 Industrial application of olefin metathesis 3

1.3.1 Production of Petrochemicals 3

1.3.2 Production of polymers 4

1.4 Historical background of catalysts in olefin metathesis 4

1.4.1. Heterogeneous catalysts in olefin metathesis 5

1.4.3 Homogeneous catalysts in olefin metathesis 6

1.4.2 Olefin metathesis catalytic cycle 6

1.4.4 Homogeneous vs. Heterogeneous catalyst 7

1.5 Literature review 10

1.5.1 Ruthenium based catalysts 10

1.5.2 Ru carbene complexes 10

1.5.2.1 Ruthenium alkenylcarbene complexes 11

1.5.2.2 Ru benzylidene complexes with bisphosphine ligands 13

1.5.2.3 Ru benzylidene complexes with N-heterocyclic-phosphine 15

1.5.2.3 Ru isopropoxy-benzylidene complexes 18

1.5.2.4 Ruthenium indenylidene complexes 20

1.6 The Ru based catalyst mechanistic study 21

1.7 Types of carbene ligands 23

1.7.1 Bonding in NHC ligands 24

1.7.2 The bonding in metal-N-heterocyclic carbene ligands 24

1.7.3 Functionalities of NHC ligands 25

1.8 Problem statement 25

1.9 Research aim and objectives 26

References 28

CHAPTER TWO 39

2. EXPERIMENTAL SECTION 39

2.1 Chemicals and solvents 39

2.2. Equipments and Instrumentation 39

2.2.1 UV-Visible Spectroscopy 39

2.2.2 Infrared spectroscopy 39

2.2.3 Elemental analysis 40

2.2.4 Melting Point 40

2.2.5 NMR spectroscopy 40

2.3. Synthesis of *N,N′*-diarylformamidines 41

2.3.1. Synthesis of *N,N′-bis*(2-methylphenyl)formamidine (F1) 41

2.3.2 Synthesis of *N,N′-bis*(4-methylphenyl)formamidine (F2) 42

2.3.3 Synthesis of *N,N′*-diphenylformamidine (F3) 42

2.3.4 Synthesis of *N,N′-bis*(4-methoxyphenyl)formamidine (F4) 43

2.3.5 Synthesis of *N,N′-bis*(3-methylphenyl)formamidine (F5) 44

2.4 Synthesis of *N,N′*-diarylimidazolinium chlorides 44

2.4.1 Synthesis of *N,N′-bis*(2-methylphenyl)imidazolinium chloride (L1) 44

2.4.2 Synthesis of *N,N′-bis*(4-methylphenyl)imidazolium chloride (L2) 45

2.4.3 Synthesis of *N,N′*-diphenylimidazolinium chloride (L3) 46

2.4.4 Synthesis of *N,N′-bis*(4-methoxyphenyl)imidazolinium chloride (L4) 47

2.4.5 Synthesis of *N,N′-bis*(3-methylphenyl)imidazolinium chloride (L5) 47

2.5 Synthesis of Ru(II) complexes with N-heterocyclic carbene ligands 48

2.5.1. Synthesis of $RuCl_2(Ind)(SIoTol)(PPh_3)$ (C1) 48

2.5.2 Synthesis of $RuCl_2(Ind)(SIpTol)(PPh_3)$ (C2) 49

2.5.2 Synthesis of $RuCl_2(Ind)(SIPh)(PPh_3)$ (C3) 50

2.5.4 Synthesis of $RuCl_2(Ind)(SIpAnis)(PPh_3)$ (C4) 50

2.5.5 Synthesis of $RuCl_2(Ind)(SImTol)(PPh_3)$ (C5) 51

2.5.6 Synthesis of [$RuCl_2$(SIoTol)(py)(Ind)] (C6) 52

2.5.7 Synthesis of [$RuCl_2$(SIpTol)(py)(Ind)] (C7) 52

2.5.8 Synthesis of [$RuCl_2$(SIPh)(py)(Ind)] (C8) 53

2.5.9 Synthesis of [$RuCl_2$(SIpAnis)(py)(Ind)] (C9) 54

References 55

CHAPTER THREE 56

RESULTS AND DISCUSSION 56

3.1 Introduction 56

3.2 Synthesis and characterization of *N,N′*-diarylformamidines 56

3.2.1 Infrared analysis of *N,N′*-diarylformamidines 58

3.2.2. NMR spectra results of *N,N′*-diarylformamidines 60

3.2.2.1 NMR analysis of *N,N′-bis*(2-methylphenyl)formamidine (F1) 62

3.2.2.2 NMR analysis of *N,N′-bis*(4-methylphenyl)formamidine (F2) 64

3.2.2.3 NMR analysis of *N,N′-di*phenylformamidine (F3) 65

3.2.2.4 NMR analysis of *N,N′-bis*(4-methoxyphenyl)formamidine (F4) 67

3.2.2.5 NMR analysis of *N,N′-bis*(3-methylphenyl)formamidine (F5) 69

3.3.1 NMR spectra results of *N,N′*-diarylimidazolinium chlorides 72

3.3.1.1 NMR analysis of *N,N′-bis*(2-methylphenyl)imidazolinium chloride (L1) 73

3.3.1.2 NMR analysis of *N,N′-bis*(4-methylphenyl)imidazolinium chloride (L2) 75

3.3.1.3 NMR analysis of *N,N′-bis*(phenyl)imidazolinium chloride (L3) 77

3.3.1.4 NMR analysis of N,N′-bis(2-methylphenyl)imidazolinium chloride (L4 78

3.3.2 FT-IR analysis of *N,N′*-diarylimidazolinium chlorides 79

3.4 Synthesis and characterization of Ru(II) complexes with N-heterocyclic carbene ligand..... 80

3.4.1 Infrared studies of Ru(II) phenyl-3-indenylidene N-heterocyclic carbene complexes 82

3.4.2 Electronic spectra of Ru(II) complexes..... 85

References..... 88

CHAPTER FOUR..... 92

SUMMARY, CONCLUSION AND RECOMMENDATIONS 92

4.1 Summary 92

4.2 Conclusion 95

4.3 Recommendations for future work 95

APPENDICES 97

Appendix A.1 Infrared spectra of *N,N′*-diarylformamidines 97

Appendix B1: Infrared spectra of *N,N′*-diarylimidazolinium chlorides 102

LIST OF FIGURES

CHAPTER ONE

Figure 1.1: Time line of catalysis development in olefin metathesis [19]. 5

Figure 1.2: General structures of Ru and Mo type complexes 8

Figure 1.3: The ruthenium vinyl carbene complexes..... 11

Figure 1.4: Structures of Grubbs first generation catalysts..... 13

Figure 1.5: Structures of Ru(II) benzylidene complex with bis(N-heterocyclic carbene ligand). 15

Figure 1.6: Structures of Ru benzylidene complexes with saturated and unsaturated NHC ligands 16

Figure 1.7: Structures of Hoveyda-Grubbs 1st and 2nd generation catalysts 18

Figure 1.8: Structures of Ru indenylidene complexes 20

Figure 1.9: Structures of bonding between metal- N-heterocyclic carbene ligand [99] 24

CHAPTER THREE

Figure 3.1: ^{1}H-NMR spectrum of F1 62

Figure 3.2: ^{13}C-NMR spectrum of F2 62

Figure 3.3: The structures of sync and *anti*- isomers [10] 63

Figure 3.4: ^{1}H-NMR spectrum of F2 64

Figure 3.5: ^{13}C-NMR spectrum of F2 64

Figure 3.6: ^{1}H-NMR spectrum of F3 65

Figure 3.7: ^{13}C-NMR spectrum of F3 66

Figure 3.8: ^{1}H-NMR spectrum of F4 67

Figure 3.9: ^{13}C-NMR spectrum of F4 68

Figure 3.10: 1H-NMR spectrum of F5 69

Figure 3.11: ^{13}C-NMR spectrum of F5 70

Figure 3.12: ^{1}H-NMR spectrum of L1 74

Figure 3.13: ^{13}C-NMR spectrum of L1 74

Figure 3.14: ^{1}H-NMR spectrum of L2 75

Figure 3.15: ^{13}C-NMR spectrum of L2 76

Figure 3.16: ^{1}H-NMR spectrum of L3 77

Figure 3.17: ^{13}C-NMR spectrum of L3 77

Figure 3.18: ^{13}H-NMR spectrum of L5 78

Figure 3.19: The infrared spectra of Ru(II)NHC-phosphine complexes 84

Figure 3.20: The infrared spectra of Ru(II)NHC-pyridine complexes 84

Figure 3.21: The electronic spectra of the Ru(II) complexes with NHC-phosphine 86

Figure 3.22: The electronic spectra of the Ru(II) complex with NHC-pyridine 87

LIST OF SCHEMES

CHAPTER ONE

Scheme 1.1: General reaction for olefin metathesis reaction [1]. 1

Scheme 1.2: Types of olefin metathesis reactions 2

Scheme 1.3: Ring opening metathesis polymerization of 2-norbenene [14]. 4

Scheme 1.4: Olefin metathesis catalytic cycle……6

Scheme 1.5: Polymerization of highly steric 2-norbornene [14]. 12

Scheme 1.6: Reactions for application of complex 4e [78] 17

Scheme 1.7: Reaction for application of Grubbs-Hoveyda catalysts [78] 19

Scheme 1.8: RCM using ruthenium indenylidene complexes [47]. 21

Scheme 1.9: The mechanism for Grubbs 1st and 2nd generation catalysts [90] 22

CHAPTER TWO

Scheme 2.1: Synthesis of N, N'-bis(2-methylphenyl)formamadine 41

Scheme 2.2: Synthesis of N, N'-bis(4-methylpheny)formamidine 42

Scheme 2.3: Synthesis of N, N'-di(phenyl)formamidine 43

Scheme 2.4: Synthesis of N, N'-bis(4-methoxyphenyl)formamadines 43

Scheme 2.5: synthesis of N, N'-bis(3-methylphneyl)formamidine 44

Scheme 2.6: Synthesis of N, N'-bis(2-methylphenyl)imidazolinium chlorides 45

Scheme 2.7: Synthesis of N, N'-bis(4-methylphenyl)imidazolium chloride 46

Scheme 2.8: Synthesis of N, N'-bis(phenyl)imidazolinium chloride 47

Scheme 2.9: Synthesis of N, N'-bis(4-methoxyphenyl)imidazolium chloride 47

Scheme 2.10: Synthesis of N, N'-bis(3-methylphenyl)imidazolinium chlorides 48

Scheme 2.11: Synthesis of [$RuCl_2$(SIoTol)(PPh_3)(Ind)] 49

Scheme 2.12: Synthesis of [$RuCl_2$(SIpTol)(PPh_3)(Ind)] 50

Scheme 2.13: Synthesis of [$RuCl_2$(SIPh)(PPh_3)(Ind)] 50

Scheme 2.14: Synthesis of [$RuCl_2$(SIpAnis)(PPh_3)(Ind) 51

Scheme 2.15: Synthesis of [$RuCl_2$(SIoTol)(PPh_3)(Ind)] 51

Scheme 2.16: Synthesis of [$RuCl_2$(SI*o*-Tol)(Py)(Ind)] 52

Scheme 2.17: Synthesis of [$RuCl_2$(SIoTol)(Py)(Ind)] 53

Scheme 2.18: synthesis of [$RuCl_2$(SIPh)(Py)(Ind)] 53

Scheme 2.19: Synthesis of [$RuCl_2$(SIpAnis)(Py)(Ind)] 54

CHAPTER THREE

Scheme 3.1: Synthetic routes to different N, N'-diarylformamidine [3] 57

Scheme 3.2. Synthetic route to different N, N'-diarylimidazolinium chlorides [3] 71

Scheme 3.3: Synthetic route to Ru(II) complexes [15, 16] 80

LIST OF TABLES

CHAPTER ONE

Table 1.1: Compares different metal ion activity towards different functionalities [22] 9

CHAPTER THREE

Table 3.1: Summary of physical parameters of synthesized N, N'-diarylformamidines..... 57

Table 3.2: Some selected vibrational frequency of N, N'-diarylformamidines..... 59

Table 3.3: NMR results of N, N'-diarylformamidines 60

Table 3.4: Summary of physical properties of synthesized N, N'-diarylimidazolinium chlorides 72

Table 3.5: NMR results of N, N'-diarylimidazolinium chlorides..... 73

Table 3.6: Some selected vibrational frequency of N, N'-diarylimidazolinium chloride 79

Table 3.7: Summary of physical parameters of synthesized Ru(II) complexes 81

Table 3.8: Selected vibration bands of Ru(II) phenyl-3-indenylidene complexes 83

TTable 3.9: UV-Vis absoprtion band of Ru(II) complexes and corresponding ligands..... 85

ABBRIVATIONS AND SYMBOLS

OM	Olefin metathesis
Ru	Ruthenium
Mo	Molybdenum
$Ru=CHR_2$	Ruthenium carbene complexes
$Mo=CHR_2$	Molybdenum carbene complexes
CM	Cross metathesis
RCM	Ring closing metathesis
ROM	Ring opening metathesis
ROMP	Ring opening metathesis polymerization
ADMP	Acyclic diene metathesis polymerization
C_2H_2	Ethylene
WO_3	Tungsten oxide
SiO_2	Silicon dioxide
$RuCl_3$	Ruthenium(III) chloride
HCl	Hydrogen chloride
Ti	Titanium

W	Tungsten
WCl_6	Hexachloridotungsten(VI)
$AlCl_2$	Aluminum chloride
$RuCl_3$(hydrate)	Ruthenim(III) chloride hydrate
NHC	N-heterocyclic carbene
PPh_3	Triphenylphosphine
PCy_3	Tricyclophenylphosphine
$RuCl_2(PPh_3)_3$	Ruthenium(II) chloride *tris*(triphenylphosphine)
IMesMe	*N,N´-bis*(mesityl)-4,5-dimethylimidazol-2-ylidene
SIPrMe	*N,N´-bis*(2,6-diisopropylphenyl)-4,5-dimethylimidazolin-2-ylidene
$PiPrPh_2$	Diphenylisopropylphosiphine
$PiPr_3$	Triisopropylphosphine
$Pt\text{-}Bu_3$	Tritetrabutylphosphine
SIPr)	*N,N´-bis*(2,6-diisopropylphenyl)-4,5-dihydroimidazolin-2-ylidene
SIPr	*N,N´-bis*(2,6-diisopropylphenyl)-4.5-imidazolin-2-ylidene
SIoTol	*N,N´-bis*(2-methylphenyl)-4,5-dihydroimidazolin-2-ylidene
(SIMes)	*N,N´-bis*(mesityl)-4,5-dihydroimidazolin-2-ylidene
FTIR	Fourier Transform Infra-Red
UV-vis	Ultra violet visible spectroscopy

H^{1}-NMR	Proton nuclear magnetic resonance
C^{13}-NMR	Carbon nuclear magnetic resonance
C	Carbon
Re_2O_7	Rhenium oxide
Al_2O_3	Aluminum oxide
py	Pyridine
KHMDS	Potassium bis(trimethylsilyl)amide
Ind	3-pheylindenylidene
DCE	1, 2-dichloroethane
DiPr	N, N-diisopropylethylamine
o-tolyl	2-methyphenyl
p-tolyl	4-methylphenyl
p-anisyl	4-methoxyphenyl
m-tolyl	3-methylphenyl

ABSTRACT

In this study, a series of Ru(II) phenyl-3-indenylidene complexes with general formula of [$RuCl_2$(NHC)(Ind)(L)] (where L= triphenylphosphine, pyridine and NHC = five different types of N-heterocyclic carbene ligands), have been synthesized and characterized using FT-IR, UV-Vis, elementally analysis and melting/decomposition point. The *N,N'*-diarylimidazolinium chlorides have been used as N-heterocyclic carbene precursors and were synthesized from their corresponding *N,N'*-diarylformamidines and further characterized using ^{1}H-NMR, ^{13}C-NMR, FTIR and melting point determination.

The infrared spectra of the *N,N'*-diarylimidazolinium chlorides show a quaternary nature ($R_2N{=}C^{+}$) with broad vibration band in region 3300-3400 cm^{-1}. The disappearance of this vibration band in the infrared spectra of the ruthenium(II) complexes was used to confirm the coordination of the ligand to the ruthenium ions. The percentage analysis of carbon, hydrogen and nitrogen obtained corresponded with the calculated percentages of these atoms in the complexes with the slight difference of less than 1%. The electronic spectra of the complexes show three distinct absorption bands. The two bands are due to intraligand charge transfers transition assigned to $\pi\rightarrow\pi^*$, $n\rightarrow\pi^*$ and third band is due to d-d transition, signifying the presence of the metal ion. The synthesized Ru(II) complexes did not show any of melting, however a change in colour was observed signifying the decomposition of the complexes.

CHAPTER ONE

INTRODUCTION AND LITERATURE REVIEW

1.1 Olefin metathesis

Olefin metathesis is a metal-catalyzed chemical transformation that involves the re-arrangement of carbon atoms on alkene chemical bonds. In this reaction, generally two carbon-carbon double bonded molecules under the presence of metal ion complex as catalyst defragment and reassembly groups to form new alkene molecules using less useful ones, as illustrated by the Scheme 1.1 below. In this reaction, R_1 and R_2 can be any alkyl groups attached to the carbon atoms with different functional groups [1, 2].

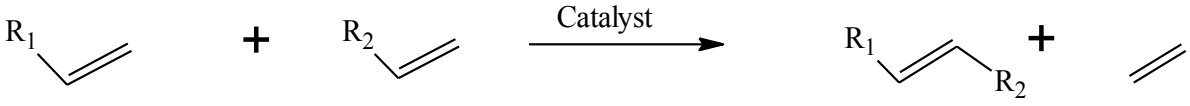

Scheme 1.1: General reaction for olefin metathesis reaction [1].

Over the last decade, metathesis transformations have received huge attention as alternative technique of synthesizing more valuable olefins in various fields of science, especially in polymer science and synthesis of heterocyclics [3, 4]. The merits of this reaction in synthesizing olefins over other conventional organic synthetic reactions are; non-generation of by-products, it is a simple organic reaction with low energy consumption, olefins are used as starting material to produce other olefins and meets the general demands for green chemistry [1, 5].

The application of olefin metathesis in different fields has grown since the introduction of ruthenium carbene ($Ru=CHR_2$) and molybdenum carbene ($Mo=CHR_2$) complexes as catalysts by Grubbs and Schrock respectively, and the elucidation of its mechanism by Chauvin, for which they jointly received Noble price in chemistry in 2005 [6-8].

1.2 Types of olefin metathesis transformation

Several types of olefin metathesis transformation are known and they are classified and named based on their reaction mechanism. The interchange of groups between two acyclic olefins is cross metathesis (CM) (Eq 1), the ring closure of terminal acyclic diene is ring closing metathesis (RCM) (Eq 2), the cleavage of cyclic double bond to form acyclic diene is ring opening metathesis (ROM) (Eq 3). The polymerization of cyclic olefins to produce polymerized acyclic diene is ring opening metathesis polymerization (ROMP) (Eq 4), and acyclic diene metathesis polymerization (ADMP) (Eq 5) is the polymerization of acyclic olefin to form long chain [9-11].

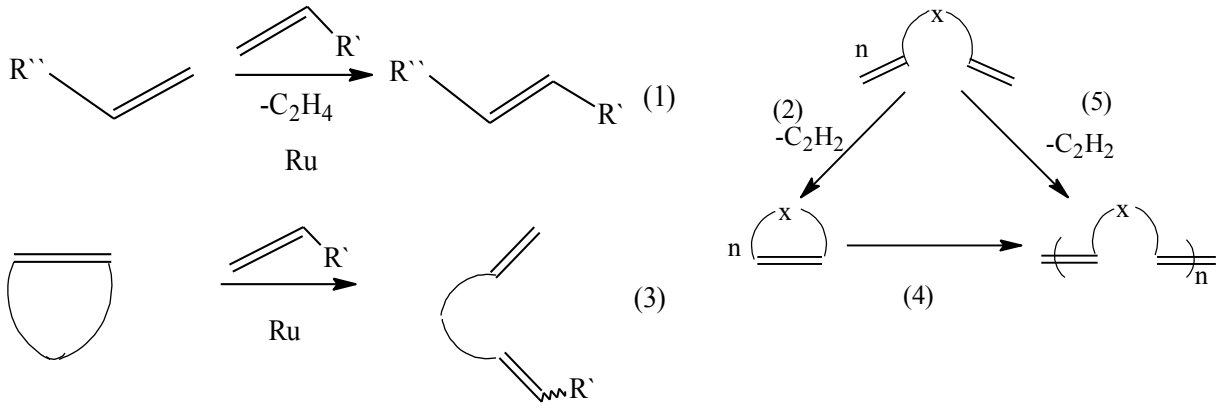

Scheme 1.2: Types of olefin metathesis reactions [11].

1.3 Industrial application of olefin metathesis

1.3.1 Production of Petrochemicals

1.3.1.1 Production of Propene

Conventionally, about 65% of propene is produced mainly from naphtha steam crackers as a co-product with ethane or as co-product from gasoline process. Very small amounts are produced through dehydration and by coal gasification through Fischer-Tropsch process, yet the demand for propene increases globally due to its useful application. Propene can be used to produce polypropene, acrylonitrile, acrylic acid, thus the high demand of propene has led to an alternative way of producing propene through the reaction of ethylene and 2-butene which is the reverse of Phillips triolefin process [2, 12].

1.3.1.2 Production of neohexene

The common name of neohexene is 3,3-dimethyl-1-butene. It is used to produce terbine fine an antifungal agent and is also useful in the synthesis of tonalide, a synthetic musk perfume. Neohexene is produced through cross metathesis between the mixture of 2,4,4 trimethyl-2-pentene and ethylene using WO_3/SiO_2 .

1.3.1.3 The Shell higher olefins process (SHOP)

Olefin metathesis is incorporated to produce linear higher olefin from ethene. Thus, 1.2 million tons of linear higher olefin per year from ethylene [13].

1.3.2 Production of polymers

1.3.2.1 Production of polynorbornene

Polynorbornene is a useful elastomers and can be used for sound barrier and oil spill recovery. It is produced by ROMP of 2-norbornene and this reaction was first commercialized in 1976 in France and 1978 in USA and Japan. The reaction used $RuCl_3$/HCl as catalyst [14].

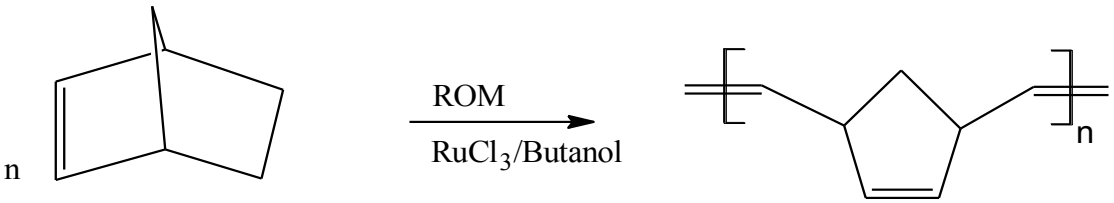

Scheme 1.3: Ring opening metathesis polymerization of 2-norbenene [14].

1.4 Historical background of catalysts in olefin metathesis

Prior the 1950`s no known catalyzed metathesis reaction existed, however the knowledge then was on non-catalyzed metathesis reaction published in 1931, by Schneider and Frolich [15] in producing butene and ethene as products through pyrolysis of propylene at 752 ^{o}C. The widely accepted name olefin metathesis was derived from two Greek vocabularies, “meta” change and “thesis” position, thus the full name means “change in position of the double bond” [16]. The first catalyzed metathesis reactions were discovered as early as 1950`s with the contribution work from the three petrochemical chemists at DuPont, Standard Oil and Phillips petroleum using, molybdenum on alumina catalyst [17, 18].

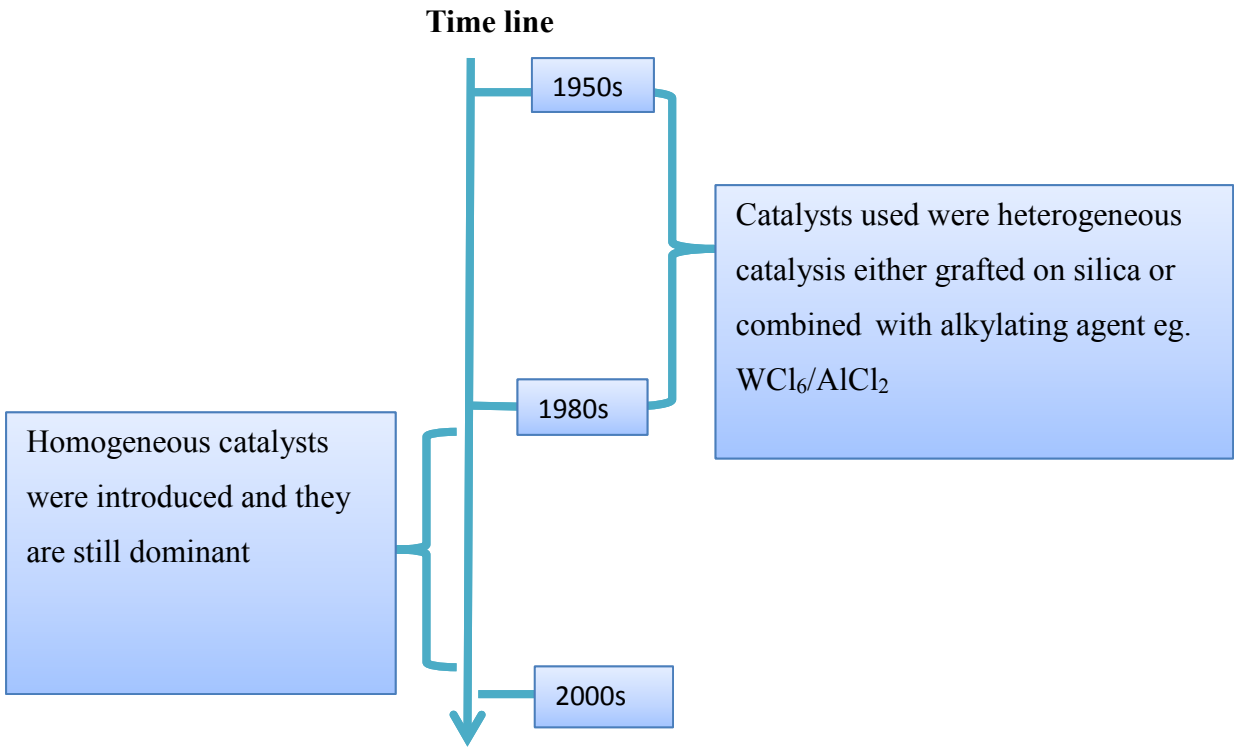

Figure 1.1: Time line of catalysis development in olefin metathesis [19].

There are two types of catalysts that have been used in catalyzing olefin metathesis reactions namely homogenous and heterogeneous catalysts. As illustrated on the time line above (Figure 1.1) between 1950- 1980`s, catalyst used were mainly ill-defined heterogeneous catalysts on alumina support and the first reaction to be recognized was the ring opening metathesis polymerization of norbornene using hexachloridotungsten(VI)/$AlEt_2Cl$ as catalyst [16, 20]. From the 1980-2000's the focus changed to development of well-defined homogeneous catalysts [19].

1.4.1. Heterogeneous catalysts in olefin metathesis

Heterogeneous catalysts are classified as catalysts on different phase with the reactants of the chemical reaction in which they are used in. They are solid materials dispersed on a second material that enhances the effectiveness or minimizes their cost. The reaction mechanism for

these types of catalysts usually occurs by substrate reacting on surface of the material through the process called adsorption. In olefin metathesis, three transition metals have been used as metal center for heterogeneous catalysts, namely molybdenum (MoO_3/SiO_2), rhenium (Re_2O_7/Al_2O_3), and tungsten (WO_3/SiO_2). The alumina, silica and other inert surfaces are used as supporting materials [6, 19].

1.4.2 Homogeneous catalysts in olefin metathesis

Homogeneous catalysts are catalysts on the same phase with reactants in which they are used in. The transition metals compounds that have been examined as metal center are molybdenum [$(OR)Mo=CH_2$], tungsten [$W=CHCMe_3$], ruthenium [$Cl_2Ru=CHR_2$], and titanium [Cp_2TiCH_2]. Titanium complexes have a profound use in metathesis polymerization of norbornene to polynorbernene [20].

1.4.3 Olefin metathesis catalytic cycle

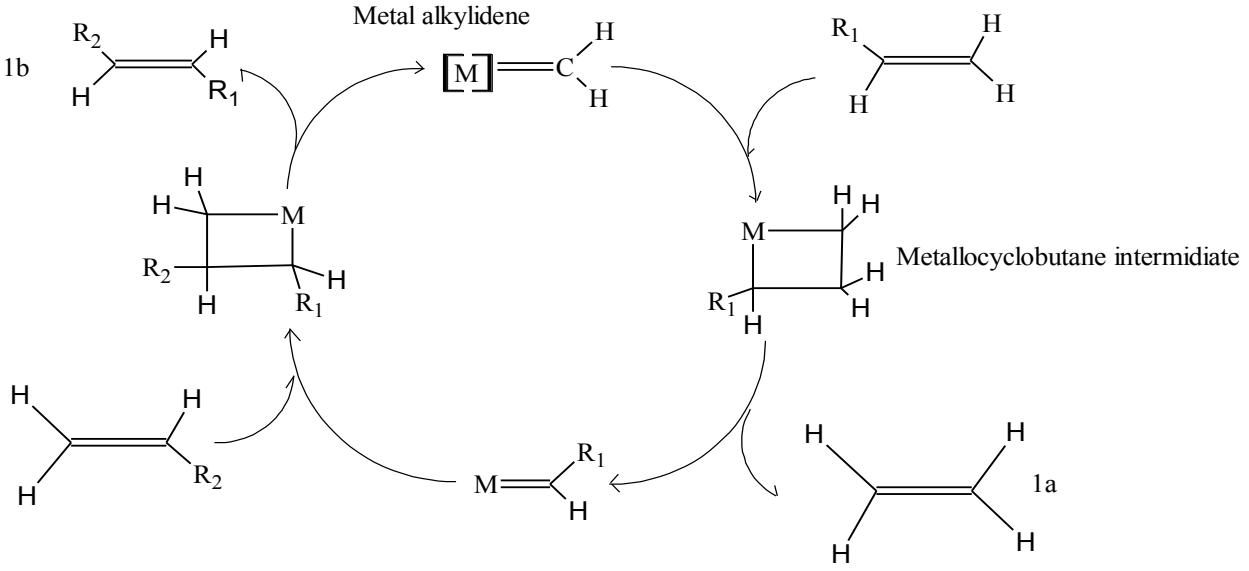

Scheme 1.4: Olefin metathesis catalytic cycle

According to the mechanism that was introduced by Chauvin and co-workers in 1971 (Scheme 1.4) [21], olefin metathesis reactions can only be initiated by a metal carbene. Firstly, (i) a metal carbene react with the olefin substrate, (ii) the metallocyclobutane intermediate is formed between the coordinated olefin and (iii) the new olefin breaks apart and it is the combination of one portion of carbene from the catalyst and the other carbene from the starting alkene. The new metal alkylidene catalyst comprises of a carbene from the substrate and this drives the reaction forward [3]

1.4.4 Homogeneous vs. Heterogeneous catalyst

Transition metals have played a significant role in the development of organometallic catalysts such as metal carbene and various different metal ions based complexes have been synthesized and tested as catalysts in metathesis reactions. About 80% of olefin metathesis reactions in the past used heterogeneous catalysts, mainly because of advantages such as easy separation process leading to long life time, high thermal stability. However, their disadvantages include: low selectivity, need of pre-treatment with co-catalyst and high energy consumption, hence over the last decade homogeneous catalysts have been considered as the future alternative to difficulties found in their counterparts, due to advantages such as excellent/good active single sites. They can be easily understood at molecular level [19, 22].

Although many of these metal based catalysts showed good metathesis activity they are non-tolerant to certain functional groups [23-26]. For instance, as illustrated in Table 1.1, tungsten complexes in solution prefer to react with ketones, alcohols, acids and become non-reactive to

the olefins substrate. This happens because tungsten-based complexes prefers ligands that are set to increase the electrophilicity of metal center resulting to high oxidation state of metal center and then become more reactive to Lewis bases [27].

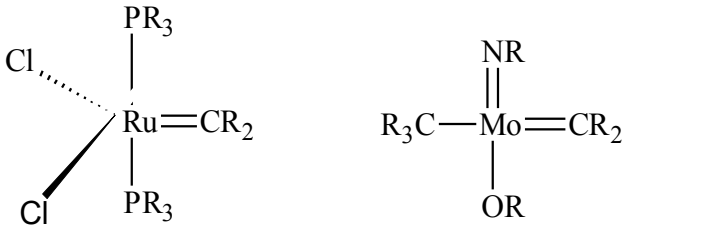

Ru proto-type complexes (1) Mo proto-type complexes (2)

Figure 1.2: General structures of Ru and Mo type complexes [28, 29]

In the contrary, ruthenium complexes of type **1** (Figure 1.2), are very stable upon storage and they prefer to react in favour of olefins and become non-reactive to other Lewis bases such as amides, aldehydes, ketones, esters, amides, alcohol and water present in solution. Hence, they are regarded as tolerant to Lewis bases **[**28-30]. So $Mo{=}CH_2$ and $Ru{=}CHR_2$ have received much attention, however Mo complexes type **2** (Figure 1.2) are difficult to handle in a small laboratory environment, hence this study will focus on the ruthenium based catalysts [31]. Table 1.1 below summarizes some of these metal ion activity towards different functional groups.

Table 1.1: Compares different metal ion activity towards different functionalities [22]

Titanium (Ti)	**Tungsten (W)**	**Molybdenum (Mo)**	**Ruthenium (Ru)**
Acids	Acids	Acids	**Olefins**
Alcohol, water	Alcohol, water	Alcohol, water	Acids
Aldehydes	Aldehydes	Aldehydes	Alcohol, water
Ketones	Ketones	**Olefins**	Aldehydes
Esters, amides	**Olefins**	Ketones	Ketones
Olefins	Esters, amides	Esters, amides	Esters, amides

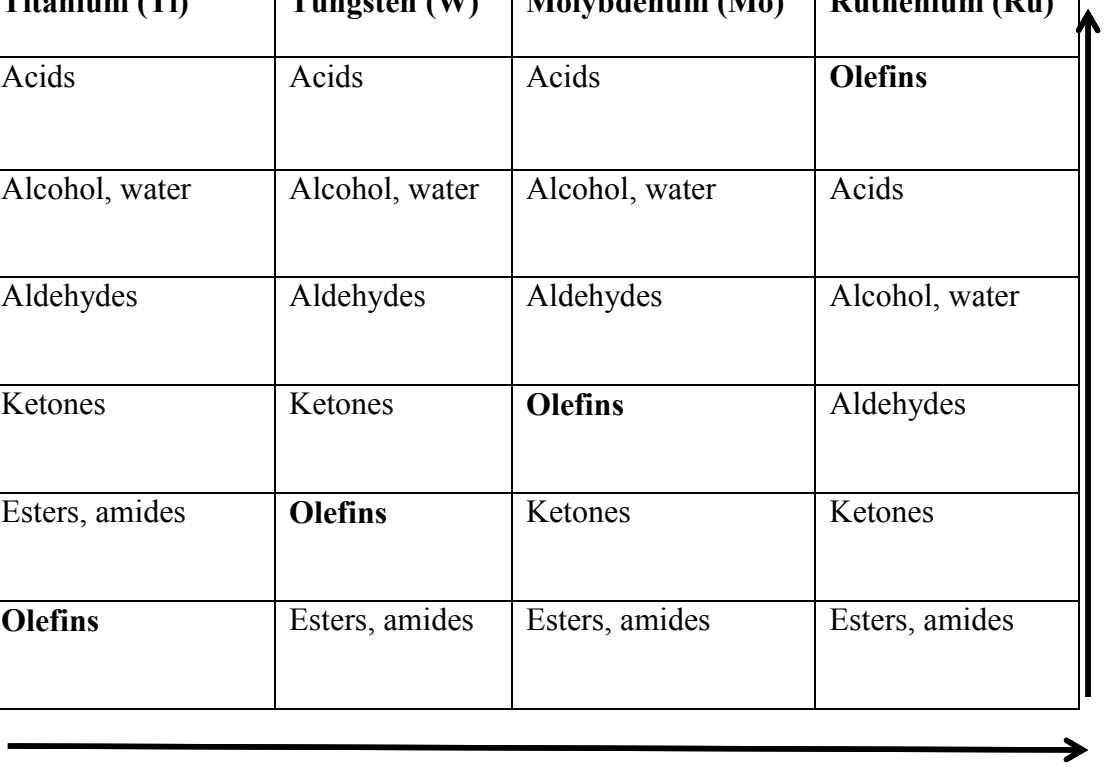

1.5 Literature review

1.5.1 Ruthenium based catalysts

Ru is one of the platinum group metals and it is a soft metal so it prefers to react with soft bases such olefins over hard bases like oxygen and other Lewis bases. It exist in different oxidation state from -2 ~ to +8 but most common oxidation states of ruthenium are +2, +3 and +4 [32-34]. It can coordinates with many different ligands to form various geometries such as octahedral and pentahedral complexes. Most ruthenium complexes have shown catalytic activity of one or more reactions and the examples are the [$RuCl_3$(hydrate)] and [$Ru(H_2O)_6$]$(OT)_2$ (OTs = toluene-4-sulfanato or tosylate ion) complexes. These complexes have successfully been used as catalysts, the [$RuCl_3$] has been used for ring opening metathesis polymerization of cyclobutene and 3-methylcycobutene and was prepared by Natta *et al.* in 1965 and the [$Ru(H_2O)_6$]$(OT)_2$ has been used for polymerization of 7-oxanorbonernene and was synthesized in 1988 by Grubbs *et al*. [35, 36].

1.5.2 Ru carbene complexes

A ruthenium carbene complex is a Ru ion coordinated to the divalent carbon ($:CR_2$) and is generally represented by the formula $X_2L_1L_2Ru{=}CR_2$ where L_1 and L_2 are ligand coordinated directly to the metal ion, X is a halogen atom and R is the alkyl group attached on the carbene. Recently these types of complexes are being consider as the best homogeneous organometallic catalysts in olefin metathesis catalysis due to their good solubility and stability in common solvents [37]. The first stable metal carbene complex with a Ru center, according to literature that was synthesized in 1971 by Green`s group is [$RuCp(=C(Me)OMe)(CO)(PCy_3)$][$PF_6$] [38]. This complex showed poor ability to catalyze OM reactions, and it was reported to form a cyclopropanation intermediate during the reaction and this was attributed to the presence of a

strong electron withdrawing ligand such as carbonyl which affects the electron density of the metal center. Due to the fascinating catalytic properties that have been shown by early ruthenium complexes such as [$RuCl_3$(hydrate)] and [$Ru(H_2O)_6$]$(OT)_2$ as catalysts, various Ru carbene complexes with different monodentate and bidentate ancillary ligands such as phosphines, N-heterocyclic carbene, pyridine, isopropyl-ether and Schiff-base around the environment of Ru center have been synthesized [39-41]. These complexes include the Ru alkenylcarbene complexes, Ru benzylidene complexes, Ru isopropoxy-benzylidene complex and Ru indenylidene complexes. These are 16 electron complexes and had shown great ability to catalyze many olefin metathesis reactions. For instance Ru indenylidene complexes have shown great stability at high temperature as compared to other complexes owing to the presence of sterically hindering 3-phenylinden-1-ylidene structure coordinated to the ruthenium center [42-46].

1.5.2.1 Ruthenium alkenylcarbene complexes

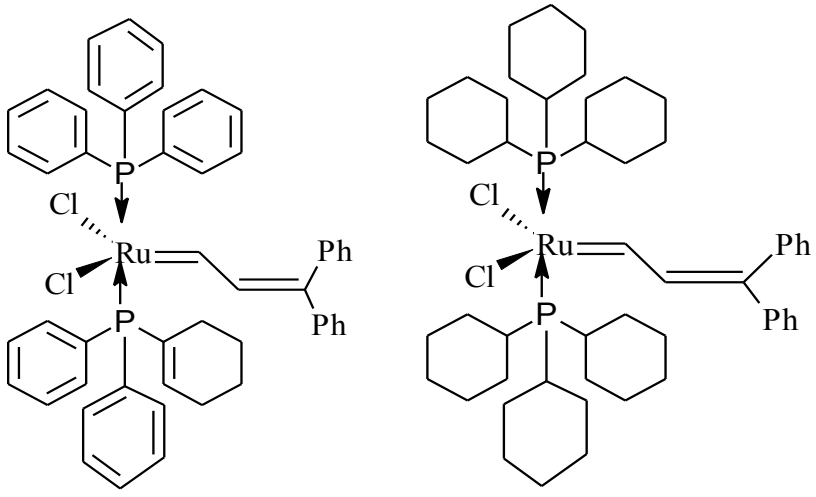

3a **3b**

Figure 1.3: The ruthenium vinyl carbene complexes [47].

Ru vinyl carbene complexes are ruthenium alkylidene complexes represented by the general formula $[RuCl_2L_2(=CHC=C(Ph)_2]$. These complexes can be synthesized by reacting 3,3-disubstituted cyclopropenes as the carbene precursor with $RuCl_2PPh_3$. They are five coordinated species in which phosphine ligands are bonded *trans* to one another to make the complex stable while chloride ligands are bonded in *cis* configuration [47-48]. Complex **3a** (Figure 3.1), $[RuCl_2(PPh_3)_3(=CHC=C(Ph)_2]$ with triphenylphosphine (PPh_3) ligands show moderate catalytic activity and tolerance in presence of water for catalyzing ring opening metathesis polymerization of high strained monomers such as 2-norbornene to polynorbornene in scheme 1.5 and 1,5-dimethy-1,5-cyclooctadiene over early ruthenium complexes but has limited activity to ROMP of low strained monomers and in catalyzing acyclic molecules [47].

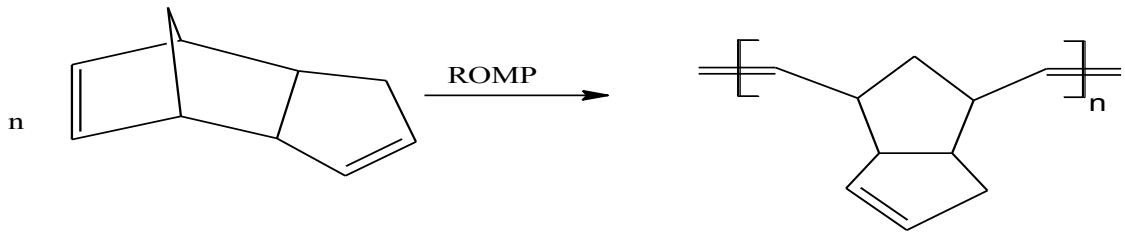

Scheme 1.5: Polymerization of highly steric 2-norbornene [14].

When the triphenylphosphines (PPh_3) is substituted with two equivalence of highly basic ligand such tricyclohexylphosphine (PCy_3), the activity of the complex becomes improved and this has been shown with complex **3b** (Figure 3.1), $[RuCl_2(PCy_3)_3(=CHC=C(Ph)_2]$. This improved activity can be explained by the difference in electron donating ability of cyclohexyl and benzene

bonded to the phosphorus atom [49-51]. Moreover, despite the successful application of complex **3a** and **3b** (Figure 3.1) in olefin metathesis, the drawbacks is the time required for their synthesis and the toxicity of diphenycyclopropene derivatives as carbene precursor.

1.5.2.2 Ru benzylidene complexes with bisphosphine ligands

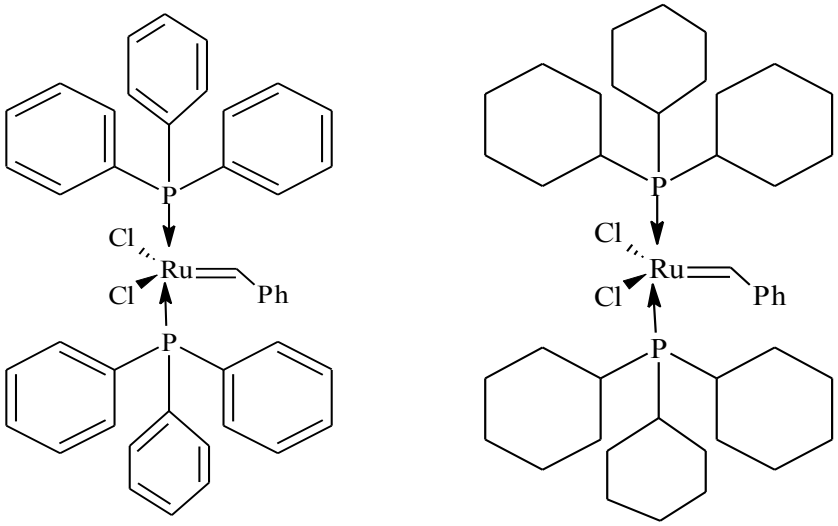

4a **4b**

Figure 1.4: Structures of Grubbs first generation catalysts [53].

Another class of ruthenium alkylidene complexes is the Ru benzylidene complexes [$RuCl_2L_2$(=C(Ph)] introduced by Grubbs and co-workers with benzylidene carbene ligand and *trans bis*(phosphines). Complexes **4a** and **4b** (Figure 1.4) shows much improved stability and activity as compared to complexes **3a** and **3b** (Figure 1.3) with conversion rate of 80% in polymerization of 2-norbornene and it also extended catalyzation of the acyclic olefins. Complex **4a**, was synthesized using ruthenium(II) dichlorido *tris*(triphenylphosphine) [$RuCl_2(PPh_3)_3$] treated with hazardous phenyl diazomethane at -78 ^oC degrees and one-pot ligand exchange of

triphenylphosphine with 2 equivalence of high basicity tricyclophosphine results in complex **4b** [52-53].

Complex **4b** (Figure 1.4) retained activity in water and acids, and shows tolerance to different function groups like many protecting groups and is able to catalyze cyclization of five-seven membered ring in good yields. Thus the catalytic activity and stability of these complexes increases with increasing electron donating ability of the phosphine ligands. The order of increasing electron donating ability is PPh_3 < P*i*PrPh$_2$ < P*i*Pr$_3$ < PCy_3 < P*t*-Bu$_3$. The steric and electronic properties of phosphines can be altered by changing the groups attached to phosphorus from less bulky to more bulky group [54, 55].

In spite of its interesting application the major shortcomings are:

(a) Proven to decompose at 80 ^{o}C which limits its application to ring opening metathesis polymerization of cyclo dienes [56].
(b) The use of poisonous diazoalkanes derivatives such as phenyl diazomethane [57, 58].
(c) It can only allow the ring closing metathesis of less sterically trisubstituted olefins only with certain substrates [59].
(d) The reagents lack stability and require huge amount of solvents [60, 61].

1.5.2.3 Ru benzylidene complexes with N-heterocyclic-phosphine

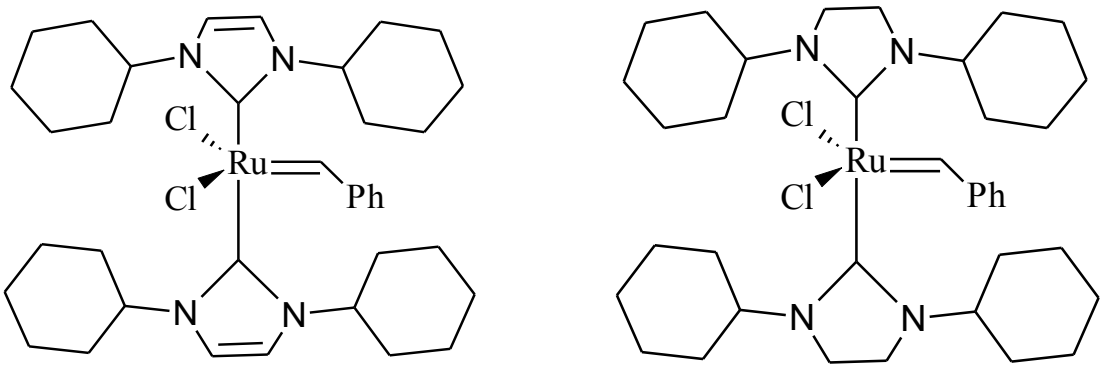

4c **4d**

Figure 1.5: Structures of Ru(II) benzylidene complex with *bis*(N-heterocyclic carbene ligand) [62].

A third and last class of ruthenium alkylidene complexes are the complexes **4c-4h** (Figure 1.5 & 1.6). The complexes **4c** and **4d** (Figure 1.5) with two NHC bonded to ruthenium ion were synthesized by Hermann`s *et al*. [62]. The two phosphines from Grubbs 1st generation pro-type complexes were replaced by strong and sterically bulky σ-sigma donor imidazolin-2-yledene ligands [63]. These ruthenium *bis*(imidazoline-2-ylidene) complexes are reported to show great stability as compared to *bis*(phosphine) complexes at high temperature but they have low activity and selectivity as compared to their phosphine ligand counter parts in ROMP of highly strained monomers. This is attributed to the fact that the *bis*(imidazoline-2-ylidene) ligands appeared to be a non-labile ligand, so they do not dissociate freely from the complexes and thus resulting in slow initiation rate because of competition in electron donating ability since they are located in the *trans* position in the complex [64-65].

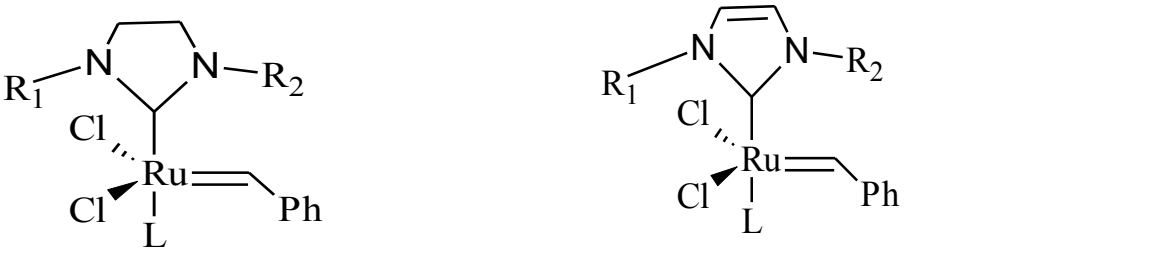

4e, R_1, R_2 = mesityl

4f, R_1, R_2 = 2,6-isopropylphenyl

4g, R_1, R_2 = mesityl

4h, R_1,R_2=2,6-disopropylphenyl

Figure 1.6: Structures of Ru benzylidene complexes with saturated and unsaturated NHC ligands [66, 67].

The presence of labile phosphine and non-labile NHC ligands t*rans* in complexes **4e-4h** (Figure 1.6) proved to complements each other very well. These complexes were obtained by substituting one triphenylphosphines from complexes **4a** and **4b** (Figure 1.4) with sterically bulky NHC ligand in Grubbs 1st generation catalyst and it resulted in complex with very good catalytic properties and these complexes are referred as Grubbs 2nd generation catalysts [66-69]. The different types of N-heterocyclic carbene that have been used for such complexes are: 1,3-bis(mesityl)-4,5-dimethy limidazol-2-ylidene (IMesMe) [70], 1-(2,6-diflourephenyl)-3-(mesityl)-4,5-dihydroimidazolin-2-ylidene [71], 1,3-bis(2,6-diisopropylphenyl)-4,5-dimethylimidazolin-2-ylidene (SIPrMe) [72], 1,3-bis(2,6-diisopropylphenyl)-4,5-dihydroimidazolin-2-ylidene (SIPr) [73], 1,3-bis(2,6-diisopropylphenyl)imidazol-2-ylidene (IPr) [74], and 1,3-bis(2-methylphenyl)-4,5-dihydroimidazol-2-ylidene (SIoTol) [75]. But the most prominent has been the 1,3-bis(mesityl)-4,5-dihydroimidazolin-2-ylidene (SIMes) reported by Grubbs *et al*. and co-workers. This complex has improved activity to even new challenging substrate shown in Scheme 1.6 [76].

The rate of activity of complex **4e** (Figure 1.6) in catalyzing olefin metathesis reaction is reported to be 10^2-10^3 times greater than the Grubbs 1st generation to catalyze ring closing metathesis of diethyl diallymalonate and ring opening metathesis polymerization of functionalized cyclo-octadiene. The Ru complexes with saturated N-heterocyclic carbene ligands have been shown to be more reactive than the unsaturated N-heterocyclic carbene ligands [77]. Contrary to Ru vinyl, carbene these complexes were superior in catalyzing ROMP of low strain monomers such as tri- and tetra-substituted substrates 1,5-dimethy-1,5-cyclooctadiene. The application also extended to tri and tetra-substituted diethyl dimalonate at very low catalysts loading shown in scheme 1.6 **[**78, 79].

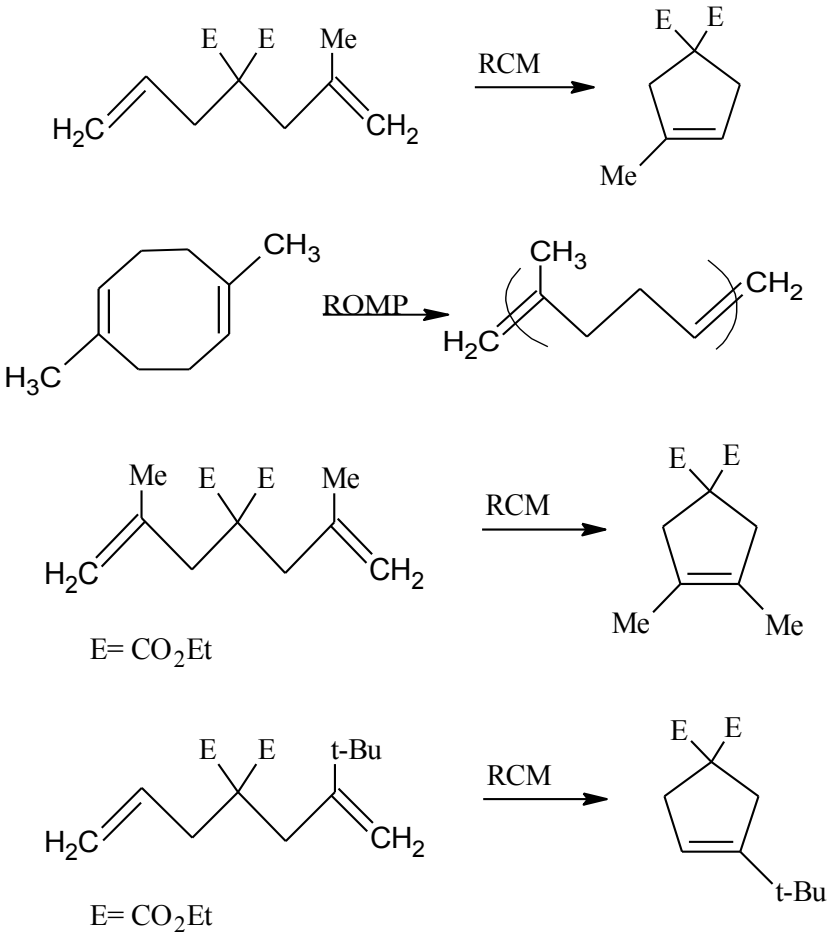

Scheme 1.6: Reactions for application of complex 4e [78]

Despite the superiority of complex **4e** (Figure 1.6) in almost all metathesis substrates, it has slow initiation rate than the first generation catalysts and complex **4f** (Figure 1.6) So to enhance the initiation rate in **4e,** pyridine is usually used instead of phosphine because it can easily de-coordinate to form 14 electron active species and complexes with pyridine are referred to as Grubb`s 3rd generation catalyst [80].

1.5.2.3 Ru isopropoxy-benzylidene complexes

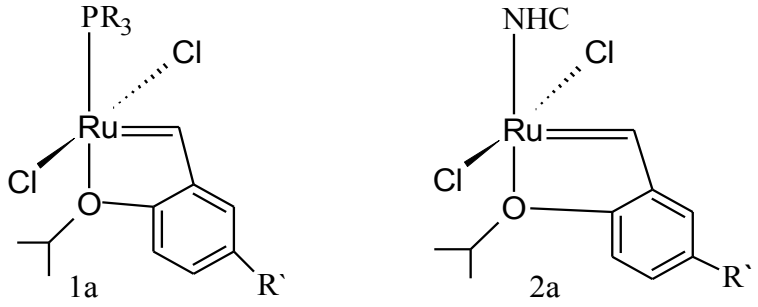

5a, R=Ph,
5b R=Cy,

5c, NHC=SIMes or IMes
5d, NHC=SiPr or iPr

Figure 1.7: Structures of Hodeida-Grubbs 1st and 2nd generation catalysts [83].

Ligands can be classified as monodentate, bidentate and multidentate depending on the number of donor sites they have. Ligands that possess more than one donor atoms coordinated to a metal center are referred as chelating ligands. These types of ligands have also found widely application in homogenous catalysts of olefin metathesis transformation. The examples of such ligands are Ru Schiff-base complexes and Ru isopropyl-ether complexes. The coordination,

solubility and steric properties of these ligands can be altered by varying of the donor atom within the ligand and examples are hemi-labile ligands [81, 82].

Complexes **5a-5d** (Figure 1.7) are referred as Grubbs-Hoveyda catalysts generations. These are synthesized by reacting isopropyl ether benzene with $[RuCl_2(PPh_3)_3]$. In general their activity is similar with Grubbs 2nd generation catalysts but the only difference is their superior selectivity [83]. The 2nd Hoveyda-Grubbs catalyst showed better selectivity for cross metathesis and ring closing metathesis with highly electron deficient compound in scheme 1.7 such as acrylonitrile and fluorinated alkenes. The mechanism of Grubbs-Hoveyda type catalyst is believed to proceed *via* the decoordination of isopropoxystyrene during the metathesis reaction to produce a 14 electron species [84].

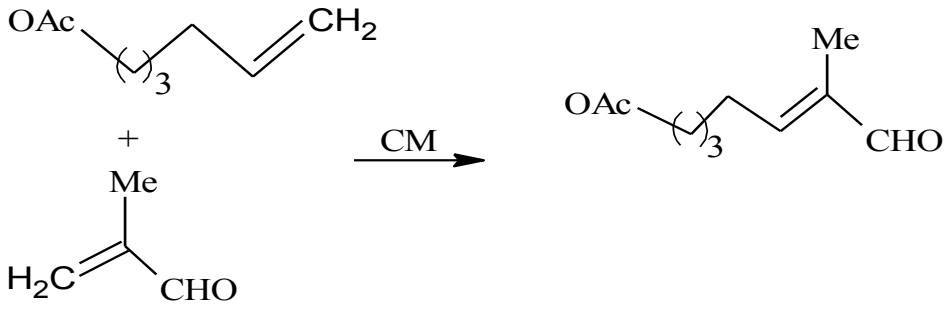

Scheme 1.7: Reaction for application of Grubbs-Hoveyda catalysts [78]

1.5.2.4 Ruthenium indenylidene complexes

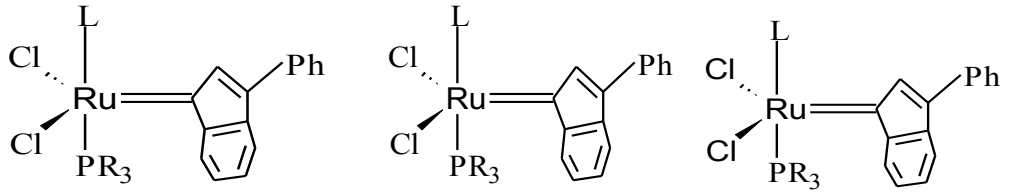

6a, L=SIMes ,R=Cy **6c,** L=SIPr ,R=Cy **6e,** L=SIoTol ,R=Cy

6f, L=SIMes ,R=py **6b**, L=SIPr ,R=py **6f**, L=SIoTol ,R=py

Figure 1.8: Structures of Ru indenylidene complexes

The more sterically the Ru carbene becomes the better stability it displays and this has been proven with the introduction of ruthenium indenylidene complexes **6a-6f** (Figure 1.8). These complexes have 3-phenylinden-1-ylidene that promote and improve the metathesis activity and stability as compared to Ru with benzylidene moiety although they often suffer from lack of selectivity [85]. They can be easily synthesized from stable and commercial starting materials and their reactivity can be extended to many different substrate with different steric functionalities. More importantly complex **6a** and **6c** displayed very good activity at high temperature in the reaction of diethyl diallyl malonate and diallyl tosylamine with very good conversion rate of 88% and 94% respectively in both reaction at room temperature within 25 min duration in Scheme 1.8 [86]. Beside their activity other advantages of using ruthenium indenylidene complexes is that they allow for the synthesis of tri and tetra-substituted cycloalkanes which earlier ruthenium catalyst could not allow and they can even be used for more challenging substrates [87].

Recent studies have been focusing on modifying the ruthenium complexes by introducing different ancillary ligands and the most notable modification has been the introduction of pyridine ligands by Mousaert *et al.* and Nolan *et al.* to produce very active and fast initiating catalyst referred as Ru indenylidene 3rd generation. Although various types of ligands have been used as the ligands to the ruthenium center but the phosphine based ligands by far are thought to be the best way because they are highly air-stable, non-toxic compounds as compared to pyridine based compounds [88, 89].

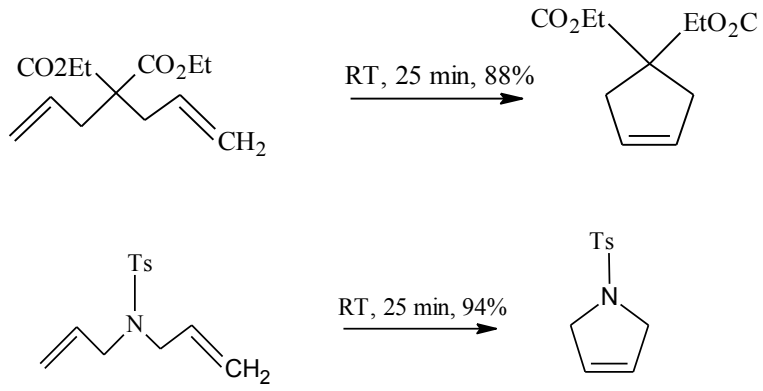

Scheme 1.8: RCM using ruthenium indenylidene complexes [47]**.**

1.6 The Ru based catalyst mechanistic study

The mechanistic and computational study of Grubbs 1st and 2nd generation catalysts in scheme 1.9 showed that the mechanism of olefin metathesis reaction involves the dissociation of phosphine ligand (PR_3) to produce active 14 electron species in high concentration with the general formula [$RuX_2(L)$=CHR`] L = NHC and PR_3. The following step is the oxidative addition of the alkene substrate to the complex to give 16 electron complexes, followed by the rearrangement of the complex to give ruthenocycle *via* insertion migration. The mechanism outlined below compares the 1st and 2nd generation catalysts [90, 91].

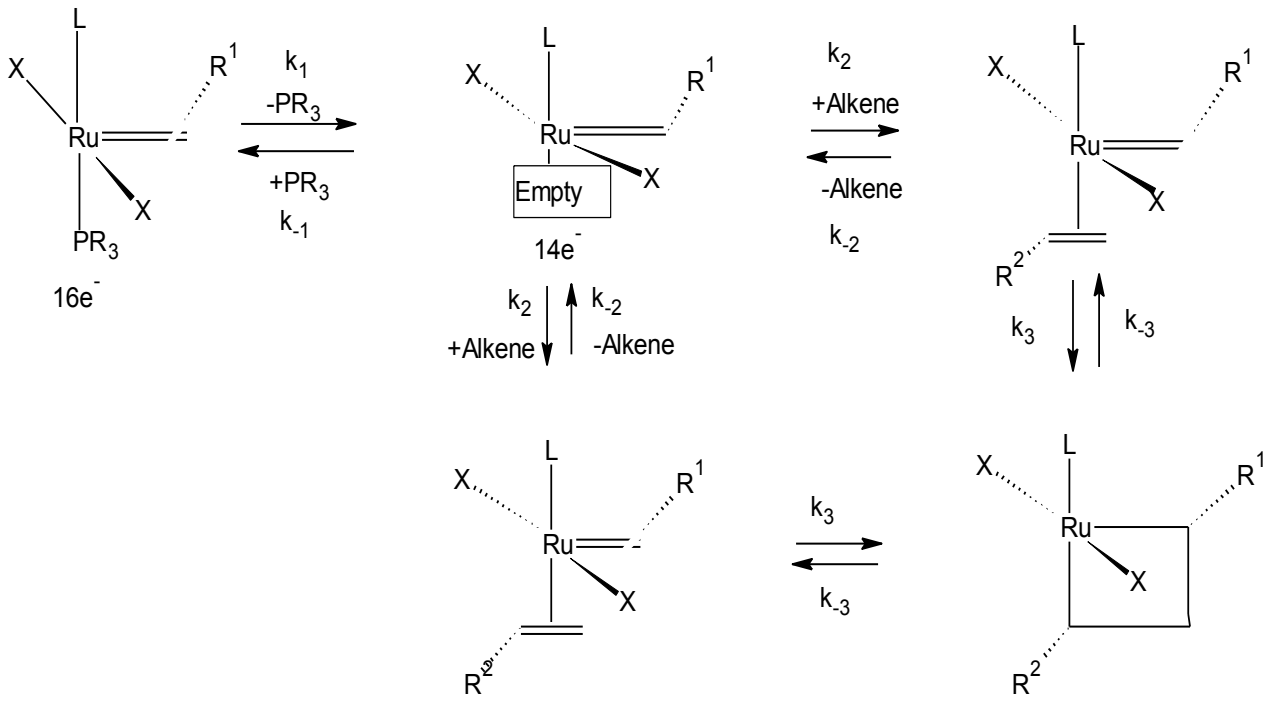

Scheme 1.9: The mechanism for Grubbs 1st and 2nd generation catalysts [90].

The Grubbs 2nd generation catalyst has slow initiation rate yet good stability and high activity as compared to the 1st generation catalyst. It was found that the activity of the catalyst is not only related to the dissociation rate k_1 of PR_3 ligand but it also depends on the coordination of an alkene substrate rate ratio of k_{-1}/k_2. This ratio determines whether the new alkene coordinate or return to the original catalyst by PR_3 rebinding to the promoted species. This means nitrogen heterocyclic carbene bearing ligands do not efficiently loose PR_3 ligand and this resulted in low initiation rate k_1 [92]. Despite the slow dissociation of phosphine ligand due to the strong sigma donation of NHC ligands which increases the electron density of ruthenium center, the strong enhancement that is achieved when a phosphine ligand is replaced with NHC ligand can be explained by the high coordination rate ratio k_{-1}/k_2 of alkene to the 14 electron species.

Electronically, it has been found that the stability and efficiency of a catalyst is achieved by varying the ligands around the metal center so the strong and efficient catalyst are anticipated to have strong sigma donor and one weak sigma donor ligand trans to each other to promote dissociation as well as insertion [93, 94].

1.7 Types of carbene ligands

Carbene ligands are divalent carbon compound with a lone pair of electrons on the carbene carbon covalently bonded with adjacent groups. These types of ligands have found important application in organic synthesis because of their high reactivity. There are three types of carbene ligand that are general known, Fischer type carbene, Shrocks type carbene and nitrogen-heterocyclic type carbenes. The Fischer type carbenes also referred to as singlet state are found with low oxidation state metal with pi accepting ligands and Shrock type carbene also referred to as triplet carbene and are found with high oxidation state metal with non π accepting ligand. The two metal carbene complexes are represented by $[M=CR_2]$.

A third and a special class of carbene ligands is the N-heterocyclic carbene ligands also referred as Arduengo type carbenes since he was the first to prepare a stable and isolable N-heterocyclic carbene ligand [95]. This class of ligands is represented by $M\text{-}CR_2$ and N-heterocyclic carbene ligands have found tremendous application because of their stability and electron donating ability when bonded to transition metal ions. They have been coordinated to many different metals for $Pd(NHC)Cl_2$, $Ni(NHC)(PPh_3)_2$, $PtCl_2(NHC)$, $RhClH(NHC)$ [96, 97].

1.7.1 Bonding in NHC ligands

NHC ligands are stabilized by the vicinal nitrogen and exhibit single state configuration. The two nitrogen lone pairs increase the energy of the empty pi orbital by mesomeric effect and the carbene lone pair is stabilized by inductive effects of electronegative nitrogen atom. N-heterocyclic carbenes are strong sigma donors and their metal complexes show better stability than phosphine complexes. There are many NHC carbene ligands with different ring such as five, six-seven etc. but recently the five–membered NHC ligand have received more attention because of they are easy to synthesize [98].

1.7.2 The bonding in metal-N-heterocyclic carbene ligands

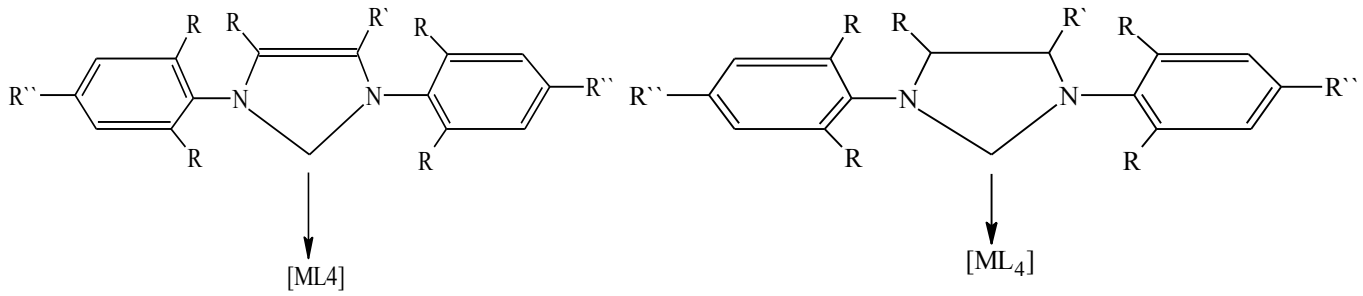

R=alkyl, aryl, halogens, esters etc.

Figure 1.9: Structures of bonding between metal- N-heterocyclic carbene ligand [99]

The NHC ligand bond to the transition metal through strong sigma bonding and pi back bonding from the metal center. The strong sigma donation is a result of strong pi donation by the N-atom, causing a highly filled p-orbital carbene carbon atom, thus reducing the tendency towards metal

to NHC-pi donation. The saturated N-heterocyclic carbene ligands have a highly electron donating ability than unsaturated N-heterocyclic carbene ligand. The better sigma donation and pi acceptor abilities of saturated NHC ensures strong M-NHC bond. Their electronics and steric properties can be altered by changing the nature of the azole ring: imidazoline > imidazole > benzimidazole (order of electron donating power). To form complexes usually the saturated imidazolinium chlorides are deprotonated in situ because of their unstable intermediate [99].

1.7.3 Functionalities of NHC ligands

The presence of NHC ligands has two functions; (i) it is strong σ donor and π acceptor, and it pushes electrons close to the metal center making it highly nucleophilic, and (ii) It promotes the stability towards decomposition due to the steric hindrance shown by these ligands [100, 102].

1.8 Problem statement

Regardless of the huge development of Ru based catalyst in the area of OM catalysis by Grubbs and co-workers, many shortcomings have been identified over the years drawn from the existing catalysts. Although most existing Ru based complexes proved to be very active in one or more of the olefin metathesis catalysis, their disadvantages are loss of thermal stability at high temperature, high catalyst loading which affect the purity of products, the difficulty in selectivity and the use of toxic diazoalkanes as carbene precursors in synthesis of Ru benzylidene complexes. So better catalysts with improved properties are still required [16, 48].

So we hypothesize that using Ru(II) phenyl-3-indenylidene proto-type complexes will results in high selective catalyst and stable catalyst with low cost. Also altering the position of alkyl groups on the phenyl ring attached to the nitrogen of imidazole with less steric alkyl substituents will enhance the steric and electronic properties of a ligand resulting to a different activity and efficiency when coordinated to the metal ion.

1.9 Research aim and objectives

1.9.1 Aim

This study seeks to synthesize and characterize Ru(II) complexes with different less steric N-heterocyclic carbenes with triphenylphosphine and pyridine.

1.9.2 Objectives

- Synthesis of *N,N′*-diaryformamidines
  - *N,N′*-bis(2-methylphenyl)formamidine
  - *N,N′*-diphenylformamidine
  - *N,N′-bis*(4-methoxyphenyl)formamidine
  - *N,N′-bis*(3-methylphenyl)formamidine
  - *N,N′-bis*(4-methylphenyl)formamidine

- Synthesis of *N,N′*-diarylmidazolinium chlorides

- *N,N′-bis*(2-methylphenyl)imidazolinium chloride
- *N,N′-bis*(3-methylphenyl)imidazolinium chloride
- *N,N′*-diphenylimidazolinium chloride
- *N,N′-bis*(4-methylphenyl)imidazolinium chloride
- *N,N′-bis*(4-methoxyphenyl)imidazolinium chloride

- The *N,N′*-diarylimidazolinium chlorides were be characterized using NMR, FTIR and melting point

- Synthesis of Ru(II) Ind complexes bearing different**:**
  - N-heterocyclic carbene, phosphine, pyridine
- The Ru(II) complexes will be characterized using FTIR, UV-Vis, Elemental analysis, decomposition/melting point and conductivity measurements.

References

1. Hoveyda, A. H.; Zhugralin, A. R. The remarkable metal-catalyzed olefin metathesis reaction. *Nature*. **2007**, 450, 243–251.
2. Hejl, A.; Day, M. W.; Grubbs, R. H. Latent olefin metathesis catalysts featuring chelating alkylidenes. *Organometallics*. **2006**, 25, 6148.
3. Nicolou, K. C.; Bugler, P. G.; Sarlah, D. Metathesis in total synthesis. *Angew. Chem. Int. Ed.* **2005**, 44, 4490- 4527.
4. Moore, J. S.; Wilson, G. O.; Caruso, M. M,; Reimer, N. T.; White, S. R.; Sottos, N. R. Evaluation of ruthenium catalysts for ring-opening metathesis polymerization-based self-healing applications. *Chem. Mat*. **2008**, 20, 3288–3297.
5. Lamaty, L.; Colacino, E.; Martinez, J. Preparation of NHC–ruthenium complexes and their catalytic activity in metathesis reaction. *Coord. Chem. Rev*. **2007**, 251, 726–764.
6. Singh, O. M. Metathesis catalysts : historical perspective, recent developments and practical applications. *J. Sci. Ind. Res*. **2006**, 65, 957–965.
7. Chauvin, Y. Olefin metathesis: the early day (Noble lecture). *Angew*. *Chem. Int. Ed*. **2006**, 25, 3740-3746.
8. Schrock, R. R. Multiple metal–carbon bonds for catalytic metathesis reactions (Nobel Lecture). *Angew. Chem. Int. Ed*. **2006**, 45, 3748-3759.
9. Furster, A. In handbook of metathesis, ed. Grubbs, R. H, Wiley-VCH, Veinheim, Germany. **2003**, 2, 423.
10. Deiters, A.; Martin, S. F. Synthesis of oxygen and nitrogen-containing heterocycles by ring-closing metathesis. *Chem. Rev*. **2004**, 104, 199.

11. Grela, K.; Michrowska, A.; Bieniek, M. Catalysts for new tasks: preparation and applications of tunable ruthenium catalysts for olefin metathesis. *Japan Chem. Forum and Wiley Period, Inc.* **2006**, 6, 146.

12. Mol, J.C. Application of olefin metathesis in oleochemistry: An example of green chemistry. *Green. Chem*. **2002**, 4, 5–13.

13. Mol, J.C. Industrial applications of olefin metathesis. *J. Mol .Cat. Chem*. **2004**, 213, 39–45.

14. Marbach, A.; Hupp, R. The evolution of polynorbornene. *Rubber World*. **1989**, 30.

15. (a) Calderon, N.; Chen, H. Y; Scott, K. S. Olefin metathesis-a novel reaction for skeletal transformations of unsaturated hydrocarbons. *Tetrahedron*. **1967**, 8, 3327-3329 (b) Calderon, N. Olefin metathesis reaction. *Acc. Chem. Res*. **1972**, 5, 127-132.

16. Owker, M, The basis and applications of heterogenous catalysis. Oxford University Press, Oxford. **1998,** 2, 3.

17. Magqi, N. Studies towards the development of novel multidentate ligands. M.S. Thesis. Rhodes University. **2007**.

18. Casey, C.P. 2005 Nobel Prize in Chemistry: development of the olefin metathesis method in organic synthesis. *J. Chem. Ed*. **2006**, 83, 192-195.

19. Rouhi, M. A. Olefin metathesis: big-deal reaction. *Chem. Eng. News*. **2002**, 80, 29-38.

20. Barrault, J.; Pouilloux, Y.; Clacens, J. M.; Vanhove, C.; Bancquart, S. Catalysis and fine chemistry. *Catalysis Today*. **2002**, 75, 177.

21. Monsaert, S.; Verpoort, F.; Vila, A. L.; Drozdzak, R.; Van Der Voort, P. Latent olefin metathesis catalysts. *Chem. Soc. Rev*. **2009**, 38, 3360-3362.

22. Eleuterio, H.S. Olefin metathesis: chance favors those minds that are best prepared. *J. Mol. Catal*. **1991**, 65, 55-61.

23. Schrock, R. R.; Hoveyda, A. H. Molybdenum and tungsten imido alkylidene complexes as efficient olefin metathesis catalysts. *Angew. Chem. Int. Ed*. **2003**, 42, 4592–4633.

24. Forman, G. S.; McConnell, A. E.; Tooze, R, P.; Van Rensburg, J.; Meyer, W. H.; Kirk, M. M.; Dwyer, C. L.; Serfontein, D. W. A stable ruthenium catalyst for productive olefin Metathesis. *Organometallic*. **2004**, 23, 4824.

25. Grubbs, R. H. The development of functional group tolerant romp catalysts. *J. Macro. Sci-Pure. Appl. Chem*. **1994**, A31, 1829.

26. Roberts, A. N.; Cochran, A. C.; Rankin, D. A.; Lowe, A. B.; Schanz, H.J. Benzylidene-functionalized ruthenium-based olefin metathesis catalysts for ring-opening metathesis polymerization in organic and aqueous media. *Organometallics*. **2007**, 26, 6515–6518.

27. Schrock, R. R. High oxidation state multiple metal–carbon bonds. *Chem. Rev*. **2002**, 102, 145–179.

28. Gallivan, J. P.; Jordan, J. P.; Grubbs, R.H. A neutral, water-soluble olefin metathesis catalyst based on an n-heterocyclic carbene ligand. *Tetrahedron*. **2005**, 46, 2577–2580.

29. Halback, T. S. Novel ruthenium-based metathesis catalysts containing electron-withdrawing ligands: synthesis, immobilization, and reactivity. *J. Org. Chem*. **2005**, 70, 4687–4694 .

30. Jafarpour, L.; Stevens, D. E.; Nolan, S. P. A sterically demanding nucleophiliccarbene: 1,3-bis(2,6-diisopropylphenyl)imidazol-2-ylidene). Thermochemistry and catalytic application in olefin metathesis. *J. Org. Chem*. **2002**, 606, 49–54.

31. Schrock, R. R. Synthesis of molybdenum imido alkylidene complexes and some reactions involving acyclic olefins. *J. Am. Chem. Soc*. **1990**, 112, 3875–3886.

32. Haas, L. K.; Franz, J. K. Application of metal coordination chemistry to explore and manipulate cell biology. *Chem. Rev*. **2009**, 109, 10.

33. Santana, S. A. A.; Carvalho Jr, V. P.; Benedito, S. L. N. DMSO molecule as ancillary ligand in Ru-based catalysts for ring opening metathesis polymerization. *J. Braz. Chem. Soc*. **2010**, 21, 279-287.

34. Wawrzycka, J. A.; Rogala, P.; Michałkiewicz, S.; Hodorowiczb, M.; Barszcza, B. Ruthenium complexes in different oxidation states: synthesis, crystal structure, spectra and redox properties. *Dalton. Tran*. **2013**, 42, 6092-6101.

35. Astruc, D. The metathesis reactions: from a historical perspective to recent developments. *New. J. Chem*., **200**5, 29, 42-56.

36. Hillmyer, M. A.; Lepetit, C.; McGrath, D. V.; Novak, B. M.; Grubbs, R. H. Aqueous Ring-Opening Metathesis Polymerization of Carboximide-Functionalized 7-Oxanorbornenes. *Macromolecules*. **1992**, 25, 3345-3350.

37. Kirk, M. M. Ruthenium based homogeneous olefin metathesis. M. S. Thesis, University of Free State. S. A. November, **2005**.

38. Green, M. L. H.; Mitchard, L. C.; Swanwick, M. G. Carbene complexes of iron, molybdenum, and ruthenium: a new route to metal–carbene derivatives. *J. Chem. Soc*. A. **1971**, 794.

39. Keisham, S. S.; Mozharivskyj, Y. A.; Carroll, P. J.; Kollipara, M. R. Syntheses and characterization of indenylidene ruthenium(II) complexes containing *N,N′* donor Schiff base ligands. Molecular structures of $[(\eta5\text{-}C_9H_7)Ru(PPh_3)_2(CH_3CN)]BF_4$ and $[(\eta5\text{-}C_9H_7)Ru(PPh_3)(C_5H_4–N_2–CHN–C_6H_4\text{-}p\text{-}CH_3)]BF_4$. *J. Org. Chem*. **2004**, 689, 1249-1256.

40. Amec, J. S. M.; Keitz, B. K.; Grubbs, R. H. Latent ruthenium olefin metathesis catalysts featuring a phosphine or an N-heterocyclic carbene ligand. *J. Org. Chem*. **2010**, 695, 1831-1837.

41. Cazin, S. J.; Bantreil, X.; Poater, A.; Urbina-Blanco, C. A.; Bidal, D. Y.; Falivence, L.; Randall, R. A. M.; Cavallo, L.; Slawin, A. M. Z. Synthesis and reactivity of ruthenium phosphite indenylidene complexes. *Organometallics*. **2012**, 31, 7415−7426.

42. Kadyrov, R.; Rosiak, A. Olefin metathesis ruthenium catalyst with unsaturated NHC. *Chem. Today*. **2009**, 27, 24-26.

43. Kuhn, K. M.; Bourg, J. B.; Chung, C. K.; Virgil, S. C.; Grubbs, R. H. Effects of NHC-backbone substitution on efficiency in ruthenium-based olefin metathesis. *J. Am. Chem. Soc.* **2009**, 131, 5313–20.

44. Lichtenheldt, M.; Kress, S.; Blechert, S. Synthesis of electronically modified Ru-based neutral 16 VE allenylidene olefin metathesis precatalysts. *Molecules*. **2012**, 17, 5177-5186.

45. Schmidt, T. E.; Bantreil, X.; Citadelle, C. A.; Slawin, A. M. Z.; Cazin, C. S. J. Phosphites as ligands in ruthenium-benzylidene catalysts for olefin metathesis. *Chem. Commun*. **2011**, 47, 7060–2.

46. Ablialimov, O.; Kędziorek, M.; Torborg, C.; Malińska, M.; Woźniak, K.; Grela, K.; New ruthenium(II) indenylidene complexes bearing unsymmetrical N-heterocyclic carbenes. *Organometallics*. **2012**, 31, 7316−7319.

47. Dragutan, V.; Dragutan, I.; Demonceau, A. Ruthenium complexes bearing n-heterocyclic carbene ligands. Part II: Recent developments in metathesis chemistry. *Platinum. Metal. Review*. **2005**, 49, 183–188.

48. Grubbs, R. H. Olefin-metathesis catalysts for the preparation of molecules and materials (Nobel Lecture 2005). *Adv. Syn. Cat*. **2007**, 349, 34–40.

49. Wu, Z.; Benedicto, A. D.; Grubbs, R. H. Living ring opening metathesis polymerization of bicycle heptane catalyzed by ruthenium alkylidene complexes, *Macro. Mol*, **1993**, 23, 4975-4977.

50. Nguyen, S. T.; Johnson, L. K.; Grubbs, R. H.; Ziller, J. W. Ring-opening metathesis polymerization (ROMP) of norbornene by a Group VIII carbene complex in protic media *J. Am. Chem. So*c. **1992**, 114, 3974-3975.

51. Schrock, R. R. Olefin metathesis by molybdenum imido alkylidene catalyst. *Tetrahedron.* **1999**, 58, 8814-8853.

52. Schwab, P.; Grubbs, R. H.; Ziller, J. W. Synthesis and application of $RuCl_2(=CHR')(PPh_3)_2$: The influence of the alkylidene moiety on metathesis activity. *J. Am. Chem. Soc*. **1996**, 118.

53. Schawb, P.; Franne, M, B.; Ziller, J. W.; Grubbs, R. H. Series of well olefin metathesis catalysts: synthesis of $RuCl_2(=CHR')$ and its reactive. *Angew. Chem. Int. End. Engl*. **1995**, 34, 2039-2041.

54. Grubbs, R. H.; Trnka, T. M.; Morgan, P. J.; Sanford, M. S.; Wilhelm, T. E.; Scholl, M.; Choi, L. T.; Ding, S.; Day, M. W. Synthesis and activity of ruthenium alkylidene complexes coordinated with phosphine and n-heterocyclic carbene ligands. *J. Am. Chem. Soc*. **2003**, 125, 2546-2558.

55. Abushhewa, S. M. A. Measuring the electronic effect of some phosphines and phosphites. University of Manchester. **2010.**

56. Love, J. A.; Sanford, M. S.; Day, M. W.; Grubbs, R. H. Synthesis, structure and activity of enhanced initiators for olefin metathesis. *J. Am. Chem. Soc*. **2003**, 125, 10103–10109.

57. Schmidt, B.; Krehl, S.; Geißler, D.; Hauke, S.; Kunz, O.; Staude, L. The catalytic performance of Ru NHC alkylidene complexes : Pcy_3 versus pyridine as the dissociating ligand. *Beil. J. Org. Chem*. **2010**, 6, 1188–1198.

58. Fürstner, A.; Guth, O.; Düffels, A.; Seidel, G.; Liebl, M.; Gabor, B.; Mynott, R. Indenylidene complexes of ruthenium: optimized synthesis, structure elucidation, and performance as catalysts for olefin metathesis- application to the synthesis of the ADE-ring system of nakadomarin A. *Chem. Eur. J*. **2001**, 7, 4811**.**

59. Schrodi, Y.; Peterson, R. L. Evolution and application of second-generation ruthenium olefin metathesis catalyst. *Mat. Inc*. **2007**, 40, 45-52.

60. Wilhelm, T. E.; Belderrain, T. R.; Brown, S. N.; Grubbs, R. H. Reactivity of $Ru(H)(H_2)Cl(PCy_3)_2$ with propargyl and vinyl chlorides: new methodology to give metathesis-active ruthenium carbenes. *Organometallics*. **1997**, 16, 3867-3869.

61. Trnka, S. T.; Nguyen, S. T.; Grubbs, R. H. The discovery and development of well defined ruthenium-based olefin metathesis catalyst. **2003**, 1, 61. Wiley. VCH.

62. Vougioukalakis, G. C.; Grubbs, R. H. Ruthenium-based heterocyclic carbene-coordinated olefin metathesis catalysts. *Chem. Rev*. **2010**, 110, 1746–87.

63. Hermann, W. A.; Kocher, C. N-Heterocyclic carbenes. *Angew. Chem. Int. Ed*. **1997**, 36, 2162.

64. Harrity, J. P. A.; La, D. S.; Cefalo, D. R.; Visser, M. S.; Hoveyda, A. H. Chromenes through metal-catalyzed reactions of styrenyl ethers. mechanism and utility in synthesis. *J. Am. Chem. Soc.* **1998**, 120, 2324.

65. Furstener, A. Olefin metathesis and beyond. *Angew. Chem. Int. Ed*. **2000**, 39, 3012-3043.

66. Chattege, H. K.; Morgan, J. P.; Scholl, M.; Grubbs, R. H. Synthesis of functionalized olefins by cross and ring-closing metatheses. *J. Am. Chem. Soc*. **2000**, 122, 3783.

67. Vehlow, K.; Maechling, S.; Blechert, S. Ruthenium metathesis catalysts with saturated unsymmetrical N-heterocyclic carbene ligands. *Organometallics*. **200**6, 25, 25-28.

68. Weber, S. G.; Loos, C.; Rominger, F.; Straub, B. F. Synthesis of an extremely sterically shielding N-heterocyclic carbene ligand. *Arkivoc*. **2012**, 3, 226-242.

69. Pump, E.; Fischer, R. C.; Slugovc, C.; Halide exchange in second-generation *cis*-dihalo ruthenium benzylidene complexes. *Organometallics*. **2012**, 31, 3972.

70. Nolan, S. P.; Urbina-Blanco, C. A.; Ba[;ntreil, X.; Clavier, H.; Slawin, A. M. Z. Backbone tuning in indenylidene-ruthenium complexes bearing an unsaturated N-heterocyclic carbene. *Beil. J. Org. Chem*. **2010**, 6, 1120-1126.

71. Vougioukalakis, G. C.; Grubbs, R. H. Ruthenium-based olefin metathesis catalysts coordinated with unsymmetrical N-heterocyclic carbene ligands: synthesis, structure, and catalytic activity. *Chem. Eur. J*. **2008**, 14, 7545-7556.

72. Dragutan, I.; Dragutan, V.; Delaude, L.; Demonceau, A. N-Heterocyclic carbenes as highly efficient ancillary ligands in homogeneous and immobilized metathesis ruthenium catalytic systems. *Arkivoc*. **2005**, 206-253.

73. Nolan, P. S.; Clavier, H.; Urbina-Blanco, C. A. Indenylidene ruthenium complex bearing a sterically demanding NHC ligand: an efficient catalyst for olefin metathesis at room temperature. *Organometallics*. **2009,** 28, 2848-285.

74. Manzini, S.; Urbina Blanco, A. C.; Slawin, A. M. Z.; Nolan, S. P. Effect of ligand bulk in ruthenium-catalyzed olefin metathesis: IPr* vs IPr. *Organometallics*. **2012**, 31, 6514-6517.

75. Grela, K.; Torborg, C.; Szczepaniak, G.; Zeilinski, A.; Malinska, M.; Wozniak, K. Stable ruthenium indenylidene complexes with a sterically reduced NHC ligand. *Chem. Comm*. **2013**, 49, 3161-3264.

76. Scholl, M.; Ding, S.; Lee, C. W.; Grubbs, R. H. Synthesis and activity of a new generation of ruthenium-based olefin metathesis catalysts coordinated with 1,3-dimesityl-4,5-dihydroimidazol-2-ylidene ligands. *Org. Lett*. **1999**, 6, 953-956.

77. Liu, S. T.; Chang, Y. H.; Fu, F. C.; liu, Y. H.; Peng, M. S.; Chen, T. J., synthesis, characterization and cataltic activity of saturated and unsaturated N-Heterocyclic carbene Iridium complexes. *Dalton. Trans.* **2008**, 861-867.

78. Grubbs, H. R.; Trnka, T. M. The development of L_2X_2Ru=CHR olefin metathesis catalysts: an organometallic success story. *Acc. Chem. Res*. **2001**, 34, 18-29.

79. Weskamp, T.; Kohl, F. J.; Hermann, W. A. N-heterocyclic carbene: novel ruthenium-alkylidene complexes. *J. Org .Chem*. **1999**, 582, 362-365.

80. Leitgeb, A.; Burtscher, D.; Bauer, T.; Slugovc, C. Ruthenium-indenylidene initiators for living ring opening metathesis polymerisation. *Chimica Oggi / Chemistry today.* **200**9, 27, 30.

81. Loock, M. M. The alkene metathesis reactivity of the Puk-Grubbs 2-precatalyst. M. S. Thesis, North West University. SA. **2009**.

82. Raju, V. V.; Balasubramanian, J.; Balakrishnan, C.; Chinnusamy, V. Synthesis, spectral characterization, catalytic and biological studies of new Ru(II) carbonyl Schiff base. *Natural science.* **2011**, 3, 542-550.

83. Kingsbury, J. S.; Harrity, P. A. J.; Bonetatesbus, P, J.; Hoveyda, A. H. A recyclable Ru-based metathesis catalyst. *J. Am. Chem. Soc*. **1999**, 121, 791-799.

84. Bruneau, C.; Shahane, S.; Toupet, T.; Fischmeister, C. Synthesis and characterization of sterically enlarged hoveyda-type olefin metathesis catalysts. *Eur. J. Inorg. Chem*. **2013**, 1, 54-60.

85. Dragutan, I.; Dragutan, V.; Delaude, L.; Demonceau, A. Exploring new achievements in olefin metathesis catalysts Part 2-compelling innovations in ruthenium complexes. *Chimica Oggi/Chemistry Today*. **2009**. 27, 13-16.

86. Dragutan, I.; Dragutan, V.; Filip, P. Recent developments in design and synthesis of well-defined ruthenium metathesis catalysts-a highly successful opening for intricate organic synthesis. *Chem. In .form*. **2006**, 37, 8, 105-129.

87. Urbina-Blanco, C. A.; Manzini, S.; Gomes, J. P.; Doppiu, A.; Nolan, S. P. Simple synthetic routes to ruthenium-indenylidene olefin metathesis catalysts. *Chem. Commun*. **2011**, 47, 5022-4.

88. Monsaert, S.; Drozdzak, R.; Dragutan, V.; Dragutan, I.; Verpoort, F. Indenylidene-ruthenium complexes bearing saturated N-heterocyclic carbenes: synthesis and catalytic investigation in olefin metathesis reactions. *Eur. J. Inorg. Chem*. **2008**, 3, 432-440.

89. Nolan, S. P.; Urbina-Blanco, C. A.; Leitgeb, A.; Slugovc, C.; Bantreil, X .; Clavier, H.; Slawin, A. Z. M. Olefin metathesis featuring ruthenium indenylidene complexes with a sterically demanding NHC ligand. *Eur. J. Chem*. **2011**, 17, 5045-53.

90. Trzaskowski, B.; Grela, K. Structural and mechanistic basis of the fast metathesis initiation by a six-coordinated ruthenium catalyst. *Organometallics*. 2013, 32, 3625-3630.

91. Romero, P. E.; Piers, W. E. Direct observation of a 14-electron ruthenacyclobutane Relevant to Olefin Metathesis. *J. Am. Chem. Soc*. **2005**, 127, 5032.

92. Grubbs, R. H.; Sanford, M. S.; Love, J. A. Mechanism and activity of ruthenium olefin metathesis catalysts. *J. Am. Chem. Soc*. **2001**, 123, 6543-6554.

93. Van Rensburg, J. W.; Steynberg, P. J.; Kirk, M. M. Meyer, W. H.; Forman, G. S . Mechanistic comparison of ruthenium olefin metathesis catalysts: DFT insight into relative reactivity and decomposition behavior. *J. Org. Chem*. **2006,** 691, 5312-5325.

94. Elias, A. J. Molecule matters N-heterocyclic carbenes-the stable form of R_2C:. *Resonance*. **2008**, 456-467.

95. Arduengo, A. J.; Krafczyk, R.; Schmutzler, R. Imidazolylidenes, imidazolinylidenes and imidazolidines. *Tetrahedron*. **1999**, 55, 14523-l4534.

96. Herrman, W. A. Heterocyclic: a new concept in organic metallic catalysts. *Angew .Chem. Int. Ed*. **2002**, 41, 1290-1309.

97. Herrmann, W. A.; Kocher, C.; Lukas, J. G.; Artus, G. R. J. Heterocyclic carbenes : a high-yielding synthesis of novel, functionalized n-heterocyclic carbenes in liquid ammonia. *Chem. Eur. J*. **1996**, 17, 1627-1636**.**

98. Scott, N. M.; Dorta, R.; Stevens, E. D.; Correa, A.; Cavallo, L.; Nolan, S. P. Interaction of a bulky N-heterocyclic carbene ligand with Rh(I) and Ir(I). Double C-H activation and isolation of bare 14-electron Rh(III) and Ir(III) complexes. *J. Am. Chem. Soc*. **2005**, 127, 3516-3526.

99. Majumdar, K. C.; Muhuri, S.; Ul Islam, R.; Chattopadhyay, B. Synthesis of five- and six-membered heterocyclic compounds by the application of the metathesis reactions. *Heterocycles*. **2009**, 78, 1109-1161.

100. Jacobsen, H.; Correa, A.; Poater, A.; Costabile, C.; Cavallo. L. Understanding the M(N HC) (NHC=N-heterocyclic carbene) bond. *Coord. Chem. Rev*. **2009**, 253, 687-703.

101. Frohlish, N.; Pidun, U.; Stahl, M.; Franking, G. Carbenes as pure donor ligands: theoric--al study of beryllium-carbene complexes. *Organometallic*s. **1997**, 16, 442.

102. Hermann, W. A.; Rurte, O.; Artus, J. Synthesis and structure of an ionic beryllium-carb--ene complex. *J. Org. Chem*. **1995**, 501, C1-C4.

103. Wang, F.; Liu, L.; Wang, W.; Li, S.; Shi, M. Chiral NHC-metal-based asymmetric cat-alysis. *Coord. Chem. Rev*. **2012**, 256, 804–853.

CHAPTER TWO

2. EXPERIMENTAL SECTION

2.1 Chemicals and solvents

Ruthenium(III) chloride hydrate, 1.1-diphenyl-2-proyl-1-ol, pyridine, *N,N*-diisopropyl ethylamine, aniline, *o*-toluidine, *p*-toluidine, *p*-anasidine, triethyl orthoformate, acetic acid, *m*-toluidine, potassium hexamethyldisilazide. Anhydrous tetrahydrofuran, methanol, hexane, anhydrous ether, dichloromethane, benzene, hexane, ethanol, pentane, toluene, acetone, 1,2-dichloroethane. All these list of solvents and chemicals were purchased from Sigma-Aldrich and used as obtained without further purification. The ruthenium precursor complexes were synthesized using literature procedures [1, 2].

2.2. Equipment's and Instrumentation

2.2.1 UV-Visible Spectroscopy

The UV–Vis (electronic) spectra were recorded on a Perkin–Elmer Lambda 25 UV–VIS spectrophotometer. The samples were placed in quartz cuvettes of 1 cm path length. High grade dichloromethane or acetonitrile as solvents were used in dissolving the complexes.

2.2.2 Infrared spectroscopy

Infrared spectra of the complexes were recorded on a Perkin–Elmer Model System 2000 FT–IR spectrophotometer in the range 4000 – 370 cm^{-1}. Firstly, the ligands were mixed with potassium bromide in 1:10 ratio. The mixture was grounded and used to prepare windows that were transparent to be used in FTIR. For sample preparation of complexes, a little amount of nujol

was mixed with the Ru(II) complexes to form a paste which was then used with NaCl disks in the FTIR instrument.

2.2.3 Elemental analysis

Elemental analyses for C, H and N were carried out on a Fison elemental analyzer.

2.2.4 Melting Point

Samples of complexes and ligands in capillary tubes were introduced into a Stuart melting point apparatus model SMP 11 to determine its melting point.

2.2.5 NMR spectroscopy

The ^{1}H and ^{13}C-NMR spectra were performed on a Varian–NMR–vnmr s600 MHz spectrometer at 25 ºC, using high–power proton decoupling, and pulse sequence: The chemical shifts of deuterated dimethylsulfoxide (DMSO-d_6) and chloroform ($CDCl_3$) were referenced as DMSO-d_6 (^{1}H-NMR, δ = 2.5 ppm; ^{13}C-NMR, δ = 40 ppm) and $CDCl_3$ (^{1}H-NMR, δ = 7.2 ppm; ^{13}C-NMR, δ = 77 ppm). Chemical shifts are reported in ppm relative to tetramethylsilane.

2.3. Synthesis of *N,N′*-diarylformamidines

2.3.1. Synthesis of *N,N′-bis*(2-methylphenyl)formamidine (F1)

F1 was synthesized, using a modified procedure of Grubbs *et al.* [3]; Glacial acetic acid (1.5 mmol, 0.086 mL) was added to a round bottom flask charged with *o*-toluidine (60 mmol, 6.377 mL) and triethyl orthoformate (30 mmol, 5mL). The mixture was heated at 140 ^{o}C for 3 hrs after which it was cooled to room temperature and a solid suspension was formed. The suspension was dissolved in cold hexane to remove unreacted *o*-toluidine. The solid was collected by vacuum filtration and the light brown product was dried at room temperature.

Yield: 6.0304 g (89%). M. p: 154-155 ^{o}C. IR (cm^{-1}): 3415 υ(N-H), 3015 υ(arom. C-H), 2871.38 υ(aliph. C-H), 1664 υ(C=N), 1590.85 υ(arom. C=C). ^{1}H-NMR: (600 MHz, $CDCl_3$ δ = 7.21): δ_H 2.20 (s, 3H), 2.34 (s, 3H), 7.04-7.86 (m, 8H), 7.83 (s, 1H), 8.08 (s, 1H). ^{13}C NMR: (600 MHz, $CDCl_3$ δ = 77) : δ_C 17.93, 30.93, 117.57, 123.40, 126.97, 130.70, 147.63.

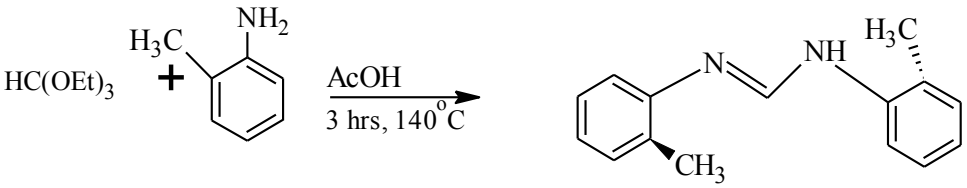

Scheme 2.1: Synthesis of *N,N′-bis*(2-methylphenyl)formamidine (**F1**)

The following *N,N′*-diarylformamidines **F2, F3** and **F5** were synthesized using the same procedure detailed above for **F1**, but different aniline derivatives were used.

2.3.2 Synthesis of *N,N′-bis*(4-methylphenyl)formamidine (F2)

Glacial acetic acid (1.5 mmol, 0.086 mL) was added to a round bottom flask charged with *p*-toluidine 6.42 g (60 mmol) and triethyl orthoformate (5 mL, 30 mmol). The mixture was heated at 140 ^{o}C for 12 hrs. A pale yellow solid was obtained.

Yield: 5.5012 g (81%). M. p: 137-138 ^{o}C. IR (cm^{-1}): 3413 υ(N-H), 3029 υ(arom. C-H), 2920 υ(aliph. C-H), 1616 υ(C=N), 1515 υ(arom. C=C). ^{1}H-NMR: (600 MHz, $CDCl_3$ δ = 7.21): δ_H 2.39 (s, 3H), 6.99-7.17 (m, 8H), 7.29 (s, 1H), 8.25 (s, 1H). ^{13}C-NMR: (600 MHz, $CDCl_3$ δ = 77): δ_C 20.83, 119.16, 129.95, 132.69, 150.02.

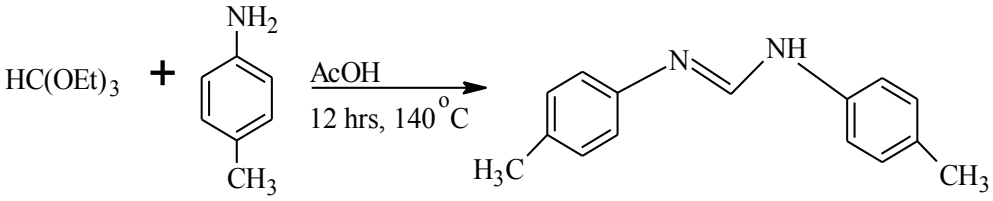

Scheme 2.2: Synthesis of *N,N′-bis*(4-methylpheny)formamidine (**F2**)

2.3.3 Synthesis of *N,N′*-diphenylformamidine (F3)

Glacial acetic acid (1.5 mmol, 0.086 mL) was added to a round bottom flask charged with aniline (60 mmol, 5.4782 mL) and triethyl orthoformate (5 mL, 30 mmol). The mixture was heated at 140 ^{o}C for 15 hrs. A yellow solid was obtained.

Yield: 4.3821 g (74%). M. p: 139-140 ^{o}C. IR (cm^{-1}): 3416 υ(N-H), 3053 υ(arom. C-H), 1619 υ(C=N), 1589.85 υ(arom. C=C). ^{1}H-NMR: (600 MHz, $CDCl_3$ δ = 7.21): δ_H 7.07-7.35 (m, 8H), 7.58 (s, 1H), 8.26 (s, 1H). ^{13}C-NMR: (600 MHz, $CDCl_3$ δ = 77): δ_C, 119.10, 123.39, 129.43, 149.43.

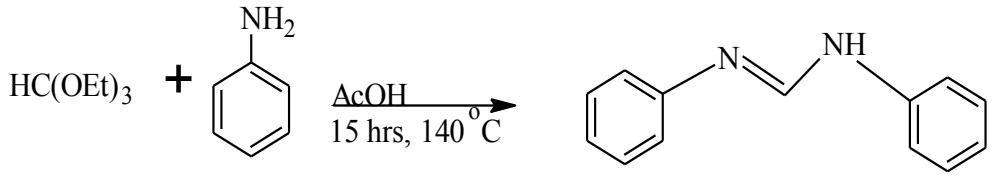

Scheme 2.3: Synthesis of *N,N′*-di(phenyl)formamidine (**F3**)

2.3.4 Synthesis of *N,N′-bis*(4-methoxyphenyl)formamidine (F4)

F4 was synthesized using modified procedure of Glorius, *et al.* [4]; Glacial Acetic acid (1.5 mmol, 86 µL, 90.1 mg) was added to a round bottom flask charged with 2-methoxyphenylaniline (60 mmol, 7.389 g) and triethyl orthoformate (30 mmol, 5 mL). The mixture was stirred and heated at 140 ºC for 4 hrs. After which, the crude suspension was collected by vacuum filtration washed with pentane (10 mL) and diethyl ether (15 mL). The suspension was then recrystallized using acetone and colorless crystallized were obtained.

Yield: 4.0120 g (52%). M. p: 130-131 ºC. IR (cm^{-1}): 3415 υ(N-H), 3055 υ(arom. C-H), 2894.38 υ(aliph. C-H), 1656 υ(C=N), 1556 υ(arom. C=C), 1027 υ(O-CH_3). ^{1}H-NMR: (600 MHz, $CDCl_3$ δ = 7.21): δ_H 3.78 (s, 3H), 6.84-8.38 (m, 8H), 8.54 (s, 1H), 8.75 (s, 1H). ^{13}C-NMR: (600 MHz, $CDCl_3$, δ = 77): δ_C 55.47, 55.56, 114.19, 114.89, 121.47, 121.92, 129.75, 130.16, 156.66, 159.40, 163.44.

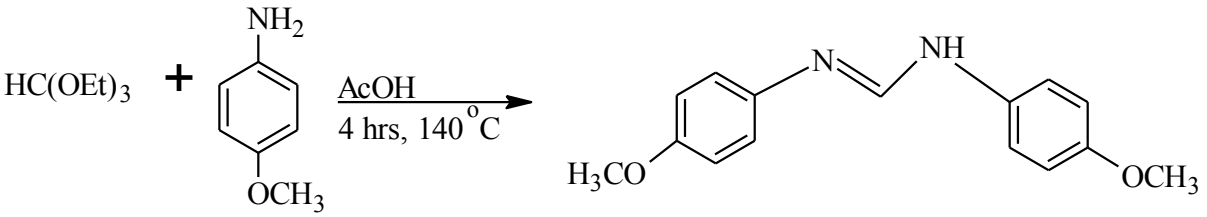

Scheme 2.4: Synthesis of *N,N′-bis*(4-methoxyphenyl)formamadines (**F4**)

2.3.5 Synthesis of *N,N′-bis*(3-methylphenyl)formamidine (F5)

Glacial acetic acid (1.5 mmol, 0.086 mL) was added to a round bottom flask charged with *m*-toluidine (8.892 g, 60 mmol) and triethyl orthoformate (5 mL, 30 mmol). The mixture was heated at 140 ^{o}C for 3 hrs. A brown solid was obtained.

Yield: 5.3021 g (79%). M. p: 149-150 ^{o}C. IR (cm^{-1}): 3405 υ(N-H), 3007 υ(arom. C-H), 2924 υ(aliph. C-H), 1610 υ(C=N), 1514 υ(arom. C=C). ^{1}H-NMR: (600 MHz, $CDCl_3$ δ = 7.21): δ_H 2.19 (s, 3H), 2.34 (s, 3H), 7.03-7.29 (m, 8H), 8.08 (s, 1H), 8.14 (s, 1H). ^{13}C-NMR: (600 MHz, $CDCl_3$ δ = 77): δ_C 17.91, 30.93, 117.55, 123.40, 126.96, 130.69, 147.60.

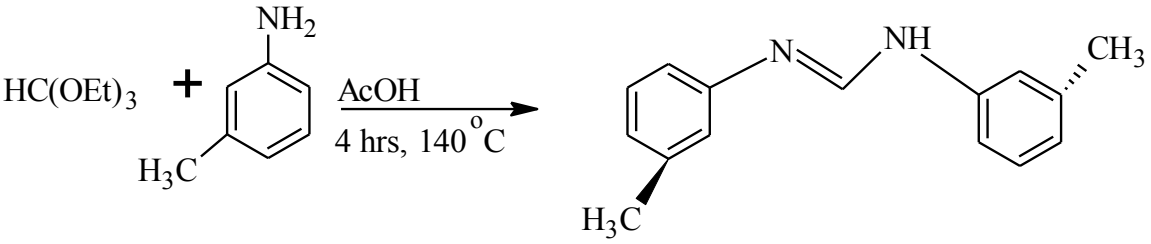

Scheme 2.5: synthesis of *N,N′-bis*(3-methylphneyl)formamidine (**F5**)

2.4 Synthesis of *N,N′*-diarylimidazolinium chlorides

2.4.1 Synthesis of *N,N′-bis*(2-methylphenyl)imidazolinium chloride (L1)

Diisopropylethylamine ($NEt(iPr)_2$) 2.562 mL (14.74 mmol) was added to a stirred solution of **F1** (3.000 g, 13.4 mmol) and 1, 2-dichloroethane (21.115 mL, 268 mmol) in a three neck flask. The mixture was heated at 110 °C for 20 hrs, after which the reaction mixture was then cooled to room temperature, and excess 1,2-dichloroethane was removed *in vacuo*. The residue was

redissolved on acetone to remove any unreacted formamidine and the product was collected by vacuum filtration, washed with excess solvent and dried *in vacuo*. A white solid was obtained.

Yield: 1.989 g (52%). M. p: > 230 ºC. IR (cm^{-1}): 3415 υ(R_2N^+=C), 3015 υ(arom. C-H), 2827 υ(aliph. C-H), 1677 υ(C=N), 1622.85 υ(arom. C=C), 1486 υ(C-N). ^{1}H-NMR: (600 MHz, $CDCl_3$ δ=7.21): δ_H 2.14 (br, 3H), 2.52 (br, 3H), 4.62 (d, 2H), 4.67 (d, 2H), 7.21-7.78 (m, 8H), 8.85 (br, 1H). ^{13}C-NMR: (600 MHz, $CDCl_3$ δ=77): δ_C 18.10, 30.83, 40.95, 52.89, 26.127, 131, 134, 157.88

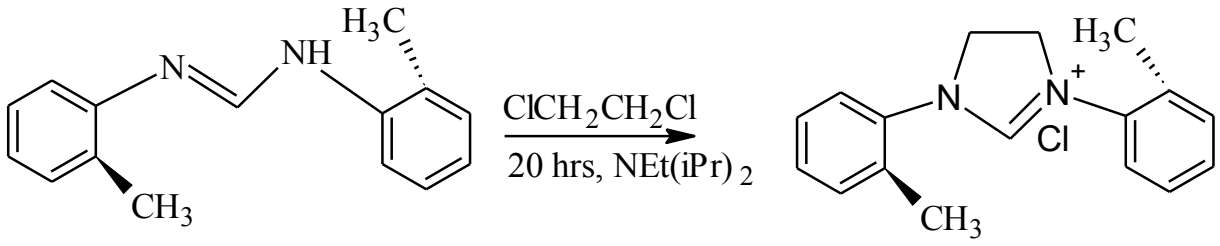

Scheme 2.6: Synthesis of *N,N′-bis*(2-methylphenyl)imidazolinium chlorides (**L1**)

L2, **L3**, **L4** and **L5** were all synthesized using the same procedure illustrated section 2.4.1, but different diarylformamidine were used.

2.4.2 Synthesis of *N,N′-bis*(4-methylphenyl)imidazolium chloride (L2)

Diisopropylethylamine ($NEt(iPr)_2$) (2.566 mL, 14.74 mmol) was added to a stirred solution of **F2** formamidine (2.985 g, 13.4 mmol) and 1, 2-dichloroethane (21.114 mL, 268 mmol) in a two neck flask. The mixture was heated at 110 °C for 16 hrs. A pale yellow solid was obtained.

Yield: 2.0432 g (53%). M. p: > 250 ºC. IR (cm^{-1}): 3415 υ(R_2N^+=C), 3086 υ(arom. C-H), 2924 υ(aliph. C-H), 1689 υ(C=N), 1610 υ(arom. C=C), 1460 υ(C-N), 819 υ(p-CH_3). ^{1}H-NMR: (600 MHz, CDCl3 δ = 7.21): δ_H 2.09 (s, 3H), 2.36 (s, 3H), 4.96 (s, 4H), 7, 28-7.58 (m, 8H) 10.03 (s, H). ^{13}C-NMR; (600 MHz, CDCl3 δ = 77): δ_C 20.92, 31.17, 48.77, 118.79, 130.48, 134.27, 136.93, 151.59.

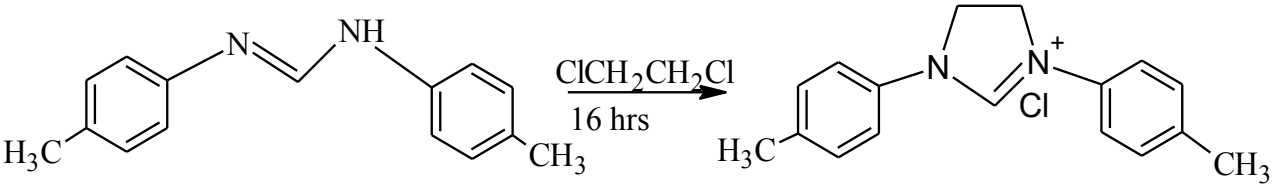

Scheme 2.7: Synthesis of *N,N′-bis*(4-methylphenyl)imidazolinium chloride (**L2**)

2.4.3 Synthesis of *N,N′*-diphenylimidazolinium chloride (L3)

Diisopropylethylamine (1.95 mL, 11.22 mmol) was added to a stirred solution of **F3** (2.0 g, 10.2 mmol) and 1, 2-dichloroethane (16.073 mL, 204 mmol) in a two neck flask. The mixture was heated at 120 °C for 24 hrs. A pale yellow solid was obtained.

Yield: 1.621 g (62%). M. p: > 250 ºC. IR (cm^{-1}): 3417 (R_2N^+=C), 3050 (arom. C-H), 1618 (C=N), 1589 (arom. C=C), 1498 (C-N) cm^{-1}. ^{1}H-NMR: (600 MHz, $CDCl_3$ δ = 7.21): δ_H 4.61 (s, 4H), 7.12-7.72 (m, 8H), 10.19 (s, 1H). ^{13}C-NMR: (600 MHz, $CDCl_3$ δ = 77): δ_C 48.77, 188.98, 127.46, 19, 130.13, 136.61, 154.30**.**

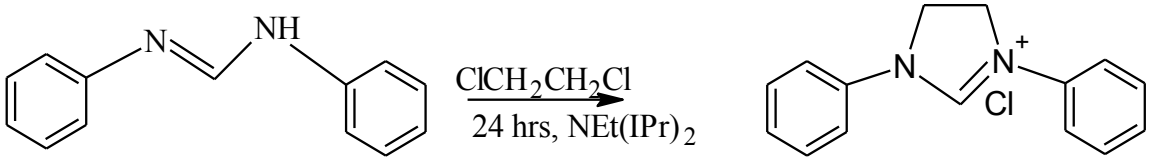

Scheme 2.8: Synthesis of *N,N′-bis*(phenyl)imidazolinium chloride (**L3**)

2.4.4 Synthesis of *N,N′-bis*(4-methoxyphenyl)imidazolinium chloride (L4)

Diisopropylethylamine (0.649 mL, 4.279 mmol) was added to a stirred solution of **F4** (1.00 g, 3.890 mmol) and 1, 2-dichloroethane (6.1298 mL, 77.8 mmol) in a two neck flask. The mixture was heated at 110 °C for 20 hrs. A pale yellow solid was obtained.

Yield: 0.963 g (78%). M. p: >250 ^{o}C. IR (cm^{-1}): 3420 (N-H), 3074 (arom. C-H), 2894.38 (aliph. C-H), 1616 (C=N), 1513 (arom. C=C), 1354 (C-N), 1247 (O-CH_3) cm^{-1}.

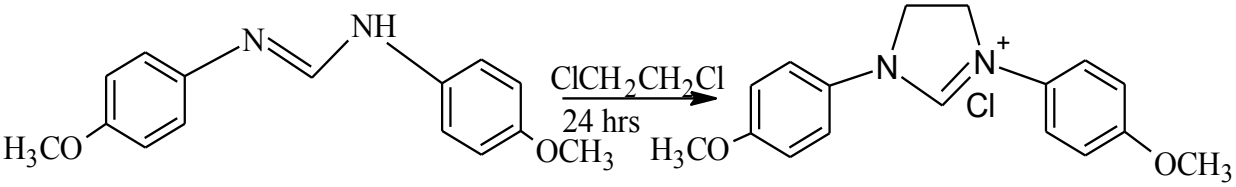

Scheme 2.9: Synthesis of *N,N′-bis*(4-methoxyphenyl)imidazolinium chloride (**L4**)

2.4.5 Synthesis of *N,N′-bis*(3-methylphenyl)imidazolinium chloride *(*L5)

Diisopropylethylamine (0.96 mL, 5.5 mmol) was added to a stirred solution of **F5** (2.5001 g, 11.1 mmol) and 1, 2-dichloroethane (17.51 mL, 222 mmol) in a two neck flask. The mixture was heated at 110 °C for 20 hrs. A white solid was obtained.

Yield: 2.1476 g (67%). M. p: > 250 ^{o}C. IR (cm^{-1}): 3416 (R_2N^+=R), 3122 (arom. C-H), 2921.38 (aliph. C-H), 1656 (C=N), 1594 (arom. C=C), 1482 ν(C-N), 778 ν(*m*-CH_3). ^{1}H-NMR: (600

MHz, $CDCl_3$ δ = 7.21): δ_H 2.14 (br, 3H), 2,52 (br, 3H), 4.62 (d, 2H), 4.67 (d, 2H), 7.27-7.79 (m, 8H), 8.95 (br, 1H).

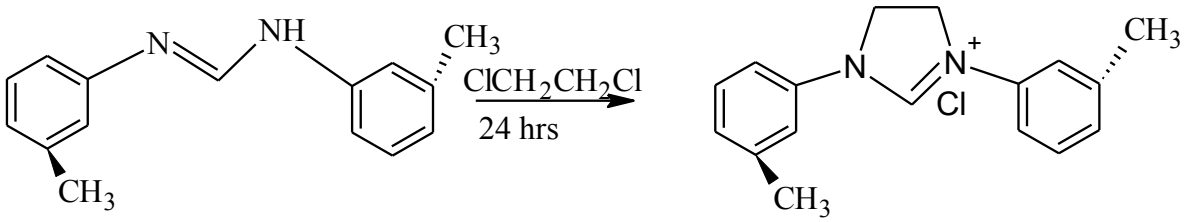

Scheme 2.10: Synthesis of *N,N′-bis*(3-methylphenyl)imidazolinium chlorides (**L5**)

2.5 Synthesis of Ru(II) complexes with N-heterocyclic carbene ligands

2.5.1. Synthesis of $RuCl_2$(Ind)(SIoTol)(PPh_3) (C1)

C1 was synthesized using modified method of Grela *et al.* [5] and Nolan *et al.* [6]. A dried three neck flask was charged with 0.16196 g (0.8119 mmol) of potassium hexamethyldisilazide (KHMDS) and 0.19379 g (0.6766 mmol) of **L1** dissolved in 10 mL of dry toluene. The solution was stirred for 10 minutes at room temperature before the solution of 300 mg (0.3383 mmol) of [$RuCl_2(PPh_3)_2$(Ind)] in 5 mL of dry toluene was added using a syringe. Then the mixture was refluxed at 50 ^oC for 3 hrs under N_2 atmosphere. After the reaction was completed the solvent was removed using a rotary evaporator and the product was re-dissolved in 5 mL of dichloromethane and precipitated using pentane (30 mL) or hexane (30 mL). The suspension formed was filtered using sintered glass and washed with 10 x 2 mL of cold methanol and 5x2 mL of cold hexanes and dried at room temperature to give a brown solid.

Yield: 0.1763 g (58%). M. p: 298 ºC. IR (cm^{-1}): 2935.38, 1947.66, 1465.6, 1373, 820, 533. Elemental analysis (%): $C_{50}H_{45}Cl_2N_2PRu$, (Cal.) Found: C= (68.49) 68.49, H = (5.17) 4.95, N = (3.19) 2.98. UV-Vis (DCM): 228, 262, 408 nm.

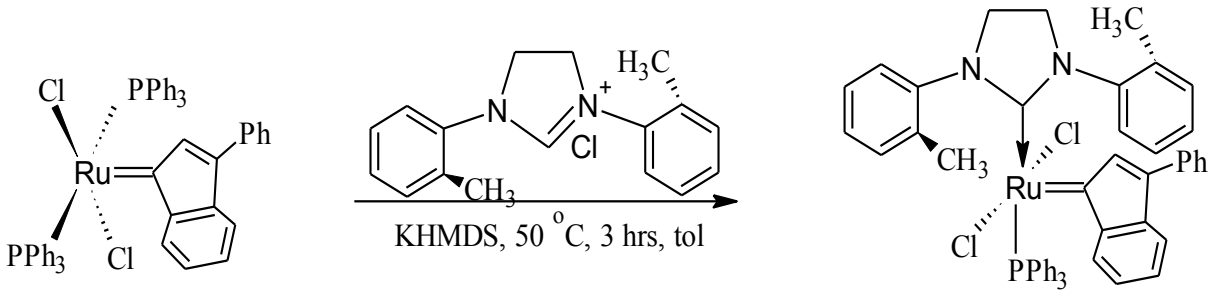

Scheme 2.11: Synthesis of $[RuCl_2(SIoTol)(PPh_3)(Ind)]$ (**C1**)

Complex **C1**, **C2**, **C3**, **C4**, **C5** have been synthesized using the method discussed above in 2.5.1

2.5.2 Synthesis of $RuCl_2(Ind)(SIpTol)(PPh_3)$ (C2)

A dried three neck flask was charged with 0.16196 g (0.8119 mmol) of potassium hexamethyldisilazide (KHMDS), 0.19379 g (0.6766 mmol) of **L2** and 300 mg (0.3383 mmol) of $[RuCl_2(PPh_3)_2(Ind)]$ as reactants. A red brown solid was obtained.

Yield: 0.15984 g (50.32%). M. p: 285 ºC IR (cm^{-1}): 2939, 1943, 1471, 1372, 812, 545.6. Elemen -tal analysis (%): $C_{50}H_{45}Cl_2N_2PRu$. (Cal.) Found: C = (68.49) 68.08, H = (5.17) 5.01, N = (3.19) 3.00. UV-Vis (DCM): 230, 247, 415 nm.

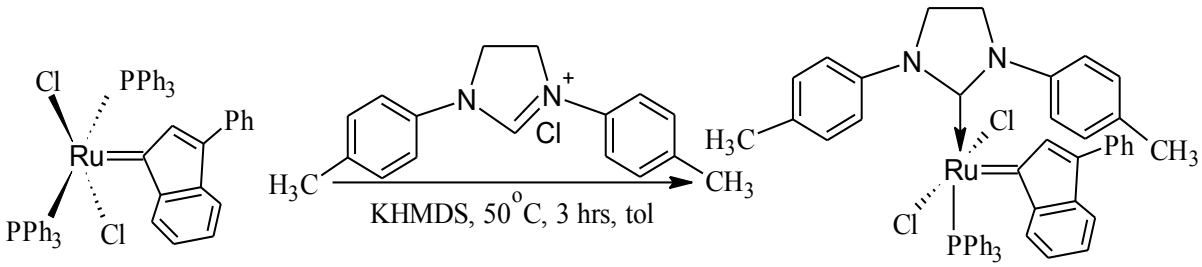

Scheme 2.12: Synthesis of $[RuCl_2(SIpTol)(PPh_3)(Ind)]$ (**C2**)

2.5.2 Synthesis of $RuCl_2(Ind)(SIPh)(PPh_3)$ (C3*)*

A dried three neck flask was charged with 0.16196 g (0.8119 mmol) of potassium hexamethyldisilazide (KHMDS), 0.17506 g (0.6766 mmol) of **L3** and 300 mg (0.3383 mmol) $[RuCl_2(PPh_3)_2(Ind)]$ as reactants. A brown solid was obtained.

Yield: 0.1672 g (55%). M. p: 276 ºC. IR (cm^{-1}): 2947, 1924, 1452, 1369, 804, 540. Elemental analysis (%): $C_{48}H_{41}Cl_2N_2PRu$. (Cal) Found: C = (67.92) 67.18, H = (4.87) 4.12, N = (3.30) 3.01. UV-Vis (DCM): 242, 256, 415 nm.

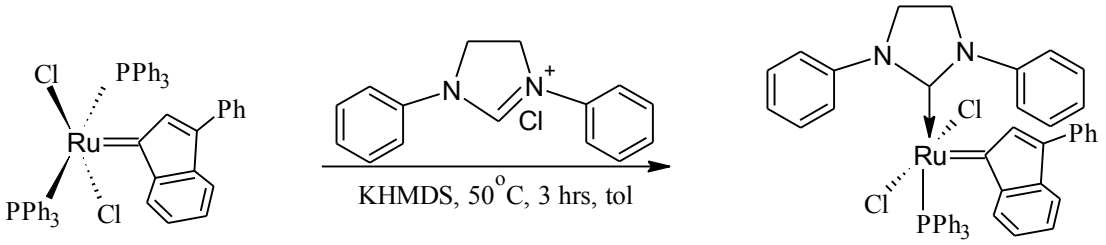

Scheme 2.13: Synthesis of $[RuCl_2(SIPh)(PPh_3)(Ind)]$ (**C3**)

2.5.4 Synthesis of $RuCl_2(Ind)(SIpAnis)(PPh_3)$ (C4)

A dried three neck flask was charged with 0.16196 g, (0.8119 mmol) of potassium hexamethyldisilazide (KHMDS), 0.215159 g, (0.6766 mmol) and 300 mg (0.3383 mmol) of $[RuCl_2(PPh_3)_2(Ind)]$ as reactants. A dark brown solid was obtained.

Yield: 0.15501 g (51.1%). M. p: > 300 ^{o}C. IR (cm^{-1}): 2950, 1946, 1471, 801, 551. Elemental analysis (%): $C_{50}H_{45}Cl_2N_2O_2PRu$: (Cal) Found: C = (66.08) 65.97, H = (4.99) 4.43, N = (3.08) 2.70. UV-Vis (DCM): 273, 257, 400 nm.

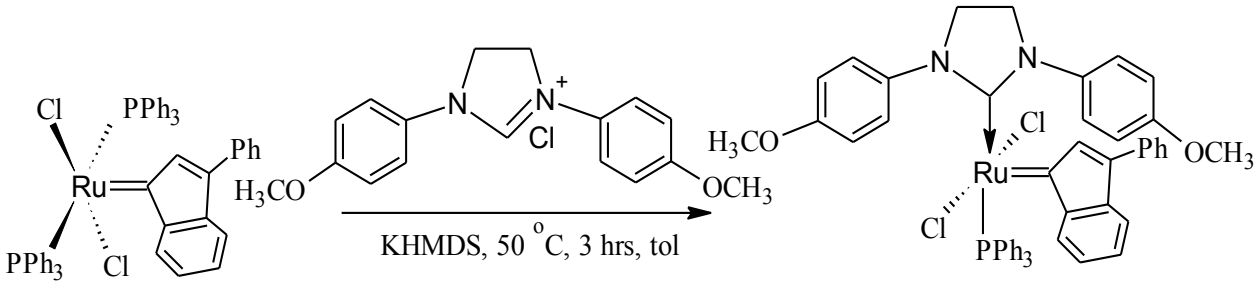

Scheme 2.14: Synthesis of [$RuCl_2$(SIpAnis)(PPh_3)(Ind)] (**C4**)

2.5.5 Synthesis of $RuCl_2$(Ind)(SImTol)(PPh_3) (C5)

A dried three neck flask was charged with 0.16196 g, (0.8119 mmol) of potassium hexamethyldisilazide (KHMDS) and 0.19379 g (0.6766 mmol) of **L5** and 300 mg (0.3383 mmol) of [$RuCl_2(PPh_3)_2$(Ind)] as starting materials. A brown solid was obtained.

Yield: 0.1620 g (60%). M. p. 294 ^{o}C IR (cm^{-1}): 2922, 1942, 1459, 1374, 821, 526. $C_{50}H_{44}Cl_2N_2PRu$: (Cal) Found. C = (68.69) 67.95, H = (5.17) (4.88), N = (3.19) 2.96. UV-Vis (DCM): 230, 263, 418 nm.

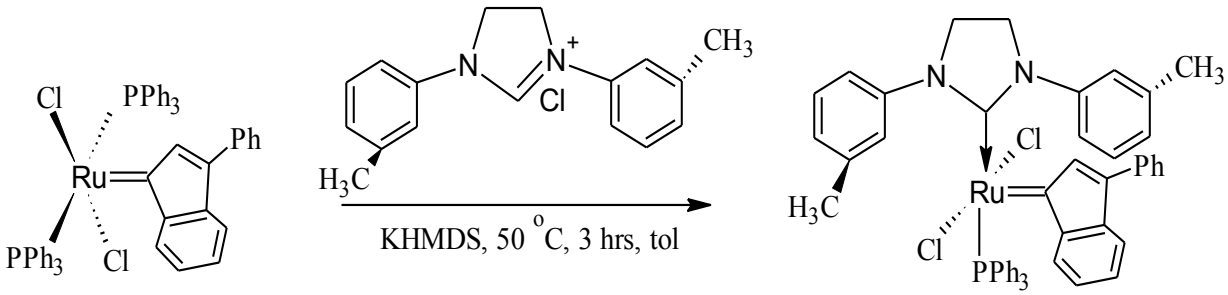

Scheme 2.15: Synthesis of [$RuCl_2$(SImTol)(PPh_3)(Ind)] (**C5**)

2.5.6 Synthesis of [$RuCl_2$(SIoTol)(py)(Ind)] (C6)

In a three neck flask under a nitrogen atmosphere 100 mg (0.1142 mmol) of [$RuCl_2$(Ind)(SIoTol)(PPh_3)] was dissolved in 0.9 mL (11.42 mmol) of dry pyridine in the fume cardboard. The solution was stirred for 1 hr before 10 ml of pentane was added, then the stirring was continued for an additional 1 hr. The mixture was kept at 0 ºC for 12 hrs. After that, the solid was filtered and washed with pentane (2x 4 mL) to give brown product.

Yield: 0.0721 g (72%). M. p: 270 ºC. IR (cm^{-1}): 2995, 1942, 1468, 1374, 736. Elemental analysis (%): $C_{37}H_{35}Cl_2N_3Ru$. (Cal) Found. C = (64.06) 63.87, H = (5.09) 4.82, N= (6.06) 5.74. UV-Vis (DCM): 275, 373, 533 nm.

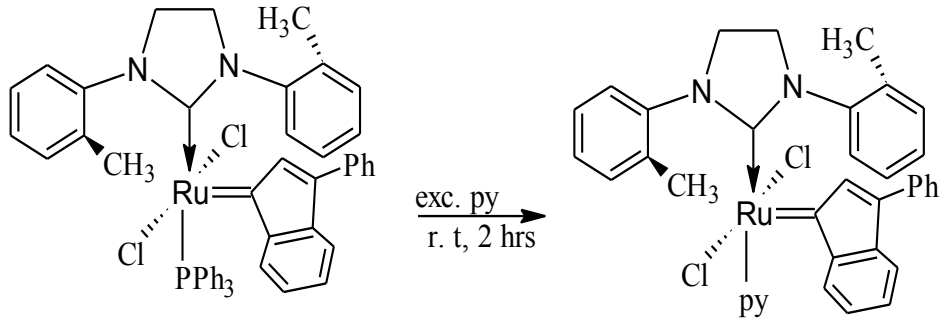

Scheme 2.16: Synthesis of [$RuCl_2$(SI*o*-Tol)(Py)(Ind)] (**C6**)

Complex **C6**, **C7**, **C8**, **C9** and **C10** have been synthesized using the detail procedure in section **2.5.6**

2.5.7 Synthesis of [$RuCl_2$(SIpTol)(py)(Ind)] (C7)

In a three neck flask under a nitrogen atmosphere 100 mg (0.1142 mmol) of [$RuCl_2$(SI*p*-Tol)(PPh_3)(Ind)] was dissolved in 0.9 mL (11.42 mmol) of dry pyridine. A red brown solid was

obtained. Yield: 0.05972 g (59 %). M. p. 256 ^{o}C IR (cm^{-1}): 2960, 1994, 1459, 1374, 733. Elemental analysis (%): $C_{37}H_{35}C_{l2}N_3Ru$. (Cal): Found. C = (64.06) 63.98, H = (5.09) 4.88, N = (6.06) 5.53. UV-Vis (DCM): 274, 370, 682 nm.

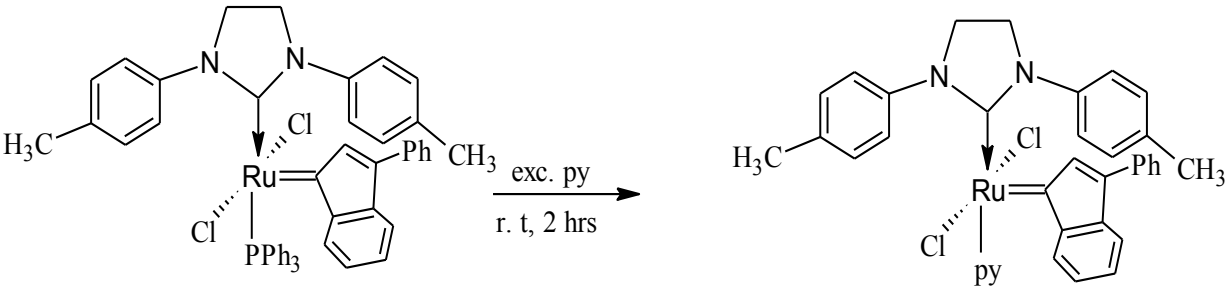

Scheme 2.17: Synthesis of [$RuCl_2$(SIoTol)(Py)(Ind)] (**C7**)

2.5.8 Synthesis of [$RuCl_2$(SIPh)(py)(Ind)] (C8)

In a three neck flask under a nitrogen atmosphere 100 mg (0.113044 mmol) of [$RuCl_2$(SIPh)(PPh_3)(Ind)] was dissolved 0.9 mL (11.30 44 mmol) of dry pyridine. The dark brown solid was obtained.

Yield: 0.053301 g (53 %). M. p: 251 ^{o}C. IR (cm^{-1}): 2995, 1949, 1481, 1374, 780. Elemental analysis (%): $C_{35}H_{32}Cl_2N_3Ru$. (Cal) Found: C = (63.16) 63.01, (4.69) 4.24, N = (6.31) 6.15. UV-Vis (Acetonitrile): 276, 439, 687 nm.

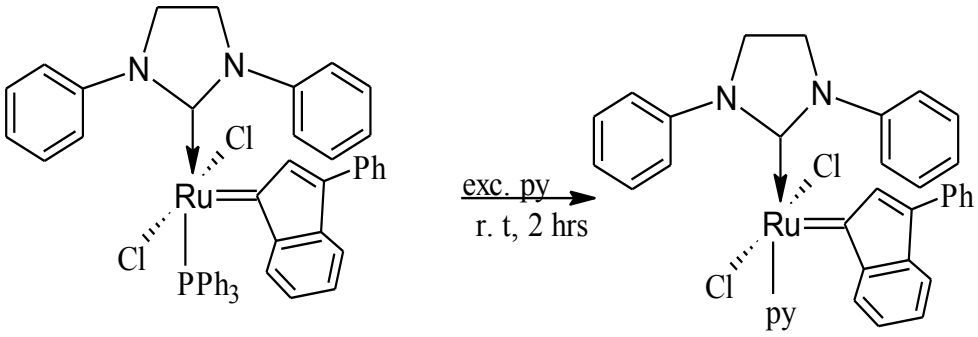

Scheme 2.18: synthesis of [$RuCl_2$(SIPh)(Py)(Ind)] (**C8**)

2.5.9 Synthesis of [$RuCl_2$(SIpAnis)(py)(Ind)] (C9)

In a three neck flask under a nitrogen atmosphere 100 mg (0.1102 mmol) of [$RuCl_2$(SIpAnis)(PPh_3)(Ind)] was dissolved in 0.9 mL (11.02 mmol) of dry pyridine. A brown-red solid was obtained.

Yield: 0.05823 g (58%). M. p: 287 ^oC. IR (cm^{-1}): 2975, 1951, 1525, 1374, 742, 523, 1023. Elemental analysis: $C_{37}H_{35}Cl_2N_3O_2Ru$. (Cal) Found: C = (61.24) 61.02, H = (4.86) 4.43, C = (5.24). UV-Vis (Acetonitrile): 285, 440, 652 nm.

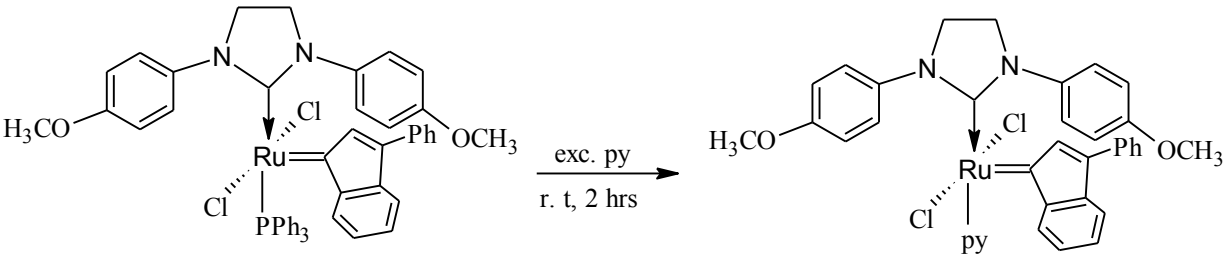

Scheme 2.19: Synthesis of [$RuCl_2$(SIpAnis)(Py)(Ind)] (**C9**)

References

1. Hallman, P. S.; Stephenson, T. A.; Wilkinson, G. Synthesis methods taken from Parry, R. W. tris(triphenylphospin)dichlororuthenium(II). *Inorg. Syn*. **1970**, 12, 238-239.
2. Fürstner, A.; Guth, O.; Düffels, A.; Seidel, G.; Liebl, M.; Gabor, B.; Mynott, R. Indenylidene complexes of ruthenium: Optimized synthesis, structure elucidation, and performance as catalysts for olefin metathesis-application to the synthesis of the ADE-ring system of nakadomarin A. *Chem. Eur. J*. **2001**, 7, 4811**.**
3. Grubbs, R. H.; Kuhn, K. M. A facile preparation if imidazolinium chlorides. *Org. Lett*. **2008**, 10, 2075-2077.
4. Glorius, F.; Hirano, K.; Urban, S.; Wang, C. A modular synthesis of highly substituted imidazolium salts. *Org. lett*. **2009**, 11, 1019-1022.
5. Grela, K.; Torborg, C.; Szczepaniak, G.; Zeilinski, A.; Malinska, M.; Wozniak, K. Stable ruthenium indenylidene complexes with a sterically reduced NHC ligand. *Chem. Comm*. **2013**, 49, 3161-3264.
6. Nolan, S. P; Clavier, H.; Urban-Blanco, C. A. Indenylidene ruthenium complexes bearing a sterically demanding NHC ligand: An Efficient catalyst for olefin metathesis at room temperature. *Organometallics*. **2009**, 28, 2848-2854.
7. Chakraborty, P. An efficient $FeCl_3$ catalyzed synthesis of *N,N'*-diarylformamidines. *Gr. Sust. Chem*. **2013**, *03*, 26-30.
8. Sadek, K. U. Cerium(IV) ammonium nitrate (CAN) mediated reactions IV. A highly efficient synthesis of *N,N'*-diarylsubstituted formamidines in water at ambient temperature. *Gr. Sust. Chem.* **2011**, *01*, 92-97.

CHAPTER THREE

RESULTS AND DISCUSSION

3.1 Introduction

N-heterocyclic carbene ligands are a class of very useful ligands in homogeneous catalysis and this has been proven by their continuous application in olefin metathesis and Suzuki-Miyaura cross coupling reactions [1]. They form very stable metal complexes when coordinated to metal ions, because of their properties such as good σ-donors and poor π-acceptors [2]. Carbene precursors can be synthesized using different methods, but in this study, a solvent free method was employed because it prevents the use of solvents and the technique is easy to handle [3]. The deprotonation of the saturated *N,N′*-diarylimidazolinium chlorides was done in-situ using potassium *bis*(trimethylsilyl)amide (KHMD). All the synthesized *N,N′*-diarylformamidines as the precursors of *N,N′*-diarylimidazolinium chlorides and their corresponding Ru(II) phenyl-3-indenylidene complexes bearing a sterically reduced N-heterocyclic carbene and phosphine or pyridine ligands were characterized using ^{1}H-NMR, ^{13}C-NMR, FT-IR, UV-Vis spectroscopy, elemental analysis and melting point determination.

3.2 Synthesis and characterization of *N,N′*-diarylformamidines

Scheme 3.1 below shows different synthetic routes that were followed to synthesize *N,N′*-diarylformamidines as the precursors to *N,N′*-diarylimidazolinium chlorides. The physical and analytic parameters of the synthesized *N,N′*-diarylformamidines are summarized in Table 3.1.

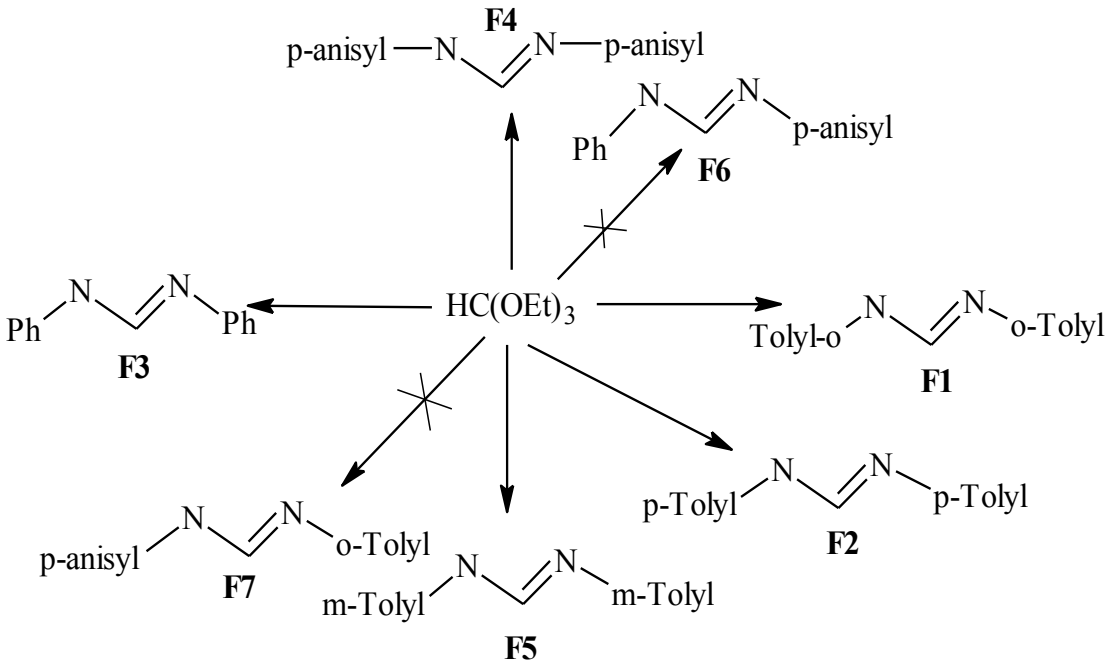

Scheme 3.1: Synthetic routes to different *N,N′*-diarylformamidine [3]

Table 3.1: Summary of physical parameters of synthesized *N,N′*-diarylformamidines

Compound	W. m. (g)	Yield (%)	M. p. (°C)	Colour	Reaction time (hrs.)
F1	6.0304	89	159-160	Light brown	3
F2	5.5012	81	137-148	Pale yellow	12
F3	4.3821	74	89-90	Yellow	12
F4	4,0120	52	130-131	Colorless	4
F5	5.3041	79	149-150	Brown	3
F6	---	---	---	Brown oil	72
F7	---	---	---	Brown oil	72

Most of the synthesized compounds gave reasonable yields except **F6** and **F7** which could not be precipitated after the reaction was left stirring for 3 days. Sample **F6** and **F7** were further kept at low temperatures and rotary evaporator was used to reduce the solvent in attempt to enhance the precipitation of the samples but these method did not yield the desired results The moderate percentage yields obtained for **F4** (52%) can be attributed to the loss of some of the product through the recrystallization process which was done in order to purify the compounds. Good percentage yields for **F1** (89%), **F2** (81%), **F3** (74%**)** and **F5** (79%) were obtained by dissolving the crude products in hexane to remove the impurities but in the case of **F4** impurities were not soluble in hexane so instead the crude products were dissolved in acetone and recrystallized at room temperature to give analytical pure compound.

3.2.1 Infrared analysis of *N,N′*-diarylformamidines

Infrared spectroscopy was used for two major purposes; (i) to confirm the presence of the anticipated functional groups in the products, and (ii) to check the presence of any impurities in our synthesized compounds. Previous studies have shown that the vibration bands expected for the *N,N′*-diarylformamidines are the secondary amine υ(N-H), υ(C=N), aromatic υ(C-H), aliphatic υ(C-H), υ(C=C) and υ(C-N). The vibration bands of υ(C=N) and υ(C=C) of the aromatic usually appear in the same region of the spectrum and this makes specific assignments of respective bands extremely difficult [4-6].

Table 3.2: Some selected vibrational frequency of *N,N′*-diarylformamidines

Compounds	υ(N-H) cm^{-1}	υ(C-H)$_{Aliph}$ cm^{-1}	υ(C=N) cm^{-1}	υ(*sub*-CH_3) cm^{-1}	υ(O-C) cm^{-1}
F1	3415	2871	1664	759	----
F2	3413	2920	1614	803	----
F3	3014	-------	1620	----	----
F4	3402	2890	1620	800	1027
F5	3405	2924	1610	770	----

The infrared spectra of **F1**, **F2** and **F5** (appendices A1.1, A 1.2, A1.5) showed two strong prominent absorption bands at 3415.34 and 1664 cm^{-1} for **F1**, 3413 and 1614 cm^{-1} for **F2** and 3405 and 1610 cm^{-1} for **F5**, respectively. These stretching vibration bands were due to the secondary amine υ(N-H) and the vibration mode of the υ(C=N) bond in the structure of the compounds [5]. The symmetrical stretching vibration band of the aliphatic υ(C-H) bond of the methyl group for **F1**, **F2** and **F5** appeared as medium absorption band at wavenumbers 2871.38, 2920.71 and 2924 cm^{-1}, respectively [4]. The difference in wavenumbers was also attributed to the difference in the position of the substituted methyl (-CH_3) groups on the phenyl ring. Although these three spectra might appeared to have the same number of absorption bands, what differentiated them was the wavenumbers for *ortho*-CH_3, *meta*-CH_3 and *para*-CH_3 for monosubstituted benzene, found in the range of 750-840 cm^{-1}. The vibrational band of methyl substituted on the *ortho* position was expected to have the lowest wavenumbers because it was more steric, while the *para* substituted phenyl would be expected to have the highest

wavenumbers because of easy rotation and its symmetrical in nature [7]. This can clearly be observed in the infrared spectra **F1**, **F2**, **F5** which have in plane vibration frequency of *o*-CH_3, *m*-CH_3, *p*-CH_3 at 759, 770 and 803 cm^{-1}, respectively. The faint vibration bands of aromatic C-H for **F1**, **F2** and **F5** appear at 3015**,** 3029 and 3007 cm^{-1}.

The infrared spectrum of *N,N′-bis*(4-methoxyphenyl)formamidine (**F4)** (appendix A1.4) showed vibration band at υ(1027) cm^{-1} due to the methoxy group (O-CH_3) present in the structure of the compound. The absorption bands at 3402, 3013, 2890 and 1620 cm^{-1} are attributed to υ(N-H), aromatic υ(C-H), aliphatic υ(C-H) and υ(C=N) already discussed above. Compound **F3** was synthesized using un-substituted aniline hence the infrared spectrum of **F3** (appendix A1.3) showed no vibration bands around 2850-3000 cm^{-1} assigned to aliphatic υ(C-H). The stretching vibration bands found are 3014, 3010 and 1620 cm^{-1} assigned υ(N-H), υ(C-H) ,υ(C=N) respectively [6].

3.2.2. NMR spectra results of *N,N′*-diarylformamidines

Table 3.3: NMR results of *N,N′*-diarylformamidines

Compounds	**Multiplicity**	**Chemical shifts** ^{1}H(ppm)	**Chemical shifts** ^{13}C (ppm)
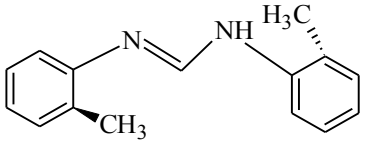	(s, 3H) (s, 3H) (m, 8H) (s, 1H) (s, 1H)	2.20 2.34 7.04-7.29 7.83 8.08	17.90, 30.93, 117.57, 123.40, 126.97, 130.70, 147.63.

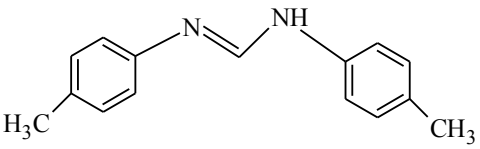	(s, 6H) (m, 8H) (s, 1H) (s, 1H)	2.39 6.99-7.17 7.29 8.25	20.83, 119.16, 129.95, 132.69, 150.02
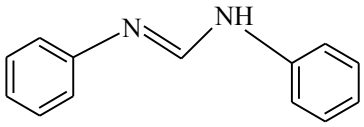	(m, 8H) (s, 1H) (s, 1H)	7.07-7.35 7.58 8.26	119.10, 123.39, 129.43,149.43
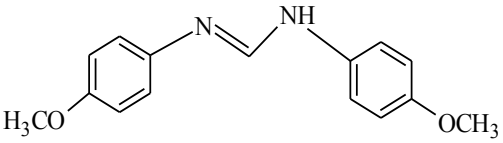	(s, 3H) (m, 8H) (s, 1H) (s, 1H)	3.78 6.84-8.28 8.54 8.75	55.47, 55.56, 114.19, 114.89, 121.47, 121.92, 129.75, 130.16, 156.66, 159.40,163.44
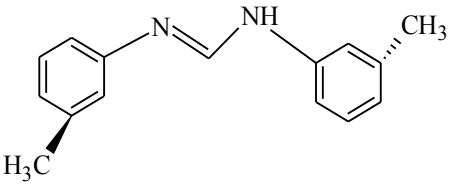	(s, 3H) (s, 3H) (m, 8H) (s, 1H) (s, 1H)	2.19 2,34 7.03-7.29 8.08 8.14	17.91, 30.93, 117.55, 123.40, 126.96, 130.69 147.60.

The ^{1}H and ^{13}C-NMR spectra results obtained were used to confirm the hydrogen and carbon framework of the synthesized compounds. The NMR results of *N,N′*-diarylformamidines are not well documented in the literature due to the possibility of isomerism, as a result not much literature has been published regarding the use of *N,N′*-diarylformamidines as the precursors for synthesis of *N,N′*-diarylimidazolinium chlorides [3]. The NMR spectra for *N,N′*-diarylformamidines were obtained using deuterated chloroform ($CDCl_3$) and dimethylsulfoxide (DMSO) and the chemical shifts and the multiplicity are presented in Table 3.3.

3.2.2.1 NMR analysis of *N,N′-bis*(2-methylphenyl)formamidine (F1)

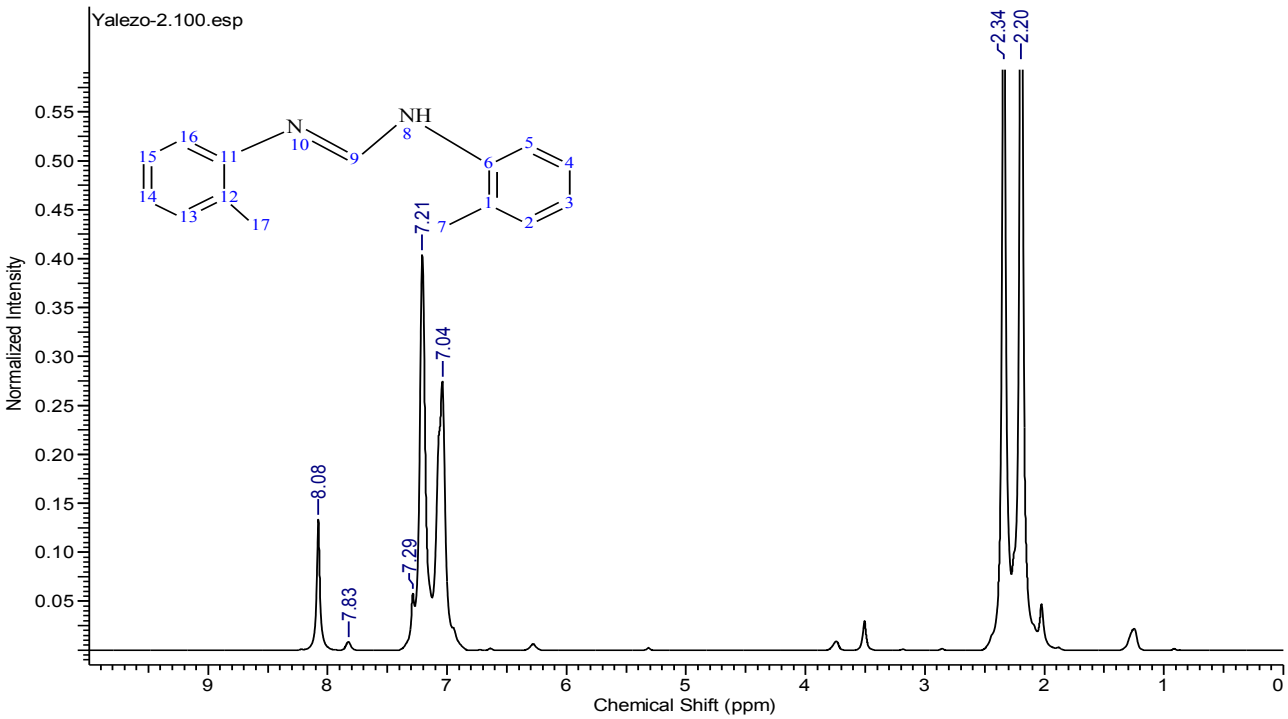

Figure 3.1: ^{1}H-NMR spectrum of **F1**

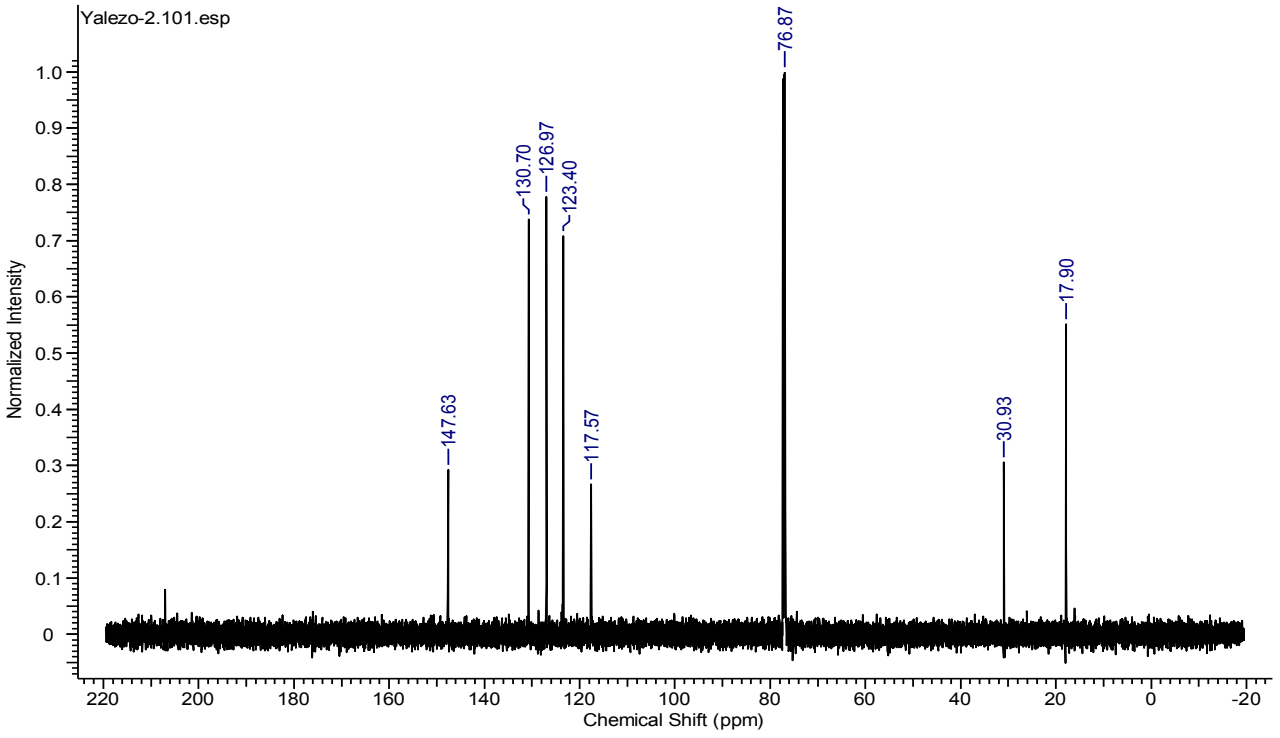

Figure 3.2: ^{13}C-NMR spectrum of **F1**

The ^{1}H-NMR spectrum of *N,N′-bis*(2-methylphenyl)formamidine (Figure 3.1) showed two singlets peaks of the methyl hydrogens (-Ar-CH_3) linked protons attached to the benzene ring at 2.20 ppm and 2.34 ppm. The two peaks appeared up-field because their proton nuclei are shielded [3]. Previous studies have reported that there are two possible geometric isomers for **F1**, the *sync*-isomer and *anti*-isomer, but the *anti*-isomer is reported to be the most stable of the two because it is less crowded [8]. The protons on the phenyl ring (Ar-H) appeared as multiplets at 7.04-7.29 ppm. The two singlets down field at 7.83 and 8.08 ppm are due to hydrogen atom on CH and NH bond.

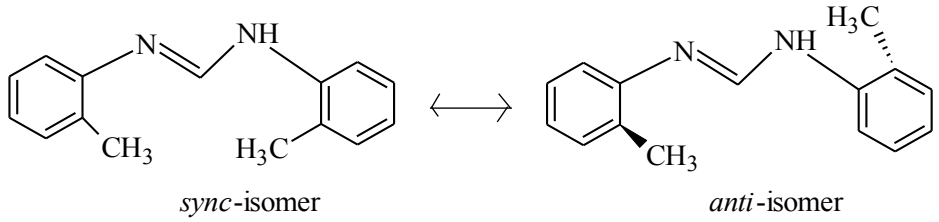

Figure 3.3: The structures of sync and *anti*- isomers [10]

The ^{13}C-NMR spectrum of **F1** (Figure 3.2) showed two (CH_3) singlets at 30.93 and 17.90 ppm of two carbon atoms on methyl group in different environments. The carbons of the benzene ring appeared as singlets at 117.57, 123.40, 126.9 and 130.70 ppm. The carbon bonded to two electron withdrawing nitrogen showed a deshielded nucleus which appeared as a singlet at 147.63 ppm down field.

3.2.2.2 NMR analysis of *N,N′-bis*(4-methylphenyl)formamidine (F2)

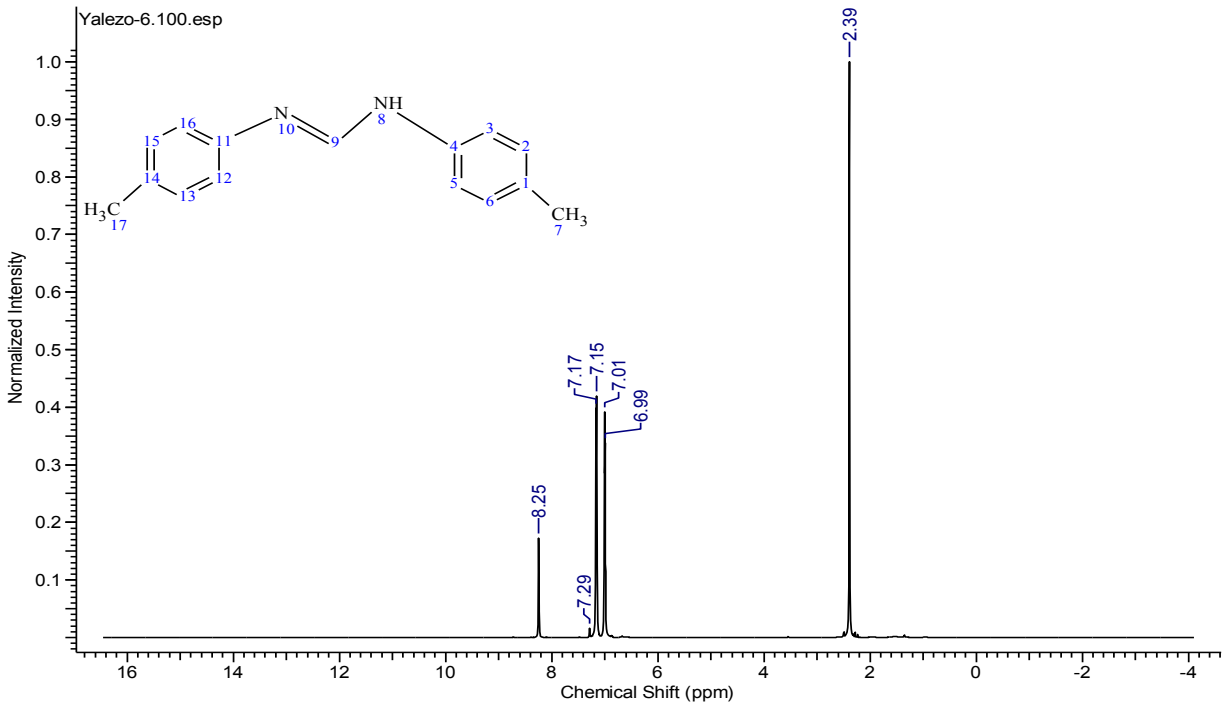

Figure 3.4: ^{1}H-NMR spectrum of **F2**

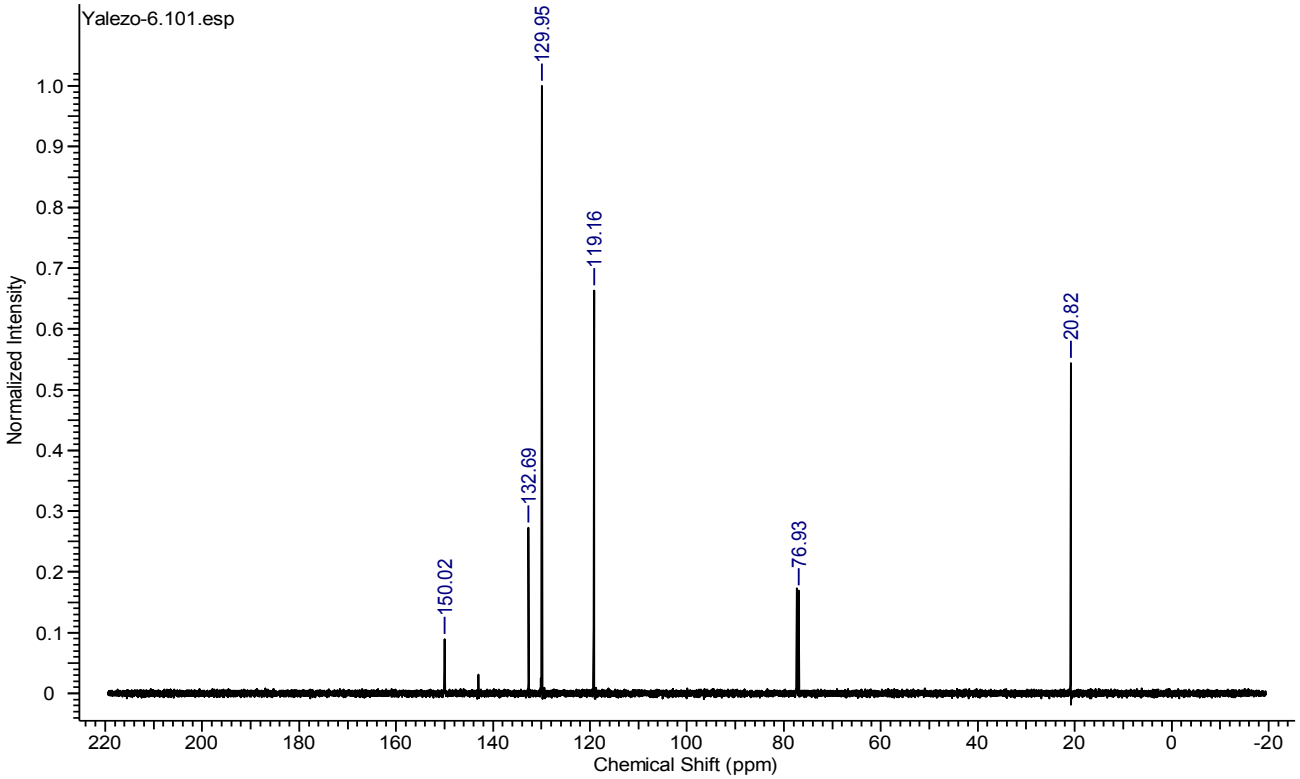

Figure 3.5: ^{13}C-NMR spectrum of **F2**

The ^{1}H-NMR spectrum of **F2** (Figure 3.4), showed one singlet peak at 2.39 ppm due to the protons linked to the (Ar-CH_3) bonded on the *para* position. The phenyl linked protons appeared as multiplets at 6.99 -7.29 ppm, and a singlet peaks at 8.21 ppm and 8.26 ppm were due to the CH and NH respectively. The ^{13}C-NMR of **F2** (Figure 3.5) showed one singlet that corresponded to the carbon in methyl group (Ar-CH_3) of both substituted benzene ring in the same chemical environment at 20.82 ppm. The signals at 119.16, 129.95, 132.69 ppm were due to the different chemical environments of carbon in the phenyl ring. The carbon bonded to two electron withdrawing nitrogen showed a deshielded nucleus which appeared as a singlet at 150.02 ppm downfield.

3.2.2.3 NMR analysis of *N,N′-di*phenylformamidine (F3)

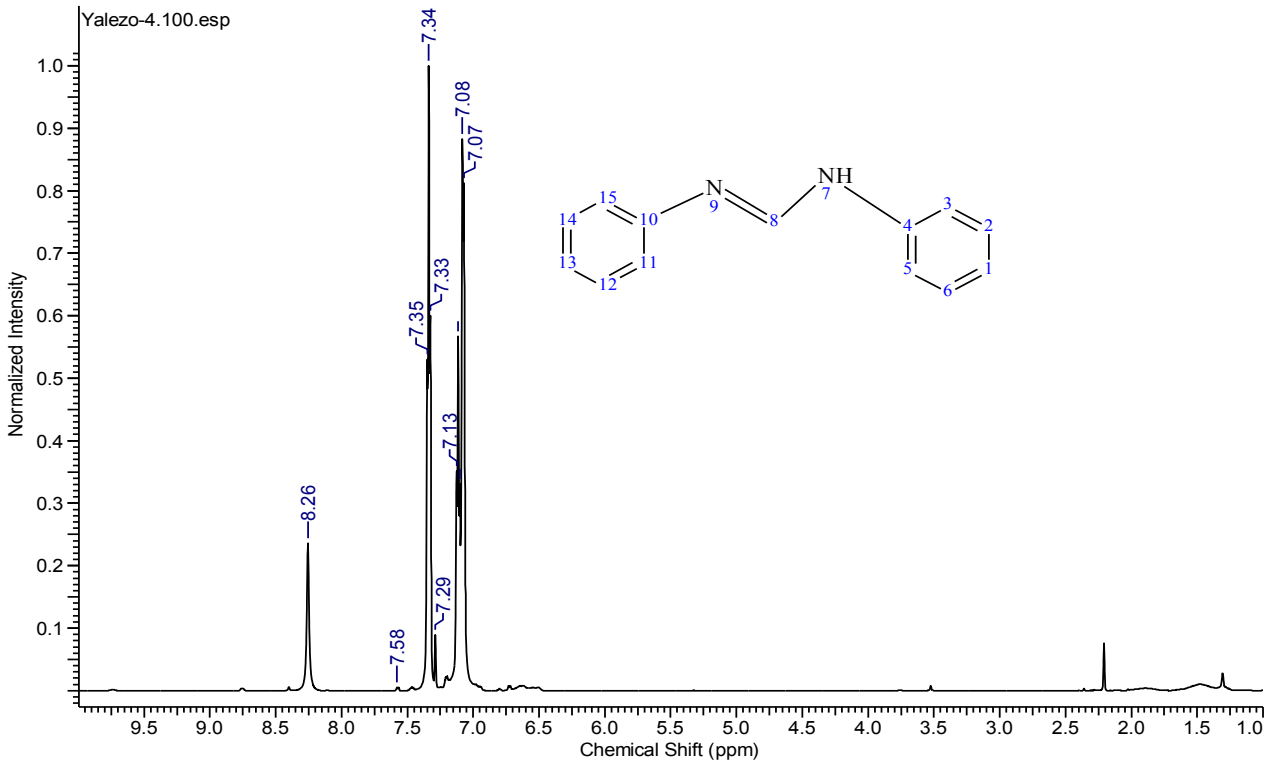

Figure 3.6: ^{1}H-NMR spectrum of **F3**

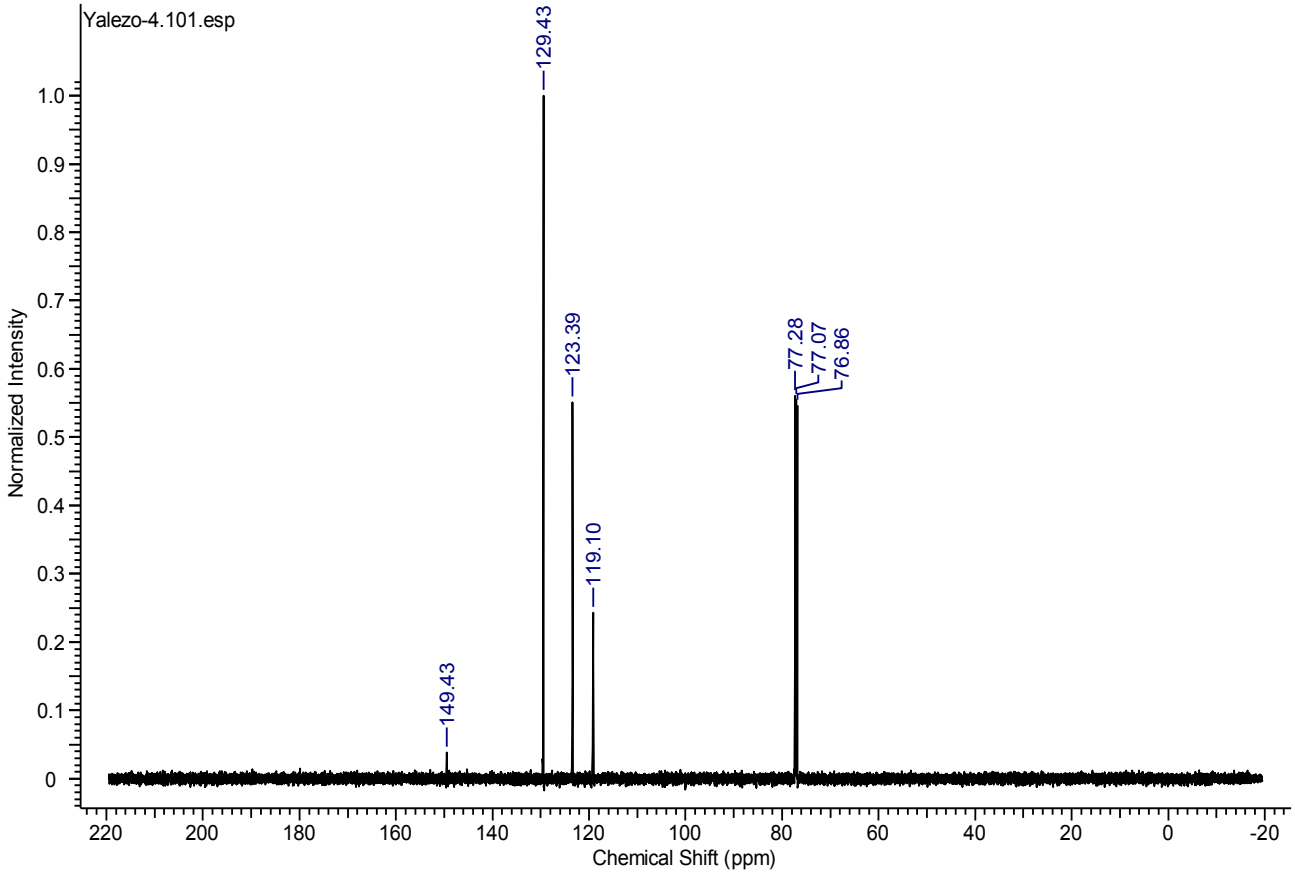

Figure 3.7: ^{13}C-NMR spectrum of **F3**

The ^{1}H-NMR spectrum of **F3** (Figure 3.6) gave no peaks up-field and this was in accordance with the structure of the compound as there are no substituents on the phenyl ring. The multiplets peaks at 7.07-7.35 ppm were due to splitting of the hydrogen linked to the phenyl ring. The signals at 7.58 and 8.26 ppm were due to CH and NH, respectively. These singlets appeared downfield because their nuclei are less shielded due the presence of the NC=N moiety. The ^{13}C-NMR spectrum of **F3** (Figure 3.7) showed no peaks downfield which is in agreement with the compound structure. The peaks at 119, 122, 129 ppm corresponded to the carbon on the phenyl ring and the peak that appeared downfield at 149 ppm is due to carbon atom of NC=C.

3.2.2.4 NMR analysis of *N,N′-bis*(4-methoxyphenyl)formamidine (F4)

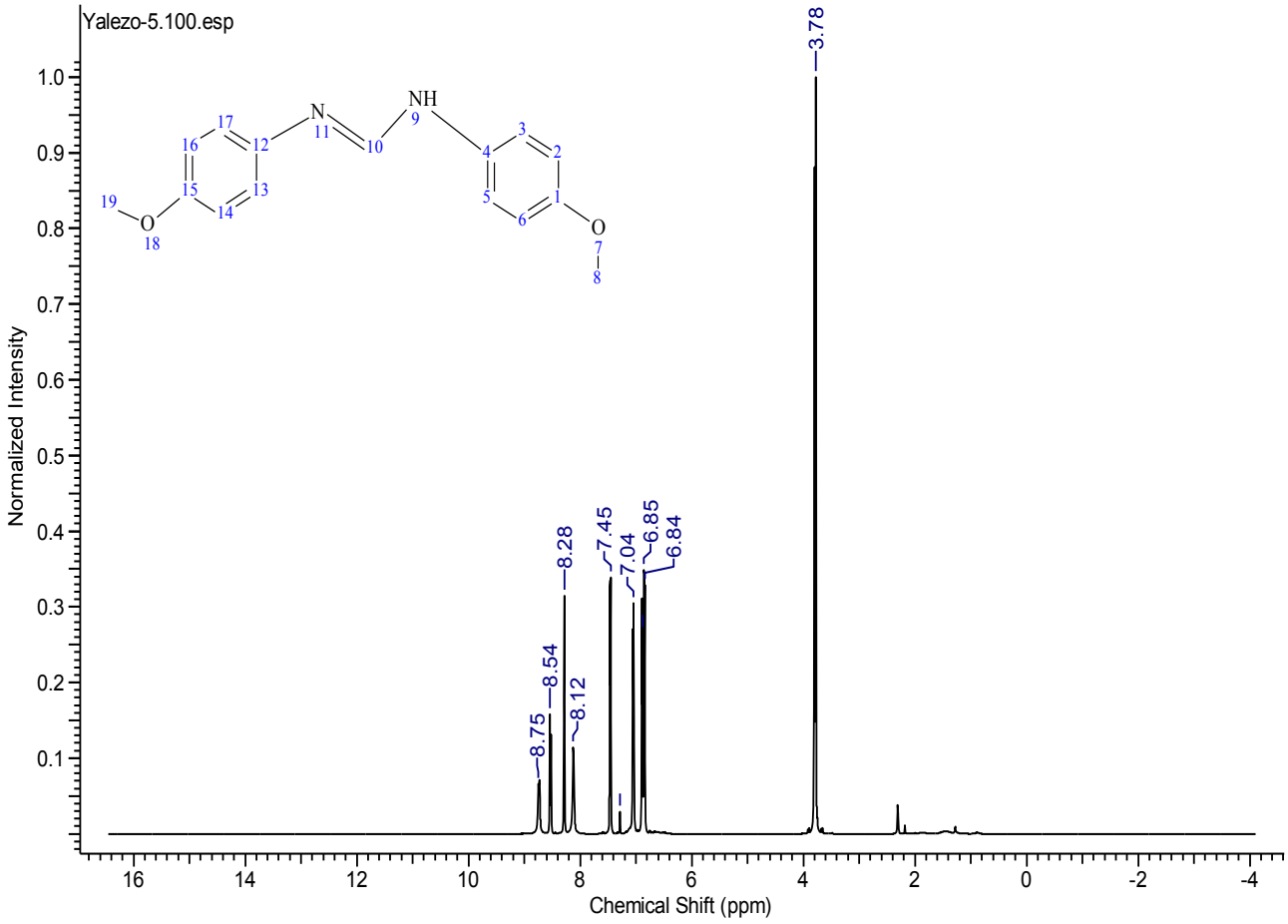

Figure 3.8: ^{1}H-NMR spectrum of **F4**

The ^{1}H-NMR spectrum of **F4** (Figure 3.8) showed one singlet peak caused by the nuclei of the CH_3 at 3.78 ppm assigned to hydrogen atoms of (O-CH_3). All the peaks in Figures 3.8 and 3.9 appear slightly downfield due to deshielding from the presence of the high electron affinity of the oxygen atom bonded to carbon that tend to pull electron density more close to itself as compared to the carbon, hence less shielding from the nucleus. Also the multiplets peaks at 6.84

- 8.28 ppm were due to the hydrogen atom on phenyl ring .and the peak at 8.54, 8.75 ppm were due to CH and NH hydrogen atoms, respectively.

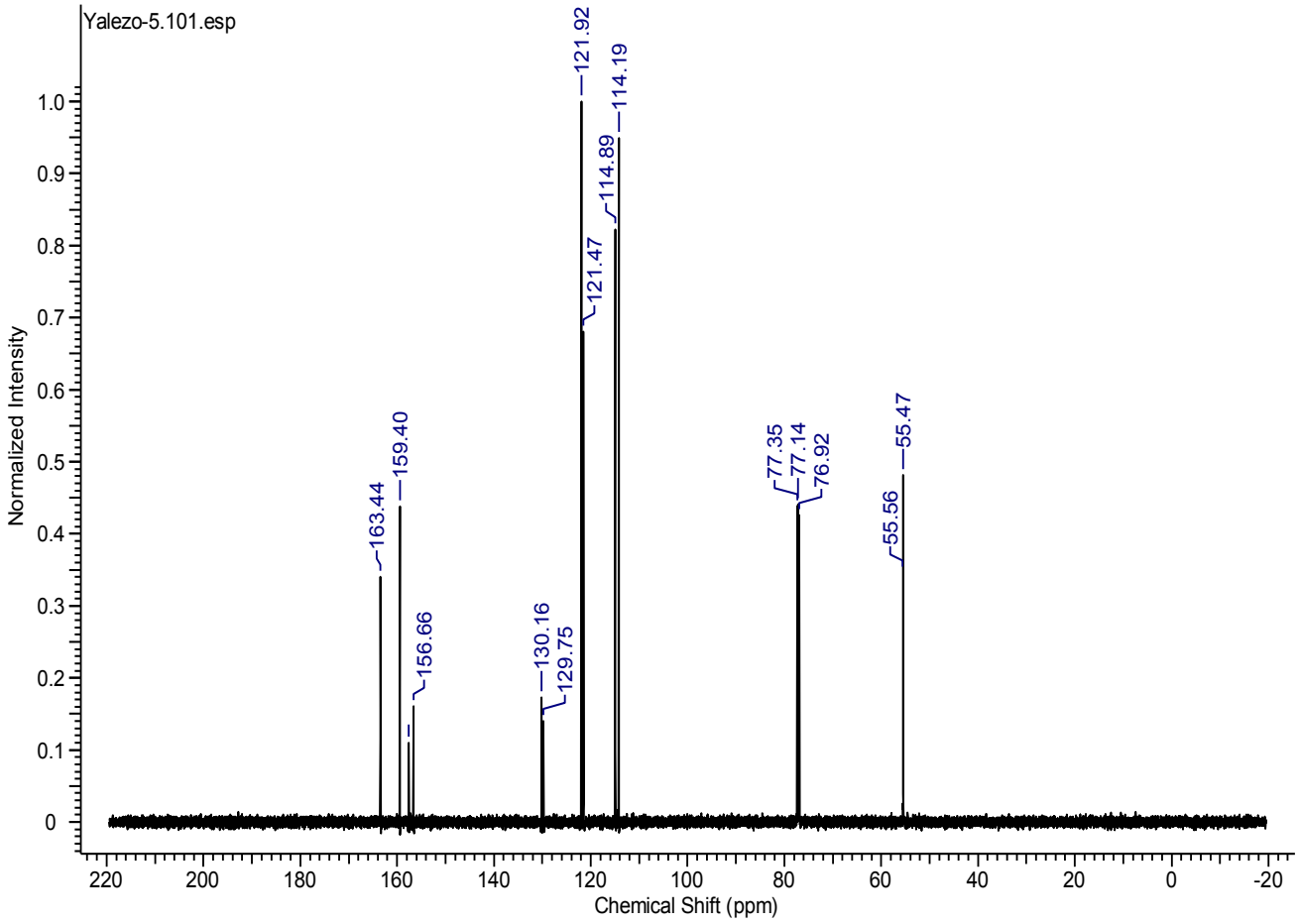

Figure 3.9: ^{13}C-NMR spectrum of **F4**

The ^{13}C-NMR spectrum of **F4 (**Figure 3.9) showed a similar deshielding of the protons atom as can be noticed from the NMR spectrum of **F4**. The peak of the methyl group appeared at 58 ppm and the peak from 114.19-159.40 ppm are due to the splitting of carbon due to the different environments on the phenyl ring. The carbon bonded to two electron withdrawing nitrogen showed a deshielded nucleus which appeared as a singlet at 163.44 ppm downfield.

3.2.2.5 NMR analysis of *N,N´-bis*(3-methylphenyl)formamidine (F5)

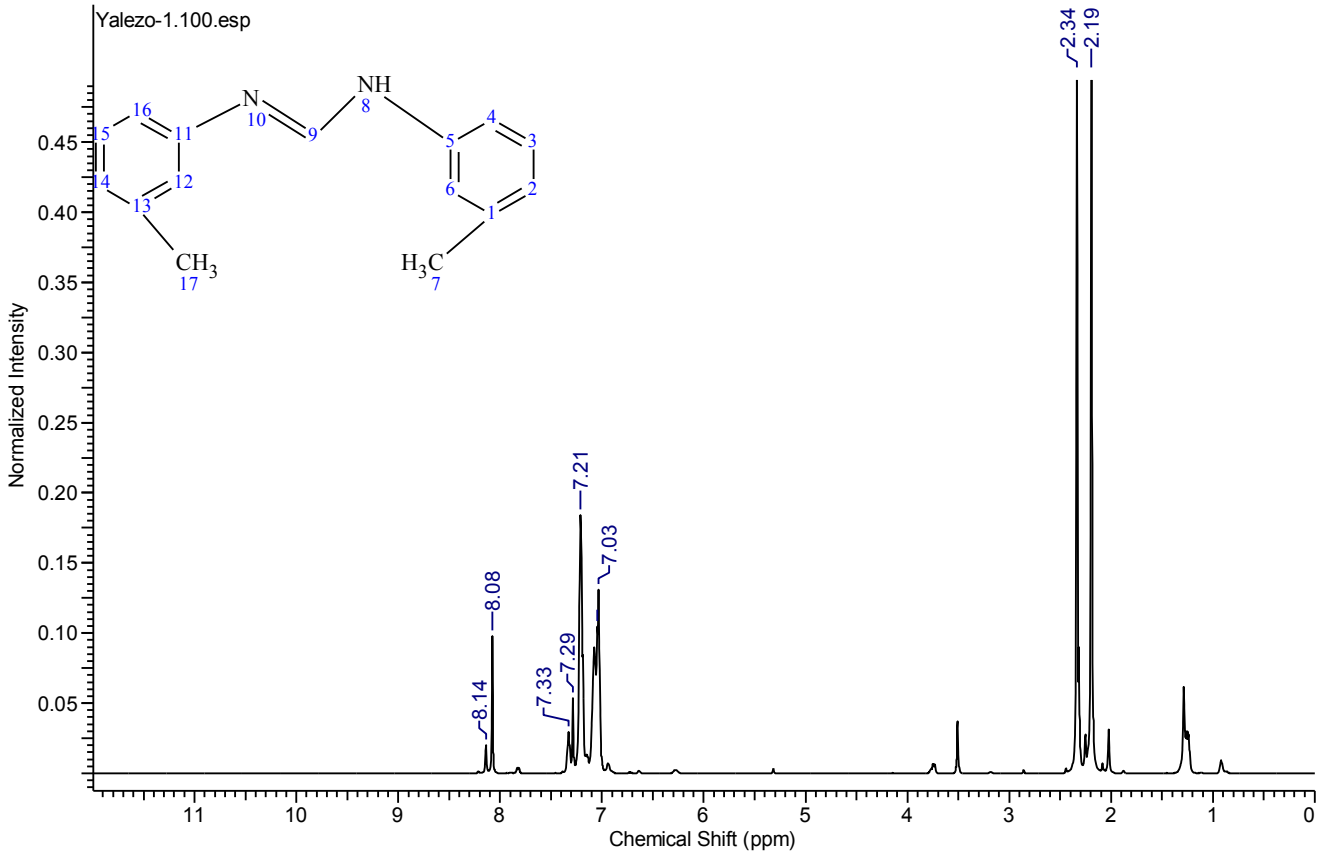

Figure 3.10: ^{1}H-NMR spectrum of **F5**

The ^{1}H-NMR spectrum of **F5** (Figure 3.10) showed two singlets peaks at 2.19 ppm and 2.34 ppm assigned to the methyl hydrogen atoms (-CH_3) and the multiplets peaks at 7.03- 7.33 ppm were assigned to the hydrogen atoms on the phenyl ring and the peaks at 8.08 and 8.14 ppm were due to the hydrogen atoms of CH and NH, respectively. The ^{13}C-NMR spectrum of **F5** (Figure 3.11) showed two singlets peaks at 17.91 and 30.93 ppm assigned to the methyl carbon (-CH_3) and the peaks at 117.55- 132.69 ppm were due to different environment of carbons on the phenyl ring . The carbon bonded to two electron withdrawing nitrogen showed a deshielded nucleus which

appeared as a singlet at 147.60 ppm downfield. The same geometric isomers exist for **F5** as explained in the discussion of **F1** [8].

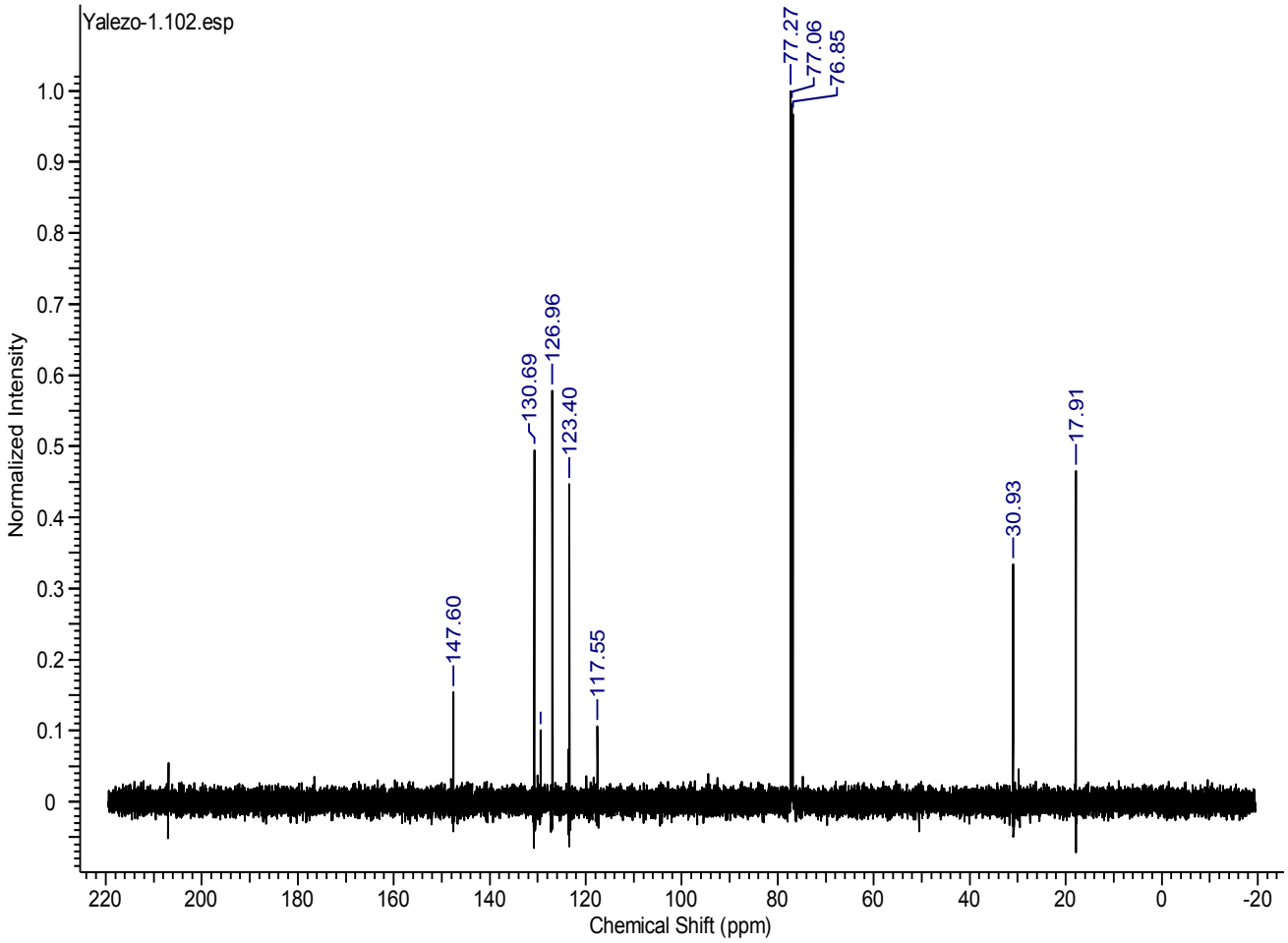

Figure 3.11: ^{13}C-NMR spectrum of **F5**

3.3. Synthesis and characterization of *N,N′*-diarylimidazolinium chlorides

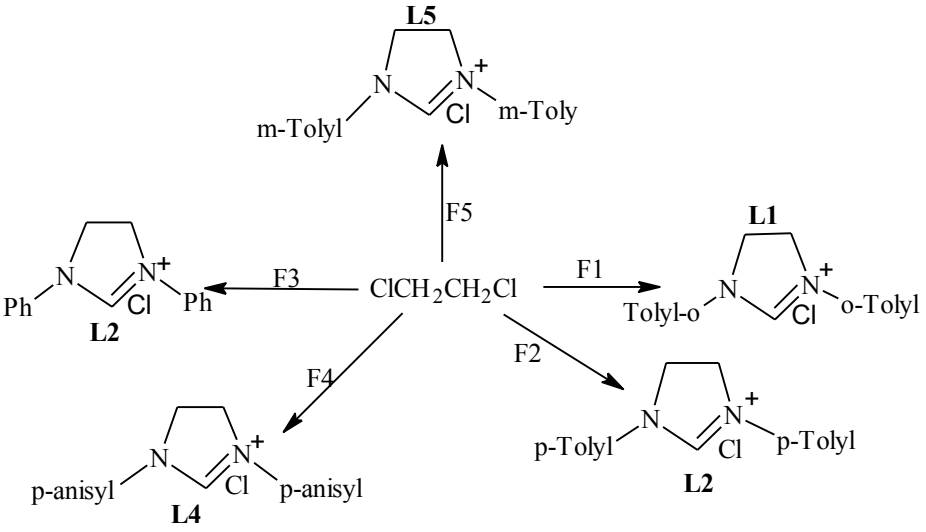

Scheme 3.2: Synthetic route to different *N,N′*-diarylimidazolinium chlorides [3]

The different symmetric *N,N′*-diarylimidazolinium chlorides were synthesized with the reaction of *N,N′*-diarylformamidines with 1,2-dichloroethane as electrophiles using the base *N,N*-diisopropylethylamine at about 100 ^{o}C, as detailed in chapter 2 [3]. The 1, 2-dichloroethane had dual function in which it was used as a solvent and as electrophile. The reaction took long hours and this can be explained by the small size of the chloride atom which requires harsh conditions in order to get substituted. Scheme 3.3 shows the different synthetic routes that were followed to obtain the different *N,N′*-diarylimidazolinium chlorides [9]. Most of the synthesized compounds gave moderate yield and in total, five *N,N′*-diarylimidazolium chlorides were synthesized and characterized using the NMR, FTIR and M. p. determination. The reaction hours varied from 16-48 hours depending on the nature of the substituent on the phenyl ring.

Table 3.4: Summary of physical properties of synthesized *N,N′*-diarylimidazolinium chlorides

Compound	Mass (g)	Yield (%)	M. p. (°C)	Colour	Reaction time (hrs)
L1	1.989	52	> 250	White	20
L2	2.0432	53	> 250	Yellow	16
L3	1.621	62	> 250	Yellow	24
L4	0.963	78	> 250	Brown	20
L5	2.1476	67	> 250	Brown	20

3.3.1 NMR spectra results of *N,N′*-diarylimidazolinium chlorides

The ^{1}H-NMR results obtained for *N,N′*-diarylimidazolinium chlorides were used to confirm the structure of synthesized *N,N′*-diarylimidazolinium chlorides from their corresponding formamidines. The major peak of interest in the NMR spectra of *N,N′*-diarylimidazolinium chlorides are the peaks due to (-CH_2CH_2) which are not present in the NMR spectra of *N,N′*-diarylformamidines [10, 11]. The NMR spectra of the *N,N′*-diarylimidazolinium chlorides are difficult to analyze because of the possible resonance structure.

Table 3.5: NMR results of *N,N′*-diarylimidazolinium chlorides

Compounds	Multiplicity	Chemical shifts ^{1}H(ppm)	Chemical shifts ^{13}C (ppm)
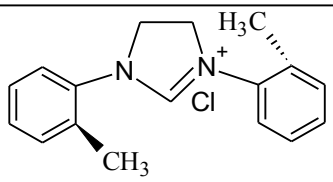	(s, 3H) (s, 3H) (d, 2H) (d, 2H) (m, 8H) (s, 1H)	2.14 2.52 4.62 4.67 7.23-7.93 8.85	18.10, 30.83, 40.95, 52.89,126,58. 127.64, 129.87, 131.65,134.84, 157.88
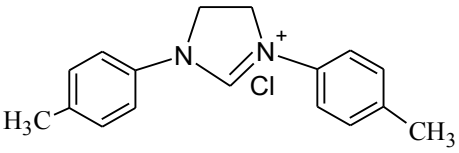	(s, 3H) (s, 3H) (s, 4H) (m, 8H) (s, 1H)	2.09 2.35 4.96 7.28-7.58 10.03	20.92, 31.17, 48.77, 118.79, 130.48, 134.27, 136.93, 151.59.
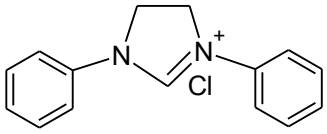	(s, 4H) (m, 8H) (s, 1H)	4.61 7.12-7.72 10.19	48.77, 188.98, 127.46.19, 130.13, 136.61, 154.30
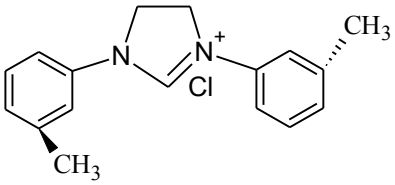	(br, 3H) (br, 3H) (d, 2H) (d, 2H) (m, 8H) (br, 1H)	2.14 2.52 4.62 4.67 7.27-7.79 8.95	

3.3.1.1 NMR analysis of *N,N′-bis*(2-methylphenyl)imidazolinium chloride (L1)

The ^{1}H-NMR spectrum of **L1** (Figure 3.12) showed two singlet peaks that corresponded to the introduction of ethyl (-CH_2CH_2-) group at 4.67 ppm and 4.62 ppm chemical shifts confirming the formation of the *N,N′*-diarylimidazolinium chlorides. The two singlets at 2.14 ppm and 2.52 ppm were due to CH_3 hydrogen linked atoms.

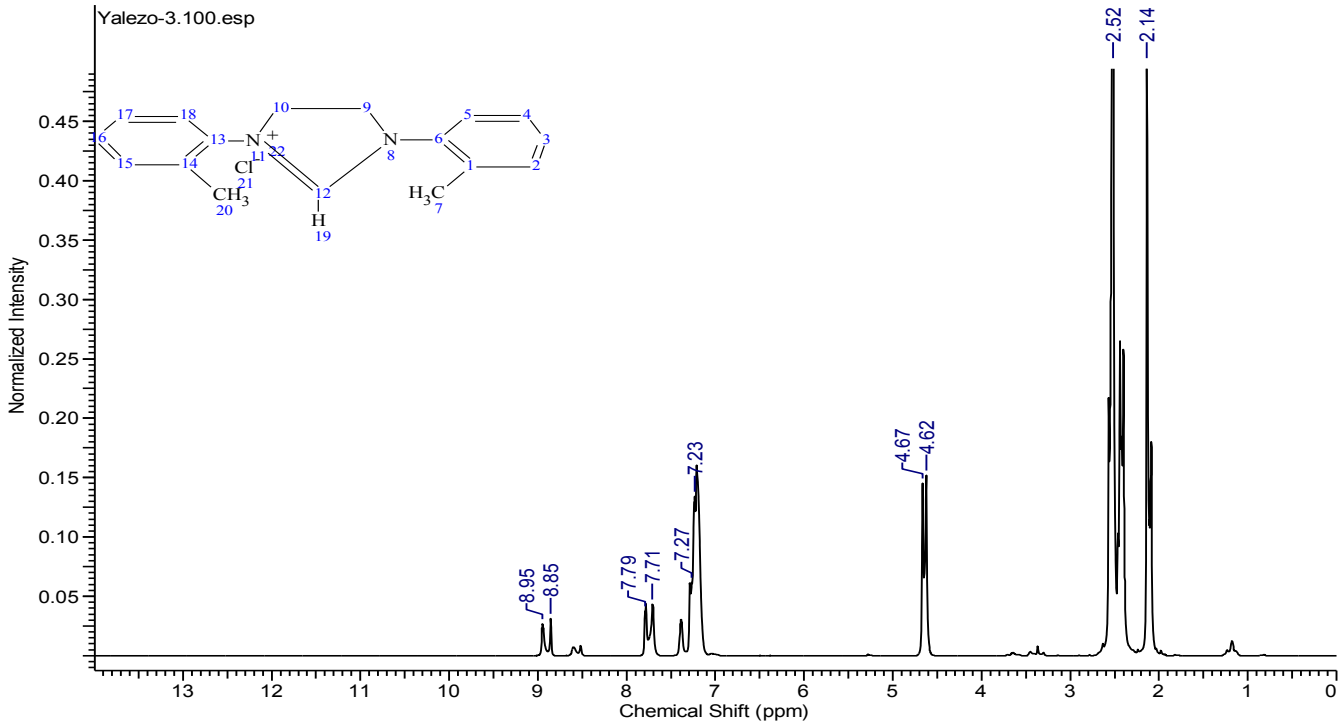

Figure 3.12: ^{1}H-NMR spectrum of **L1**

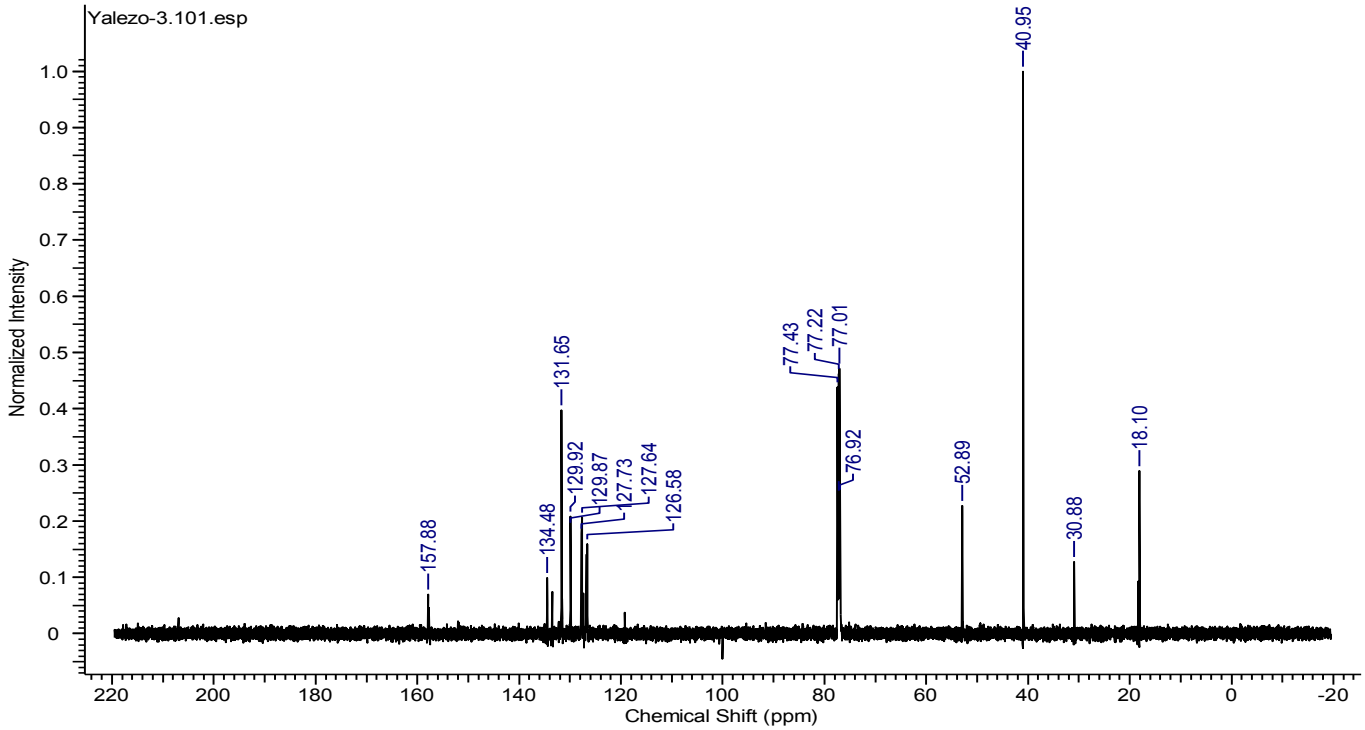

Figure 3.13: ^{13}C-NMR spectrum of **L1**

The introduction of the ethyl group (C_2H_4) caused a shifting to the peaks originally observed in the NMR spectrum of **F1**. The same shift was observed in the ^{13}C-NMR spectrum of the **L1** (Figure 3.13). The signals at 18.10 and 30.88 ppm corresponded to the carbon of the methyl group (CH_3) at different chemical environment. The singlet peaks at 40.95 ppm and 52. 89 ppm was due to the carbon atoms on the backbone of the synthesized *N,N′*-diarylimidazolinium chloride. The rest of the peaks have already been assigned in **F1.**

3.3.1.2 NMR analysis of *N,N′-bis*(4-methylphenyl)imidazolinium chloride (L2)

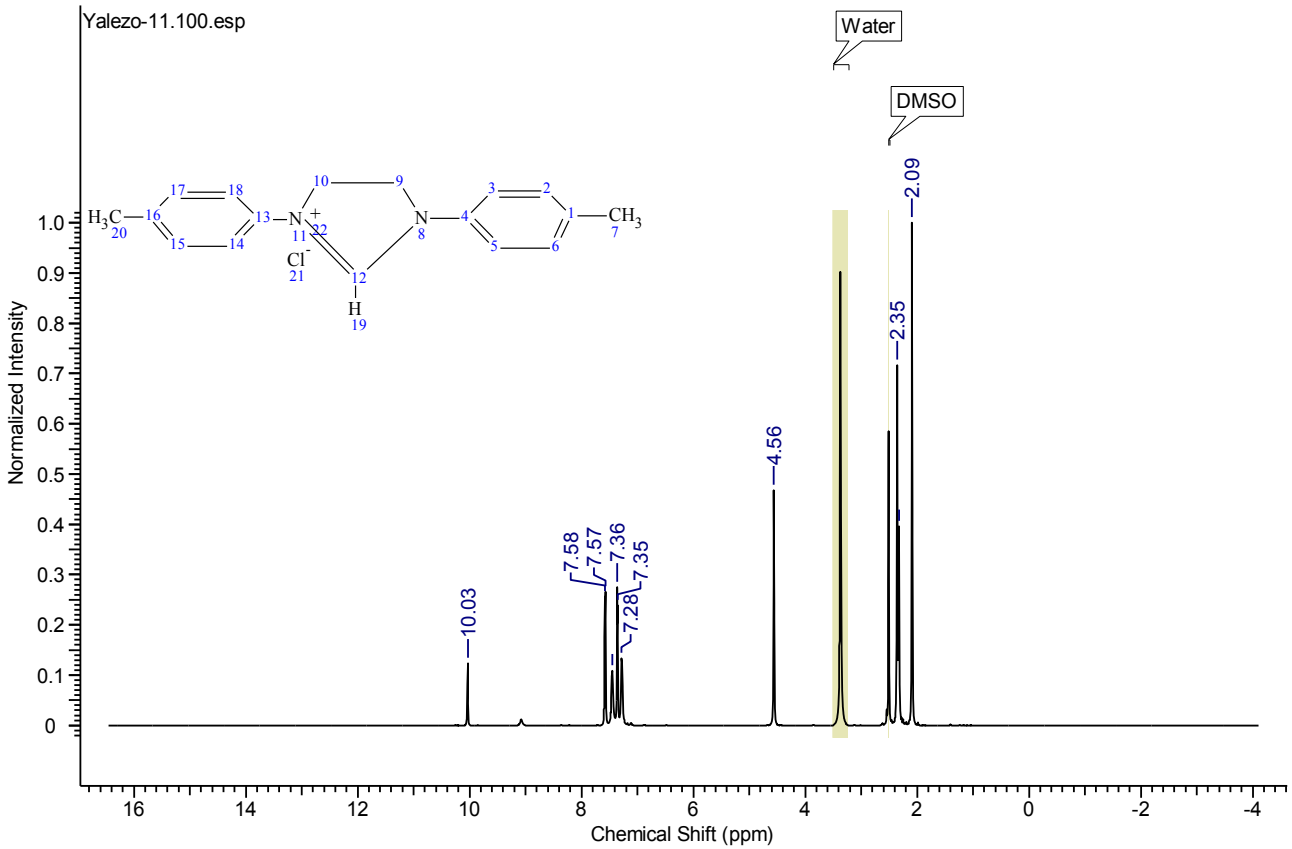

Figure 3.14: ^{1}H-NMR spectrum of **L2**

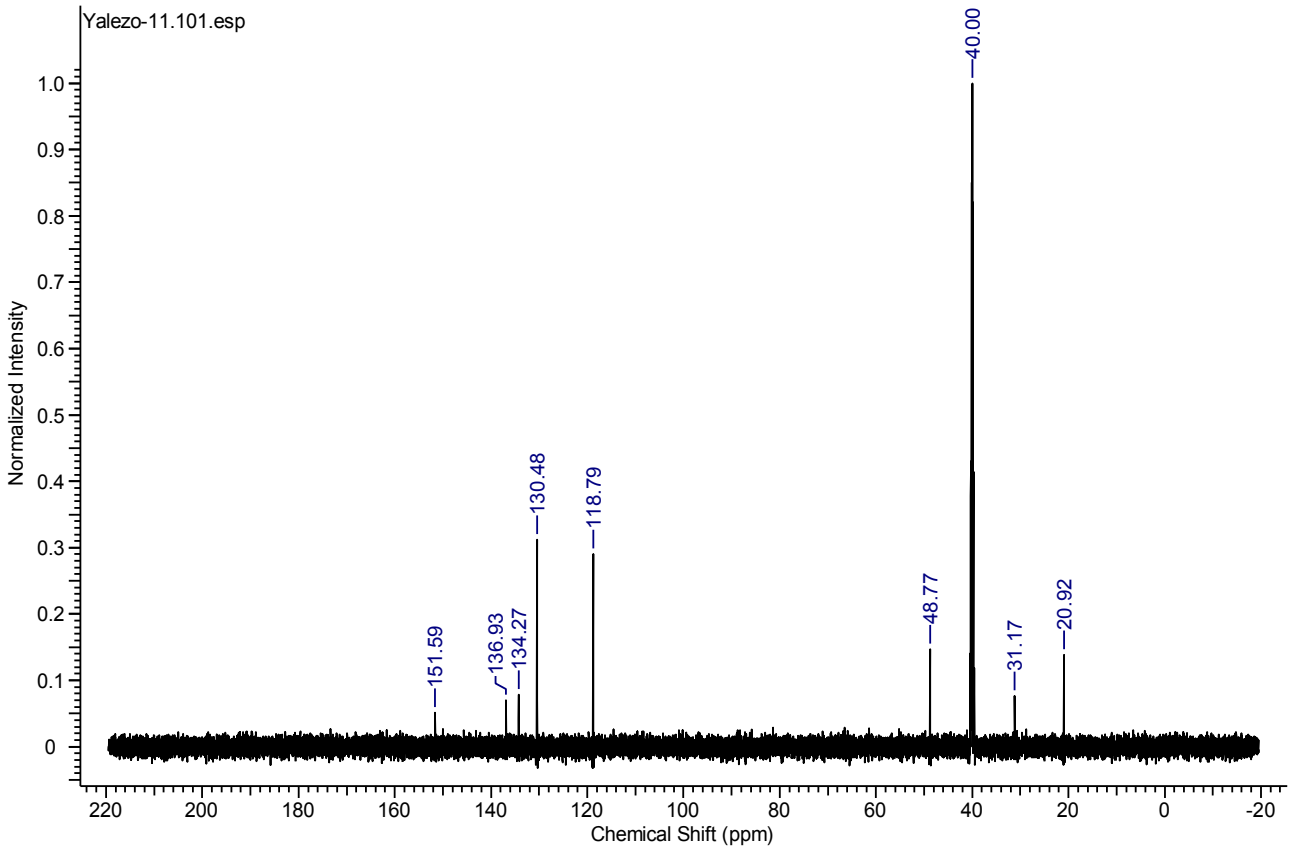

Figure 3.15: ^{13}C-NMR spectrum of **L2**

Compound **L2** was not soluble in chloroform ($CHCl_3$) so instead the ^{1}H and ^{13}C-NMR were ran using (DMSO). The ^{1}H-NMR of **L2** (Figure 3.14) showed a singlet peak at 2.35 ppm referenced as DMSO and highlighted peak between 2.5-2.8 ppm was due to the presence of water. The presence of water might be due to heating of frozen DMSO before it was used. As already discussed with **LI**, the most interested peaks that differentiate **L2** with **F2** were the appearance of the peak at 4.56 ppm due to the non-split methylene of the backbone. Furthermore, the ^{13}C-NMR of **L2** (Figure 3.15) showed a singlet peak of the two equivalent carbon atoms of the introduced ethyl group at 48.77 ppm on the backbone of the *N,N′*-diaryimidazolinium chlorides.

3.3.1.3 NMR analysis of *N,N′-bis*(phenyl)imidazolinium chloride (L3)

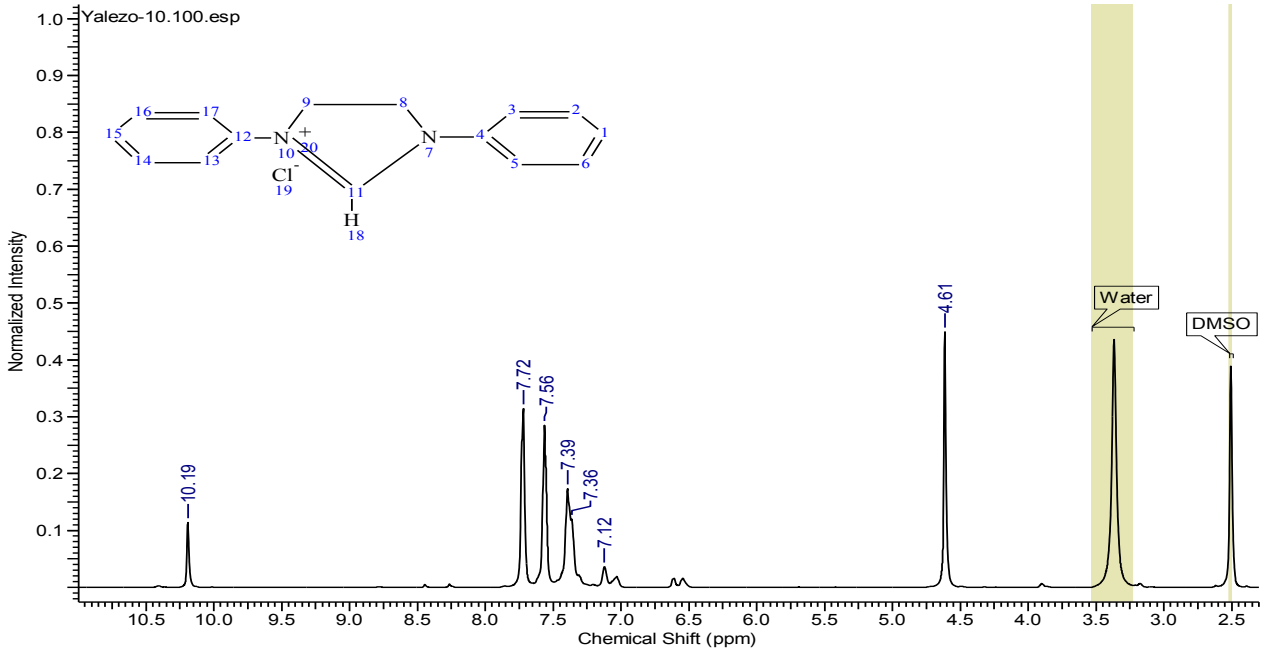

Figure 3.16: ^{1}H-NMR spectrum of **L3**

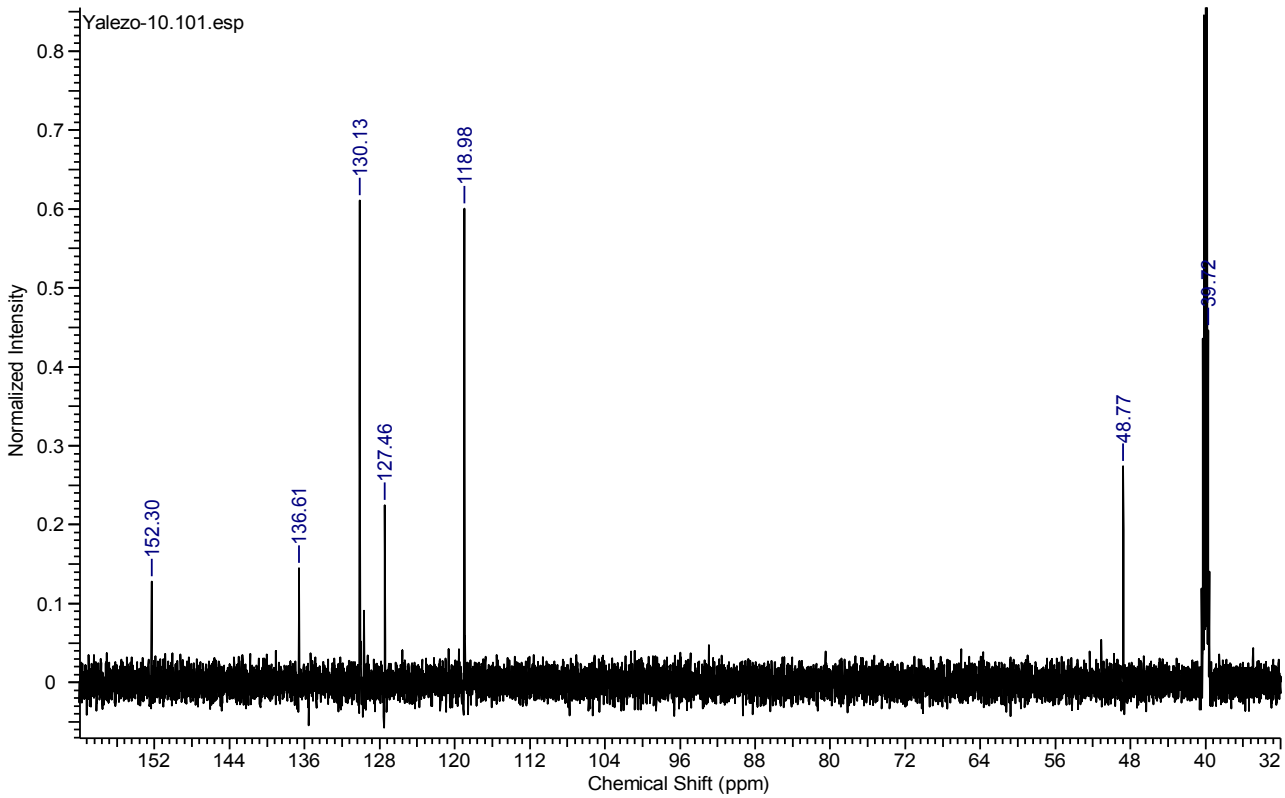

Figure 3.17: ^{13}C-NMR spectrum of **L3**

Similarly to **L2**, the ^{1}H and ^{13}C-NMR spectra of **L3** were obtained using DMSO. In Figure 3.16, the peaks at 2.50 ppm and 3.5-3.8 ppm corresponded to the reference peaks from the DMSO and the presence of water. The singlet peak at 4.61 ppm differentiates the structure of **F3** and **L3**. This peak is assigned to the introduction of the four non spit hydrogens from the ethyl group (-CH_2CH_2). In Figure 3.17, the presence of the singlet at 48.77 ppm further confirmed that the two carbon atoms are equivalent.

3.3.1.4 NMR analysis of N,N´-bis(2-methylphenyl)imidazolinium chloride (L4)

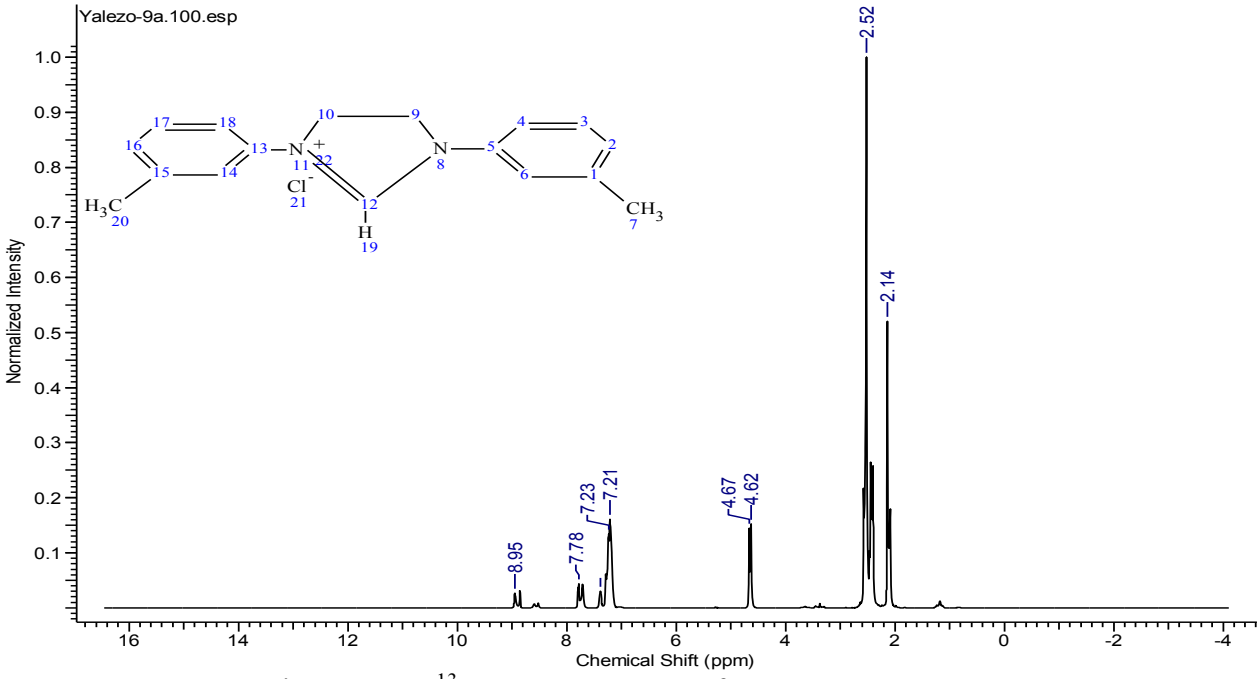

Figure 3.18: ^{13}H-NMR spectrum of L5

The ^{1}H-NMR spectrum of **L5** (Figure 3.18) showed two singlet peaks that corresponded to the introduction of ethyl (-CH_2CH_2-) group at 4.67 ppm and 4.62 ppm chemical shifts confirming the formation of the *N,N´-bis*(3-methylphenyl)imidazolinium chlorides. The proton bonded to carbon on two electron with drawing nitrogen showed a deshielded nucleus which appeared as a singlet at 8.95 ppm downfield.

3.3.2 FT-IR analysis of *N,N′*-diarylimidazolinium chlorides

Table 3.6: Some selected vibrational frequency of *N,N′*-diarylimidazolinium chloride

Compounds	$\upsilon(R_2N^+=C)$ cm^{-1}	$\upsilon(C\text{-}H)_{Aliph}$ cm^{-1}	$\upsilon(C=N)$ cm^{-1}	$\upsilon(C=C)$ cm^{-1}	$\upsilon(o\text{-}CH3)$ cm^{-1}	$\upsilon(O\text{-}C)$ cm^{-1}
L1	3415	2827	1677		753	----
L2	3415	2924	1689		819	----
L3	3417	-------	1618		----	----
L4	3420	2894	1616		810	1272
L5	3405	2924	1610		778	----

The infrared spectra of *N,N′*-diarylimidazolinium chlorides are well documented in the literature mainly because of the application as precursors to synthesis of free N-heterocyclic carbene ligands and their stability at room temperature [3, 6]. The significant difference between the spectra of the parent *N,N′*-diarylformamidines and *N,N′*-diarylimidazolinium chlorides was the peak at 3300-3500 cm^{-1} which was due to the quaternary amine cation instead of the υ(N-H). The FT-IR spectra of the **L1** and **L2** (appendices B 1.1, B 1.2) showed weak broad vibration band at 3401 cm^{-1} attributed to the presence of the quaternary amine salt formation with chloride ion as the counter ion and the vibration bands at 2881 and 2901 cm^{-1} are due to the aromatic υ(C-H) [12, 13]. The strong band at 1655 cm^{-1} was due to the stretching vibration band of υ(C=N). The decrease in the intensity of this vibrational band can be attributed to the use of electron in nitrogen in bonding with ethyl cation [14].

The infrared spectra of **L3** and **L4** are found in (appendices B 1.3-1.4). The infrared spectrum of **L3** showed only two major vibration bands at 3413 and 1618 cm^{-1} due to $\upsilon(R_2N^+=C)$ and $\upsilon(C=N)$. Table 3.6 showed the summary of the selected vibrational band of *N,N′*-diarylimidazolinium chlorides.

3.4 Synthesis and characterization of Ru(II) complexes with N-heterocyclic carbene ligand

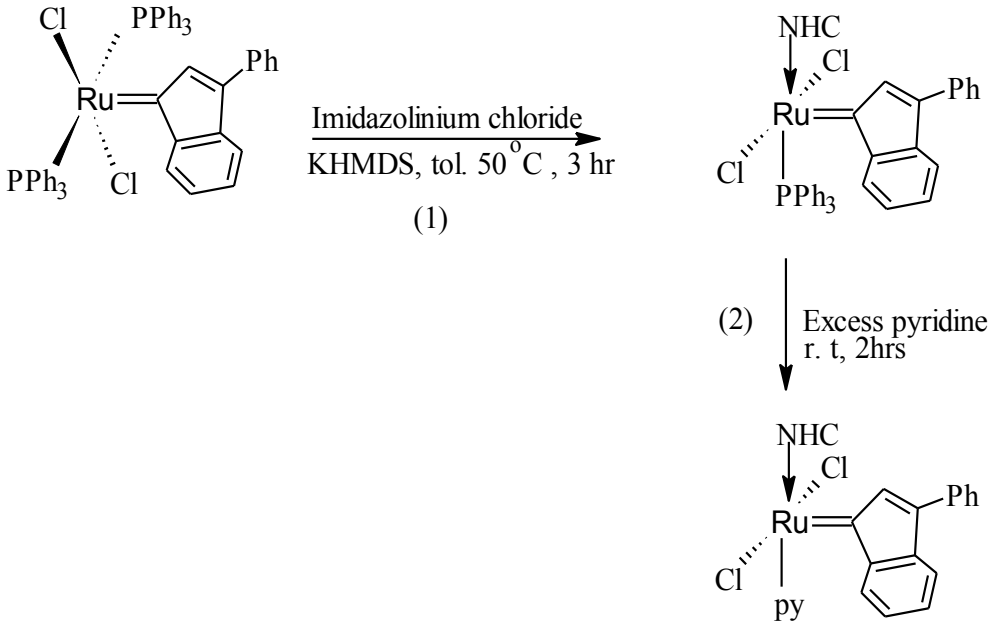

Scheme 3.3: Synthetic route to Ru(II) complexes [15, 16]

The Ru(II) phenyl-3-indenylidene complexes were synthesized through the exchange of triphenylphosphine molecule with the N-heterocyclic carbene ligand generated in-situ. Scheme 3.4 shows the two stage synthetic route that was followed to obtain the two types of ruthenium complexes. The ruthenium(II) complexes with NHC-pyridine were synthesized using the ruthenium(II) with NHC-triphenyelphosphine as starting material. The pent-coordinated geometry is the proposed structure for both type of complexes with N-heterocyclic carbene

ligand bonded either *trans* to triphenylphosphine ligand or to pyridine ligand. The two chlorides are bonded *cis* to each other. The complexes were obtained in good yield through crystallization and precipitation using hexane and pentane as non-polar solvents. Some calculated analytical results and physical parameters of the synthesized complexes are presented in Table 3.7.

Table 3.7: Summary of physical parameters of synthesized Ru(II) complexes

Complexes	Yield (%)	M.F	Colour	M.p (°C)	Anal. Data (%) (Calc.) found C	H	N
$[RuCl_2(Ind)(SIoTol)(PPh_3)]$	89	$C_{50}H_{44}Cl_2N_2PRu$	Brown	298	68.49 (68.01)	5.17 (4.95)	3.19 (2.98)
$[RuCl_2(Ind)(SIpTol)(PPh_3)]$	81	$C_{50}H_{44}Cl_2N_2PRu$	Dark brown	285	68.49 (68.08)	5.17 (5.01)	3.19 (3.00)
$[RuCl_2(Ind)(SIPh)(PPh_3)]$	74	$C_{48}H_{40}Cl_2N_2PRu$	Red brown	276	67.92 (67.18)	4.87 (4.12)	3.30 (3.01)
$[RuCl_2(Ind)(SIpAnis)(PPh_3)]$	52	$C_{50}H_{44}Cl_2N_2O_2PRu$	Brown	> 300	66.08 (65.97)	4.99 (4.43)	3.08 (2.90)
$[RuCl_2(Ind)(SImTol)(PPh_3)$	79	$C_{50}H_{44}Cl_2N_2PRu$	Brown	294	68.49 (67.95)	5.17 (4.88)	3.19 (2.96)
$[RuCl_2(Ind)(SIoTol)(py)]$	89	$C_{37}H_{34}Cl_2N_3Ru$	Brown	270	64.06 (63.87)	5.09 (4.82)	6.06 (5.74)
$[RuCl_2(Ind)(SIpTol)(py)]$	81	$C_{37}H_{34}Cl_2N_3Ru$	Brown	256	64.06 (63.98)	5.09 (4.88)	6.06 (5.83)
$[RuCl_2(Ind)(SIPh)(py)]$	74	$C_{35}H_{30}Cl_2N_3Ru$	Red brown	251	63.16 (63.01)	4.69 (4.24)	6.31 (6.15)
$[RuCl_2(Ind)(SIpAnis)(py)]$	52	$C_{37}H_{34}Cl_2N_3O_2Ru$	Brown	287	61.24 (6102)	4.86 (4.43)	5.79 (5.24)

3.4.1 Infrared studies of Ru(II) phenyl-3-indenylidene N-heterocyclic carbene complexes

The infrared spectra of the ruthenium complexes with N-heterocyclic carbene ligands were ran and carefully compared with the IR spectra of the ligands. The most notable differences between the infrared spectra was the disappearance of the broad vibration due to $\upsilon(NH_2^+=C)$ of the quaternary salts found in the region of 3300-3400 cm^{-1} and the disappearance of vibration band due to υ(C=N) in the range of 1550-1730 cm^{-1} (which had very high intensity in the infrared of the ligands). This difference could be attributed to the bonding mode of N-heterocyclic carbene carbon to the ruthenium ion, and it confirmed that the N, N'-diarylimidazolinium chlorides were successfully deprotonated. Besides this change, other vibrational band formally found in the infrared spectra of the ligands are still present, however they have either slightly shifted or their intensity has increased due to the use of electrons in bonding with metal ion.

Reports from previous studies have shown that the most interesting vibration band in the infrared spectra of Ru(II) complexes are found in the region of 1323-1432, 2850-2850, 500-800 and 490 - 550 cm^{-1} due to the presence of υ(N-C), υ(P-Ph), υ(aliph. C=H), υ(C=C), υ(Ru-N), υ(Ru-P) and υ(Ru-Cl) [17-20]. Figures 3.19-3.20, showed the infrared spectra of $[RuCl_2(NHC)(PPh_3)(Ind)]$ and $[RuCl_2(NHC)(py)(Ind)]$ type complexes. The major difference between the infrared spectra of these complexes was observed in the region of 400-800 cm^{-1} due to the vibrational bands of υ(R-Ph) and υ(Ru-N) present in their structures. The ruthenium complexes with NHC *trans* to pyridine ligand have the vibration mode of υ(Ru-N) found in the region of 500-800 cm^{-1} and for the ruthenium complexes with NHC *trans* to triphenylphosphine the vibration mode υ(Ru-P) was red shifted to 400-550 cm^{-1} [21-22]. From the infrared spectrum of complex (**C1**) $[RuCl_2(SIoTol)(PPh_3)(Ind)]$, the prominent peaks at 503, 802, 2930, 2843 cm^{-1} were due to

vibration mode of υ(Ru-P), υ(aliph. C-H), υ(C=C), and υ(C-N). However, the vibration band of υ(C-N) and υ(P-Ph) lies in the same region of spectrum in the range 1300-1453 cm^{-1} which makes specific assignment extremely difficulty because of the overlap [23]. In literature, the vibration mode of υ(Ru-Cl) was expected to appear in 200-380 cm^{-1} [24] but the Fourier transform infrared spectroscopy that was used in this study had capacity in the range of 4000-370 cm^{-1}, hence the bands could not be observed. Some relevant vibrational bands of the nine synthesized complexes are represented in Table 3.8 and the infrared spectra are shown in Figures 3.19 and 3.20.

Table 3.8: Selected vibration bands of Ru(II) phenyl-3-indenylidene complexes

Complexes	υ(Ru-P) cm^{-1}	υ(C=C) cm^{-1}	υ(C-N) cm^{-1}	υ(Ru-N) cm^{-1}
$[RuCl_2(Ind)(SIoTol)(PPh_3)]$	533	2935	1465	--------
$[RuCl_2(Ind)(SIpTol)(PPh_3)]$	545	2939	1471	--------
$[RuCl_2(Ind)(SIPh)(PPh_3)]$	540	2947	1472	--------
$[RuCl_2(Ind)(SIpAnis)(PPh_3)]$	551	2950	1471	--------
$[RuCl_2(Ind)(SImTol)(PPh_3)]$	526	2943	1479	--------
$[RuCl_2(Ind)(SIoTol)(py)]$	------	2995	1468	736
$RuCl_2(Ind)(SIpTol)(py)]$	-------	2960	1476	733
$[RuCl_2(Ind)(SIphenyl)(py)]$	------	2995	1481	780
$[RuCl_2(Ind)(SIpAnis)(py)]$	-------	2975	1525	742

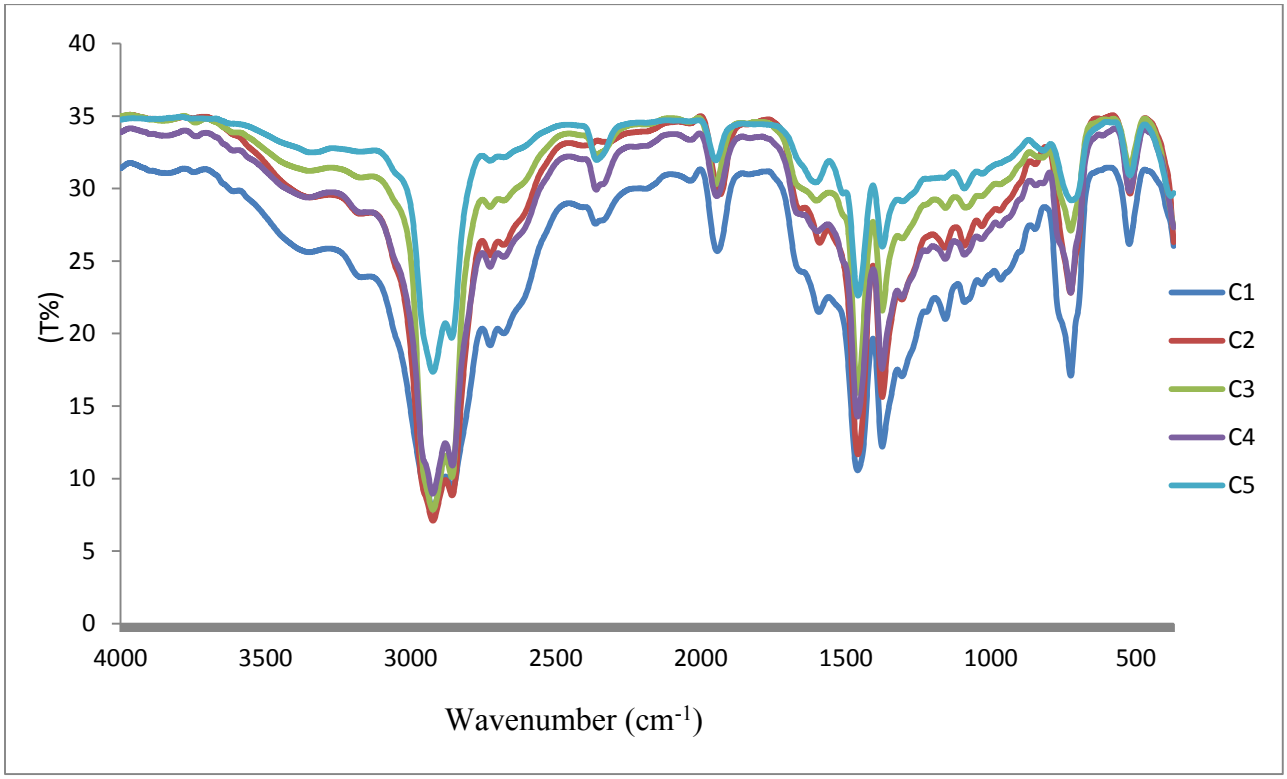

Figure 3.19: The infrared spectra of Ru(II)NHC-phosphine complexes

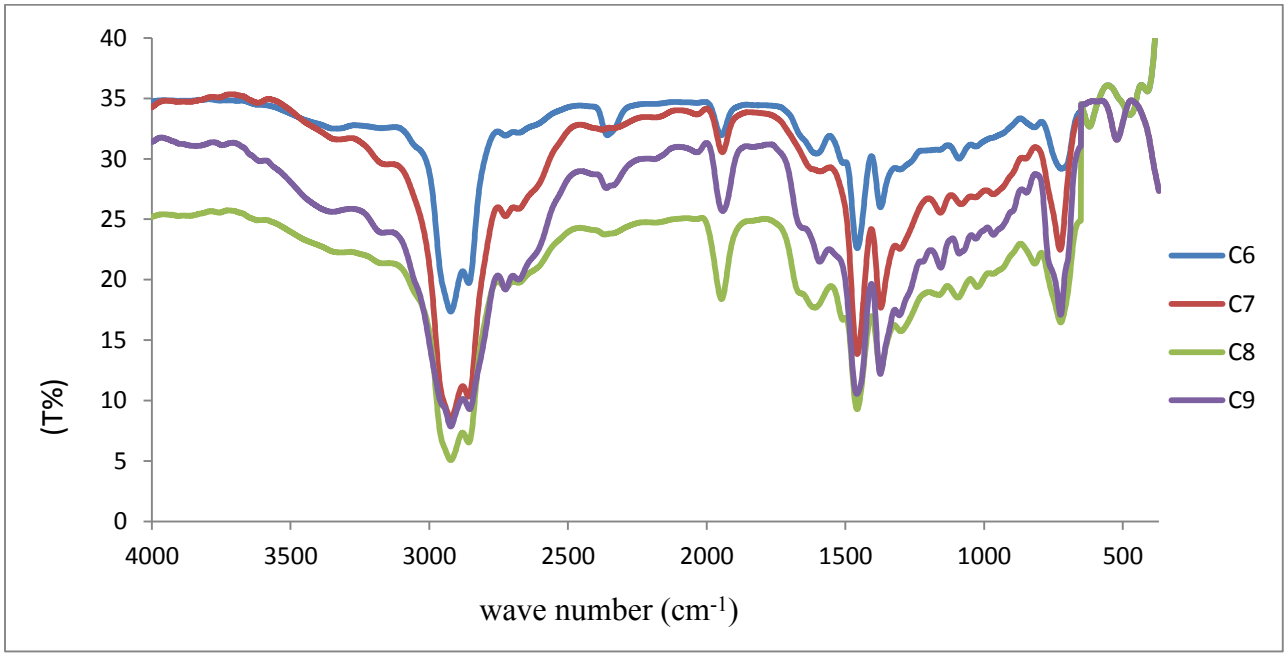

Figure 3.20: The infrared spectra of Ru(II)NHC-pyridine complexes

3.4.2 Electronic spectra of Ru(II) complexes

Table 3.9: UV-Vis absoprtion band of Ru(II) complexes and corresponding ligands

Compounds	π→ π * nm	n→ π*/ LMCT (nm)	d-d (nm)
C1	228	263	408
C2	230	254.	415
C3	232	257	415
C4	273	307	400
C5	230	263	418
C6	275	373	533
C7	274	320	682
C8	276	439	687
C9	285	440	652

The electronic spectra of the the synthesized complexes were ran using dichloromethane (DCM) and acetonitrile at 25 ^{o}C in order to establish the stereochemistry of the synthesized complexes. Figures 3.21 and 3.22, showed the electronic spectra of the Ru(II) complexes and they consist of three distinct bands. Two bands are due to intraligand charge transfers and for the filled d-d transition, signifying the presence of the metal ions [25]. The two absorption bands due to the

intraligand charge transfers transtions are π →π* and n→π*,and caused by the electronic transtions from HOMO to LUMO of the NCN chromophere [26-27]. Figure 3.1 shows the electronic spectra of Ru(II)NHC-phosphine type complexes and Figure 3.21 shows the electronic spetra of Ru(II)NHC-pyridine complexes. The electronic spectra of Ru(II) NHC-pyridine (Figure 3.22) is red shifted as compared to the phosphine countparts with d-d transtion in the region 530-700 nm, while the MLCT of Ru(II)NHC-phosphine is in the region 400-420 nm [28]. This may be atttributed to the fact that phosphorus is a soft donor atom and nitrogen is a borderline hard/soft atom. The absorption bands of MLCT in both type of complexes is due to the electron transfer from filled d-obirtal to unfilled anti-bonding π orbitals (Md_T-Lπ*($_{Nitrogen}$) and MdT-Lπ*($_{Phosphorus}$)) [29]. The types of electronic transions and the wavelenght are summarised in Table. 3.9

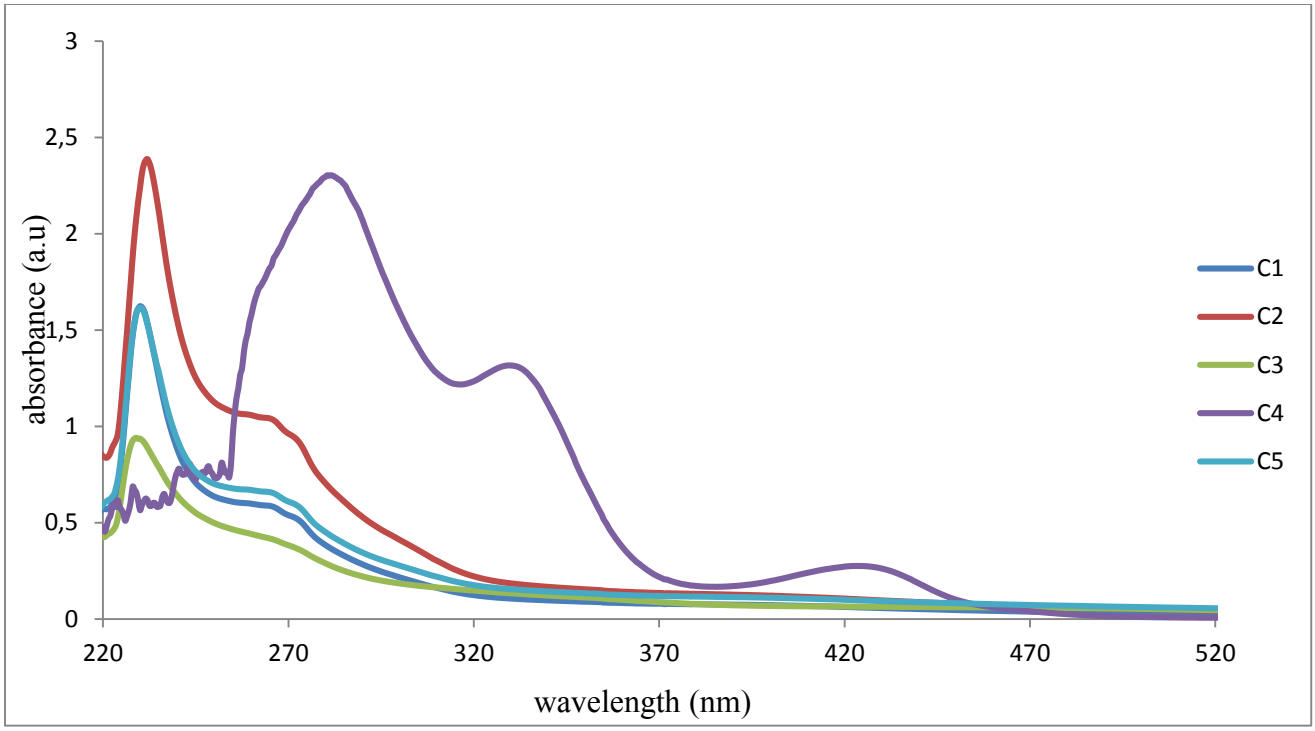

Figure 3.21: The electronic spectra of the Ru(II) complexes with NHC-phosphine

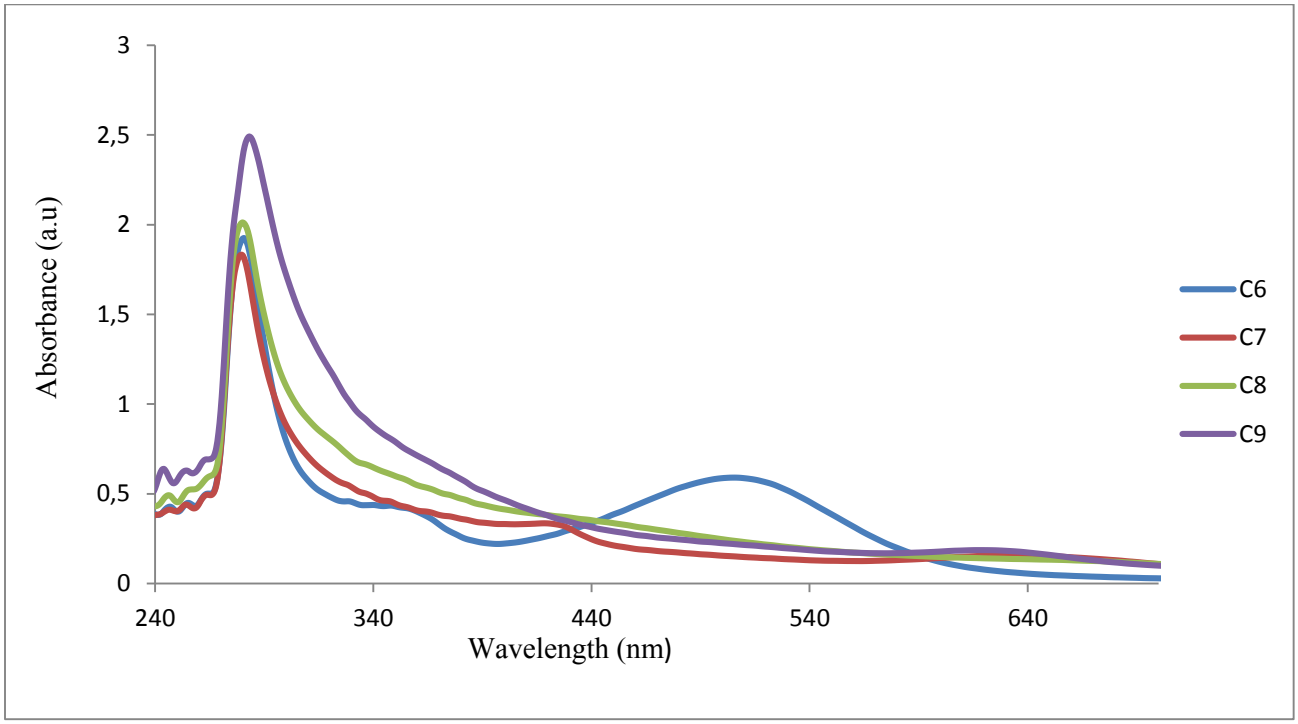

Figure 3.22: The electronic spectra of the Ru(II) complex with NHC-pyridine

References

1. Guo, X. G.; Wang, N. Y.; Wang, D.; Cai, L. H.; Chen, Z. X.; Hou, X. F. Palladium, iridium and ruthenium complexes with acyclic imino-N-heterocyclic carbenes and their application in aqua-phase Suzuki-Miyaura cross-coupling reaction and transfer hydrogenation. *Dalton. Trans*. **2012**, 41, 14557-67.
2. Herrman, W. A. Heterocyclic: A new concept in organic metallic catalysts. *Angew .Chem. Int. Ed*. **2002**, 41, 1290-1309.
3. Grubbs, R. H.; Kuhn, K. M. A facile preparation if imidazolinium chlorides. *Org. lett*. **2008**, 10, 2075-2077.
4. Chakraborty, P. An efficient $FeCl_3$ catalyzed synthesis of *N,N'*-diarylformamidines. *Green Sustain. Chem.* **2013**, *03*, 26–30.
5. Sadek, K. U. Cerium(IV) Ammonium nitrate (CAN) mediated reactions IV. A highly efficient synthesis of *N,N'*-diarylsubstituted formamidines in water at ambient temperature. *Green Sustain. Chem.* **2011**, *01*, 92–97.
6. Glorius, F.; Hirano, K.; Urban, S.; Wang, C. A modular synthesis of highly substituted imidazolium salts. *Org. Lett*. **2009**, 11, 1019-1022.
7. Diaz, D.; Lewis, W. G.; Finn, M. G. Acid-mediated amine exchange of *N,N'*-dimethylformamidines: Preparation of electron-rich formamidines. *Chem. In-form*. **2005**. 37. 2214-2218.
8. Kaji, K.; Matsubara, H .; Nagashima, H .; Kikugawa, Y.; Yamada, S. I. Synthesis of formamidines from carbodi- imides with sodium borohydride in isopropanol. *Chemical & Pharmaceutical Bulletin*. **1978**, 26, 2246-2249.

9. McGarrigle, M. E.; Fritz, P. S.; Favereau, L.; Yar, M.; Aggarwal. V. K. An efficient synthesis of imidazolinium salts using vinyl sulfonium salts. *Org. Lett*. **2011**, 13, 3060-3063.
10. Scholl, M.; Ding, S.; Lee, C. W.; Grubbs, R. H. Synthesis and activity of a new generation of ruthenium-based olefin metathesis catalysts coordinated with 1,3-dimesityl-4,5-dihydroimidazol-2-ylidene ligands. *Org. Lett*. **1999**, 6, 953-956.
11. Van der Westhuizen, B. Synthesis of investigation of Mn(l) and Rh(l) N-heterocyclic carbene complexes. M. S. Thesis. University of Pretoria. S.A. Nov. **2011**.
12. Seethalakshmi, J. V.; Padmavathy, R. E. R.; Radha, N. FTIR spectral analysis of imidazolium chloride. *Int. J. Cur. Res. Rev*. **2012**, 4, 31-36.
13. Dharaskar, S. A.; Varma, M. N.; Shende, D. Z; Yoo, C. K.; Wasewar, K. L. Synthesis, characterization and application of 1-butyl-3-methylimidazolium chloride as green material for extractive desulfurization of liquid fuel. *J. Sc. W*. **2013**. 1-9.
14. Abia, J. A.; Ozer, R. Development of polyoxometalate-ionic liquid compounds for processing cellulosic biomass. *Bioresources*. **2013**, 8, 2924-2933.
15. Grela, K.; Torborg, C.; Szczepaniak, G.; Zeilinski, A.; Malinska, M.; Wozniak, K. Stable ruthenium indenylidene complexes with a sterically reduced NHC ligand. *Chem. Commun*. **2013**, 49,3161–3264.
16. Nolan, S. P.; Urbina-Blanco, C. A.; Leitgeb, A.; Slugovc, C.; Bantreil, X .; Clavier, H.; Slawin, A. Z. M. Olefin metathesis featuring ruthenium indenylidene complexes with a sterically demanding NHC ligand. *Eur. J. Chem*. **2011**, 17, 5045-53
17. Hallman, P. S.; Stephenson, T. A.; Wilkinson, G. Synthesis methods taken from Parry, R. W. tris(triphenylphosphine)dichlororuthenium(II). *Inorg. Syn*. **1970**, 12, 238-239.

18. Małecki, J. G. Two phosphine ruthenium(III) and ruthenium(II) complexes with the pyrazole ligand-synthesis, characterisation and DFT calculations. *Polyhedron*. **2012**, 45, 15-22.

19. Prabhakaran, B.; Santhi, N.; Emayavaramban. M. Synthesis and spectral studies of Ru(II) carbonyl Schiff base complexes. *Int. Lett. Chem. Physic Astronony.* **2013**, 3, 53-66.

20. Drozdzak, R.; Ledoux, N.; Allaert, B.; Dragutan, I.; Dragutan, V.; Verpoort, F. Rational design and convenient synthesis of a novel family of ruthenium complexes with O,N-bidentate ligands. *Cent. Eur. J. Chem.*, **2005**, 3, 404-416.

21. Adeniyi, A. A.; Ajibade, P. A. The spectroscopic and conductive properties of Ru(II) complexes with potential anticancer properties. *J. Spectr.* **2014**, 1–14.

22. Garza-Ortiz, A.; Uma Maheswari, P.; Siegler, M.; Spek, A. L.; Reedijk, J. A new family of Ru(II) complexes with a tridentate pyridine Schiff-base ligand and bidentate co-ligands: synthesis, characterization, structure and *in vitro* cytotoxicity studies. *New. J. Chem.* **2013**, 37, 3450.

23. Małecki, J. G. Synthesis, crystal, molecular and electronic structures of thiocyanate ruthenium(II) complexes with pyrazole, benzimidazole and triazole ligands. *Polyhedron*. **2010**, 29, 1237-1242.

24. Warad, I. Synthesis, spectral and structural charcterization of novel dichloro-complex/triphenylphosphine/(3.4-diamnophenyl)metanone complex. *J. Mat. Envir. Sci*. **2013**, 4, 822-827.

25. Thiel, V.; Hendann, M.; Wannowius, K. J.; Plenio, H. On the mechanism of the initiation reaction in Grubbs-Hoveyda complexes. *J. Am. Chem. Soc.* **2012**, 134, 1104-14.

26. Das, A. K.; Peng, S. M.; Bhattacharya, S. Ruthenium-mediated reduction of oximes to imines. Synthesis, characterization and redox properties of imine complexes of ruthenium. *J. Chem. Soc. Dalton. Trans.* **2000**, 181-184.

27. Wilson, G. O.; Porter, K. A.; Weissman, H.; White, S. R.; Sottos, N. R.; Moore, J. S. Stability of second generation Grubbs' alkylidenes to primary amines: Formation of novel ruthenium-amine complexes. *Adv. Synth. Catal*. **2009**, 351, 1817-1825.

28. Borah, G.; Boruah, D. Coordination chemistry of the multi-funtionalized 3-(diphenylphosphino) -1-propylamine ligand with ruthenium(II). *Indian. J. Chem*. **2012**, 51, 444-452.

29. Małecki, J. G. Synthesis, crystal, molecular and electronic structures of ruthenium complexes with a benzoxazole derivative ligand. *Polyhedron*. **2012**, 31, 159–166.

CHAPTER FOUR

SUMMARY, CONCLUSION AND RECOMMENDATIONS

4.1 Summary

In summary, nine pent-coordinated ruthenium(II) complexes of general formula $[RuCl_2(NHC)(L)]$ (where L = triphenylphosphine, pyridine ligands and where NHC stand for five different less sterically N-heterocyclic carbene ligands), have been synthesized and characterized using the elemental analysis, FTIR, UV-Vis and melting point determination. All the synthesized complexes were found to be air stable and red-brown in colour. A green colour of the complexes actually meant the was oxygen present and that was avoided with running the reactions under nitrogen atmosphere. The free N-heterocyclic carbene ligands were generated through the in-situ deprotonation of their corresponding *N,N′*-diarylimidazolinium chlorides with potassium bis(trimethylsilyl)amide (KHMD) as base at room temperature.

The five symmetrical *N,N′*-diarylimidazolinium chlorides with different position of methyl (CH_3) group have been synthesized using a solvent free method in two spot syntheses: (i) reacting the triethyl orthoformate with different aniline derivatives under acidic condition to form *N,N′*- diarylformamidines and (ii) reacting the 1, 2-dichloroethane with the synthesized *N,N′*-diarylformamidines under basic condition to form *N,N′*-diarylimidazolinium chlorides salts.

General all the synthesized *N,N′*-diarylformamidines are non-soluble in common organic solvents hence they were washed with hexane or pentane. Attempts to synthesize unsymmetrical *N,N′*-diarylformamidines such as *N*-(phenyl)-*N′*-4-methoxyphenyl)formamidine and *N*-(4-methoxyphenyl)-*N′*-(2-methylphenyl)formamidine were unsuccessfully. The synthesized *N,N′*-diarylformamidines and *N,N′*-diarylimidazolinium chlorides have been further characterized using both ^{1}H and ^{13}C-NMR, FTIR and melting point determination.

To determine the functional groups present in these compounds infrared spectra were recorded on a Perkin–Elmer Model System 2000 FT–IR spectrophotometer in the range 4000 – 400 cm^{-1}. The FT-IR spectra of these compounds (appendix A and B) showed four major common bands due to vibrational bands of υ(N-H) or υ(R_2N^+=C), υ(C=N), υ(C-H)$_{Aliph.}$ and υ(C-H)$_{Arom.}$ in the region 3300-3500, 1450-1650, 2800-2900, 2950-3010 cm^{-1}. The significant difference between the infrared spectra of the *N,N′*-diarylformamidines and *N,N′*-diarylimidazolinium chlorides is the broad peak in the region 3300-3500 cm^{-1} which is due to the quaternary amine cation (R_2N^+=C) in *N,N′*-diarylimidazolinium chloride instead of the υ(N-H) found in the structure of *N,N′*-diarylformamidines. The decrease in the intensity of this vibration band is attributed to the use of electrons in nitrogen in bonding with ethyl cation to form the imidazoline ring.

Furthermore to determine the structure of the synthesized *N,N′*-diarylformamidines and *N,N′*-diarylimidazolinium chlorides the ^{1}H and ^{13}C-NMR spectra were performed on a Varian–NMR–vnmr s600 MHz spectrometer at 25 ºC. The ^{1}H and ^{13}C-NMR chemical shifts and multiplicity results of these compounds are summarized in Table 3.3 and 3.5 and the results obtained correspond with the proposed structures. The melting points results obtained for *N,N′*-diarylimidazolinium chlorides are >250 ºC, whilst the melting points obtained for the *N,N′*-

diarylformamidines are between 130 -160 ^{o}C. This information can also be used to confirm the conversion of the *N,N´*- diarylformamidines to *N,N´*-diarylimidazolinium chlorides salts.

The FT-IR spectra of the synthesized Ru(II) complexes showed a disappearance of vibration band due to $\upsilon(R_2N^{+}=C)$ in the region 3300-3400 cm^{-1} and this was attributed to coordination of the N-heterocyclic carbene ligands to the ruthenium ion. The found and calculated percentage results of carbon (C), hydrogen (H) and nitrogen (N) atoms in the synthesized Ru(II) complexes were comparable, with the difference of not more than 1 % in each of the atoms. The electronic spectra of the Ru(II) complexes were recorded on a Perkin–Elmer Lambda 25 UV–Vis spectrophotometer. The electronic spectra of Ru(II)NHC-pyridine complex is red shifted with the d-d transtion in the region 530-700 nm as compared to the Ru(II)NHC-phosphine complexes with the MLCT in the region 400-420 nm.

4.2 Conclusion

Very few studies have reported the synthesis of *N,N′*-diarylimidazolinium chlorides from their corresponding *N,N′*-diarylformamidines [1, 2]. This represents an efficient and simple method of producing such carbene precursors. Also very few studies [3, 5] have synthesized Ru(II) phenyl-3-indenylidene complexes with less sterically N-heterocyclic carbene ligands. With regards to the results obtained and reported in this dissertation it can be conclusively stated that the synthesis and characterized the Ru(II) type olefin metathesis complexes coordinated with triphenyelphosphine, pyridine and the N-heterocyclic carbene ligands was successfully achieved. However, it was our attention to run and report cyclic voltammetry for the complexes but the instrument got broken at Postdam lab in Walter Sisulu University, East London, days before we were supposed to use it in December 2014. Moreover, it is also our attention to grow single crystals for X-ray analysis for structure verification of the proposed Ruthenium(II) complexes.

4.3 Recommendations for future work

Apart from the synthesis and characterization of these Ru(II) complexes with N-heterocyclic carbene ligands, the efficiency of these complexes in catalyzing olefin metathesis reaction such as ring closing metathesis (RCM), ring opening metathesis (ROM), cross metathesis (CM) and ring opening metathesis polymerization (ROMP), still need to be evaluated using standard substrates. This will give us clear indication of their catalytic ability as compared to already existing catalysts.

It is also recommended to synthesize unsymmetrical chiral N-heterocyclic carbene ligands since they impose chiral catalysts, and compare their efficiency with the symmetrical N-heterocyclic carbene ligands reported in this study. In addition, to use different types of phosphites as complimentary ligands instead of phosphine to produce very stable catalyst which can be used for ring opening metathesis at high temperature and to do the electrochemistry of the synthesized complexes.

References

1. Glorius, F.; Hirano, K.; Urban, S.; Wang, C. A modular synthesi of highly substituted imidazolium salts. *Org. Lett*. **2009**, 11, 1019-1022.
2. Grubbs, R. H.; Kuhn, K. M. A facile preparation if imidazolinium chlorides. *Org. Lett*. **2008**, 10, 2075-2077.
3. Urbina-Blanco, C. A.; Manzini, S.; Gomes, J. P.; Doppiu, A.; Nolan, S. P. Simple synthetic routes to ruthenium-indenylidene olefin metathesis catalysts. *Chem. Commun*. **2011**, 47, 5022-4.
4. Monsaert, S.; Drozdzak, R.; Dragutan, V.; Dragutan, I.; Verpoort, F. Indenylidene-ruthenium complexes bearing saturated N-heterocyclic carbenes: synthesis and catalytic investigation in olefin metathesis reactions. *Eur. J. Inorg. Chem*. **2008**, 3, 432-440.
5. Nolan, S. P.; Urbina-Blanco, C. A.; Leitgeb, A.; Slugovc, C.; Bantreil, X .; Clavier, H.; Slawin, A. Z. M. Olefin metathesis featuring ruthenium indenylidene complexes with a sterically demanding NHC ligand. *Eur. J. Chem*. **2011**, 17, 5045-53.

APPENDICES

Appendix A.1 Infrared spectra of *N,N´*-diarylformamidines

A 1.1 Infrared spectrum of *N,N´-bis*(2-methylphenyl)formamidine (F1)

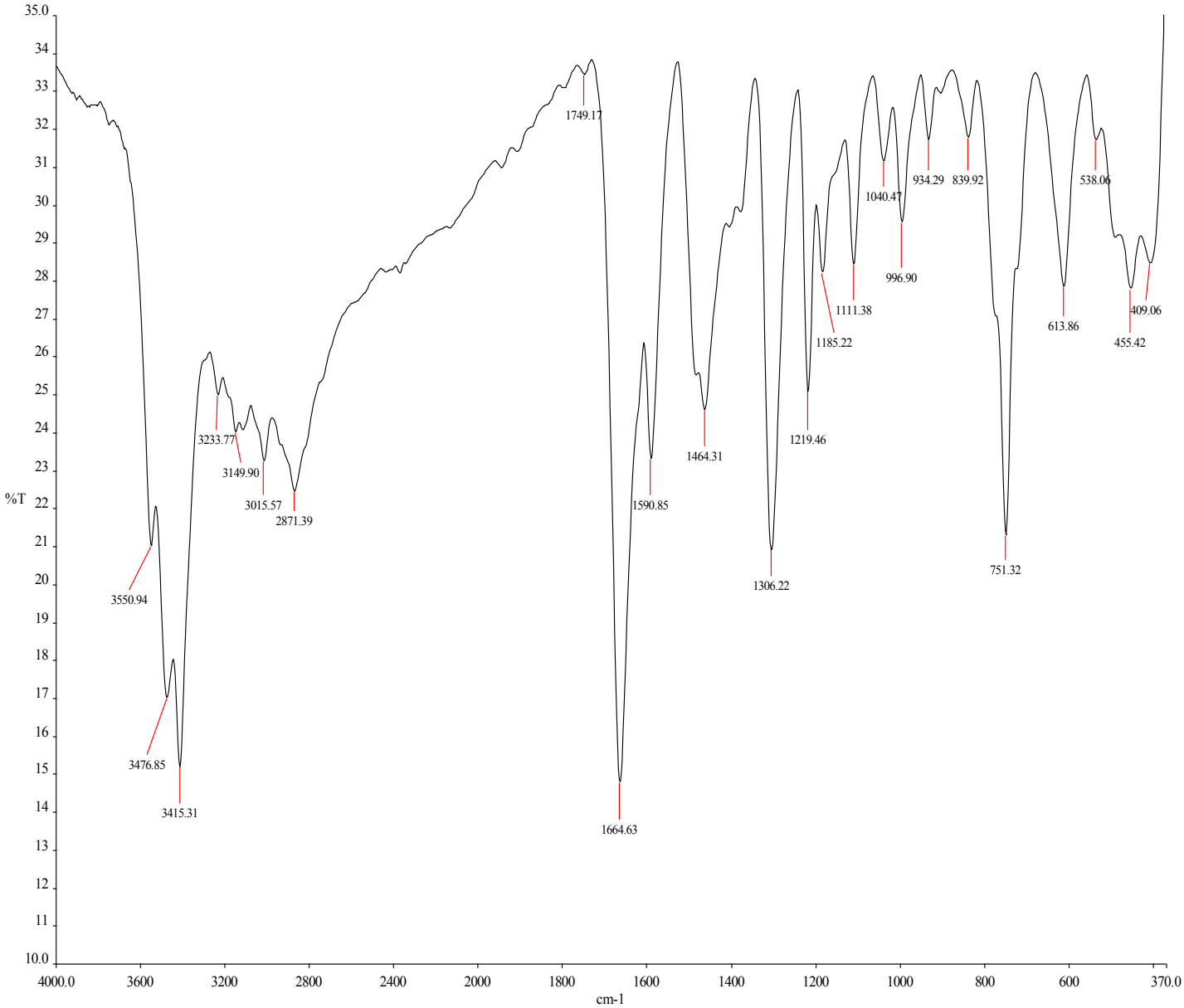

A 1.2 Infrared spectrum *N,N´-bis*(4-methylphenyl)formamidine (F2)

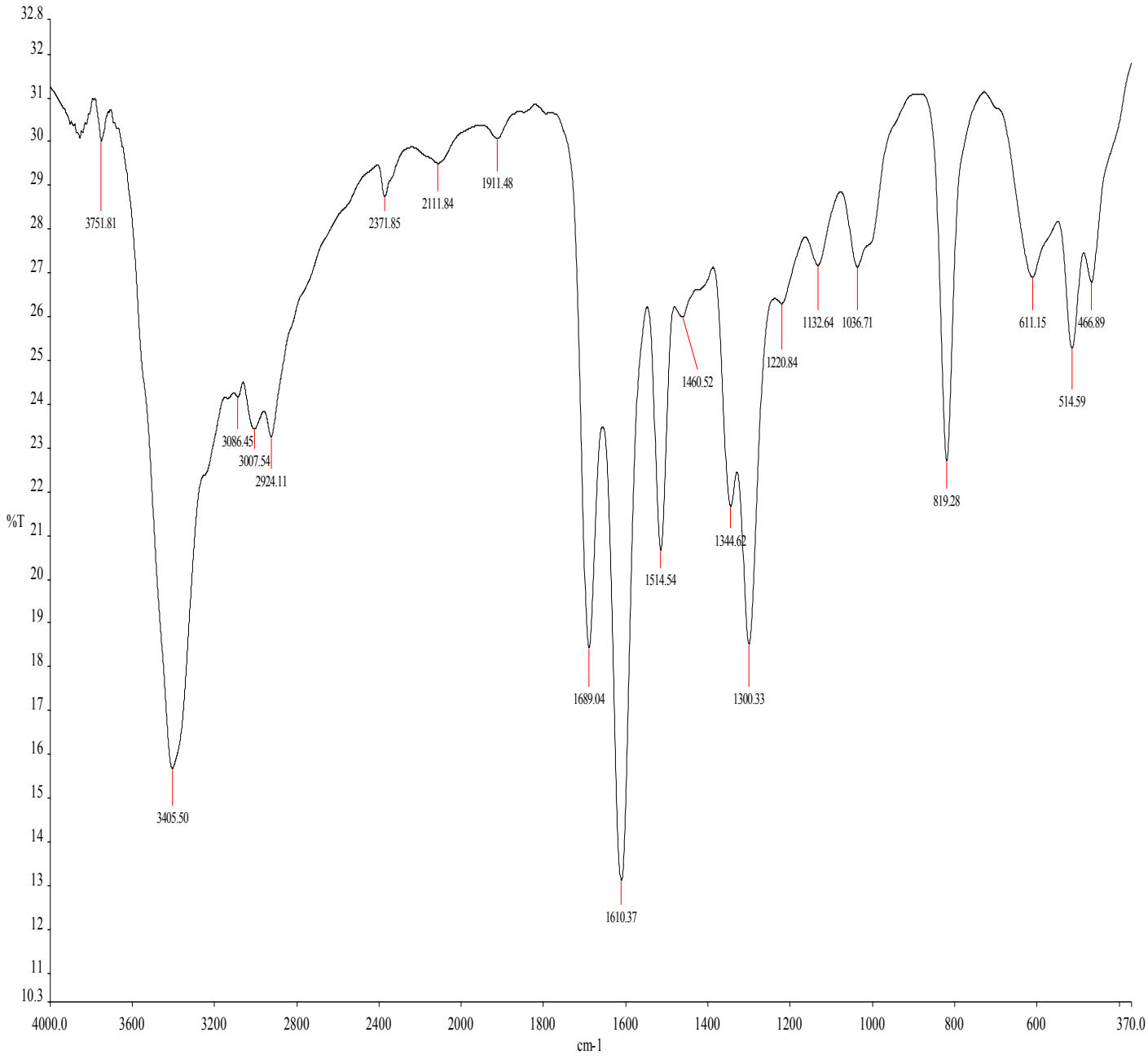

A1.3 Infrared spectrum of *N,N′*-diphenylformamidine (F3)

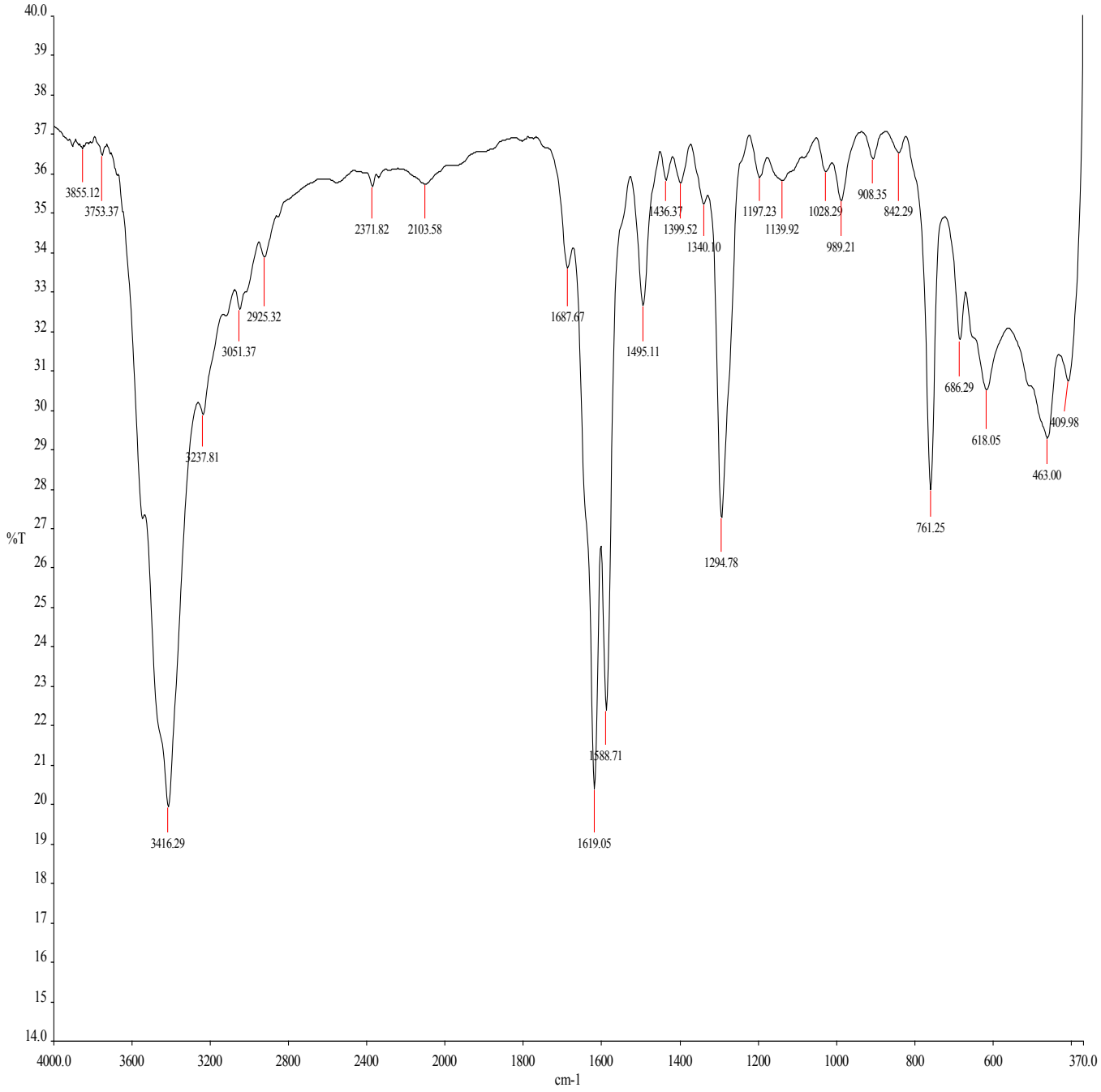

A1.4 Infrared spectrum of *N,N´-bis*(4-methoxyphenyl)formamidine (F4)

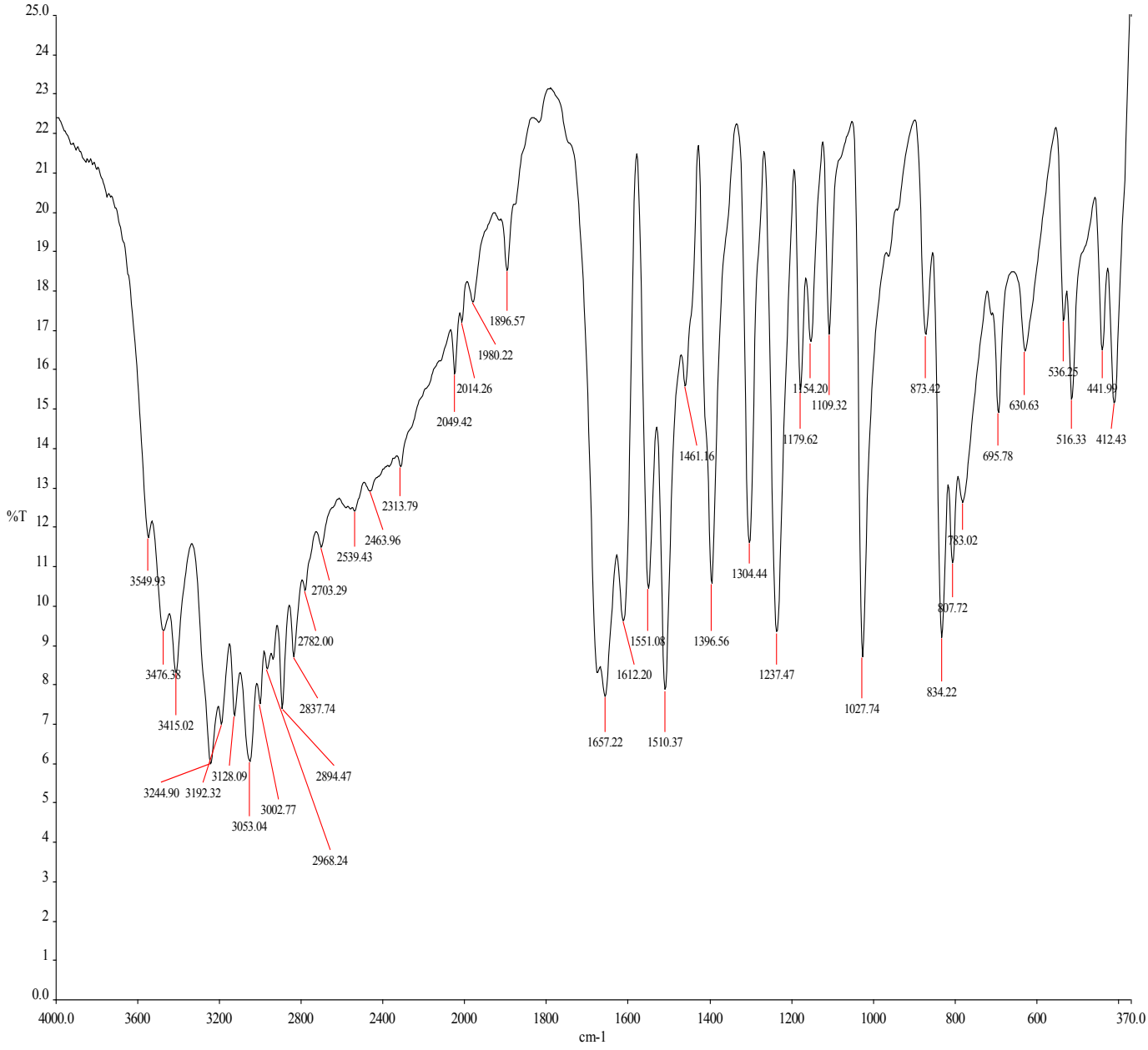

A1.5 Infrared spectrum of *N,N´-bis*(3-methyphenyl)formamidine (F5)

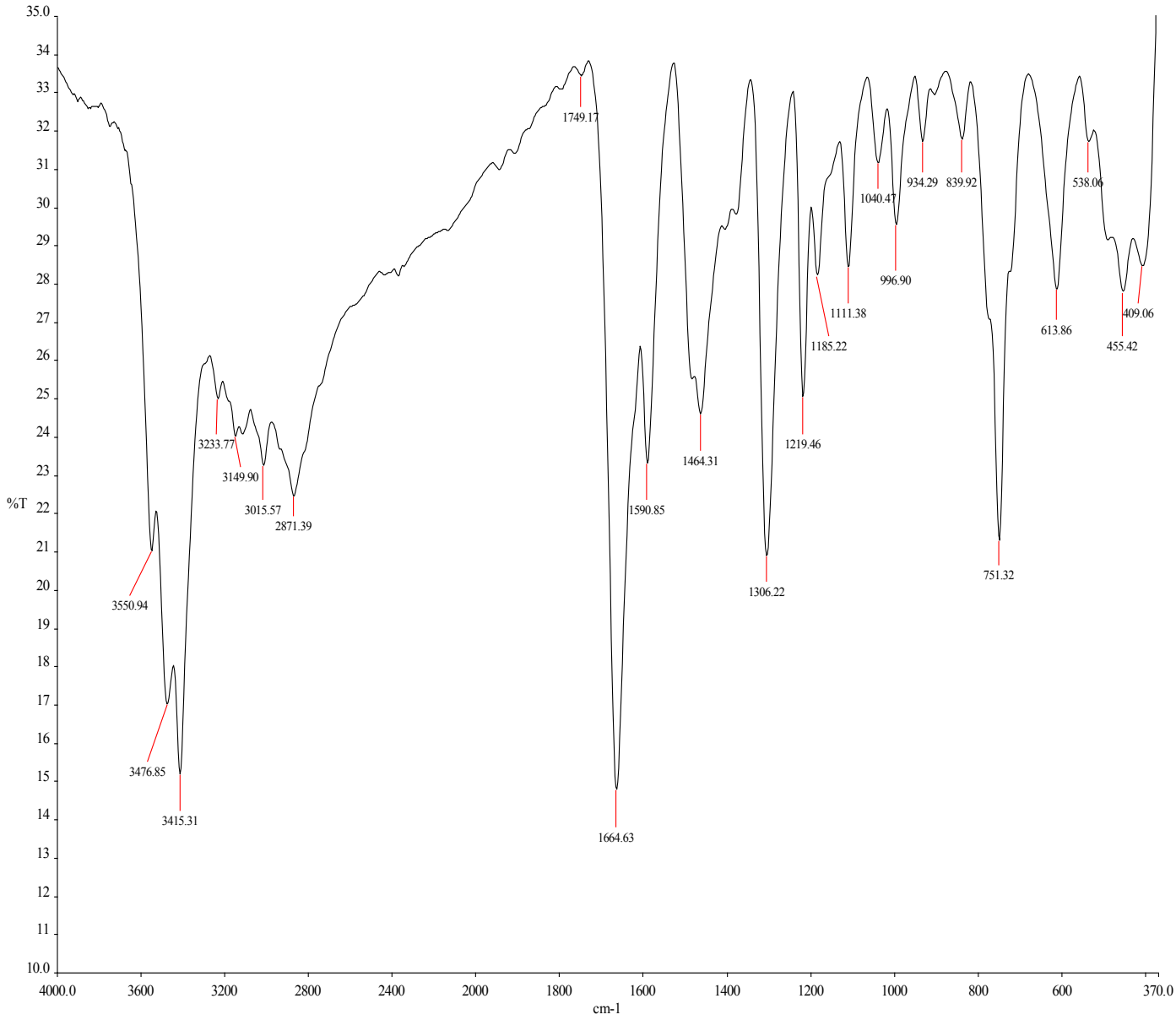

Appendix B1: Infrared spectra of *N,N′*-diarylimidazolinium chlorides

B 1.1 Infrared spectrum of *N,N′-bis*(2-methylphenyl)imidazolinium chloride (L1)

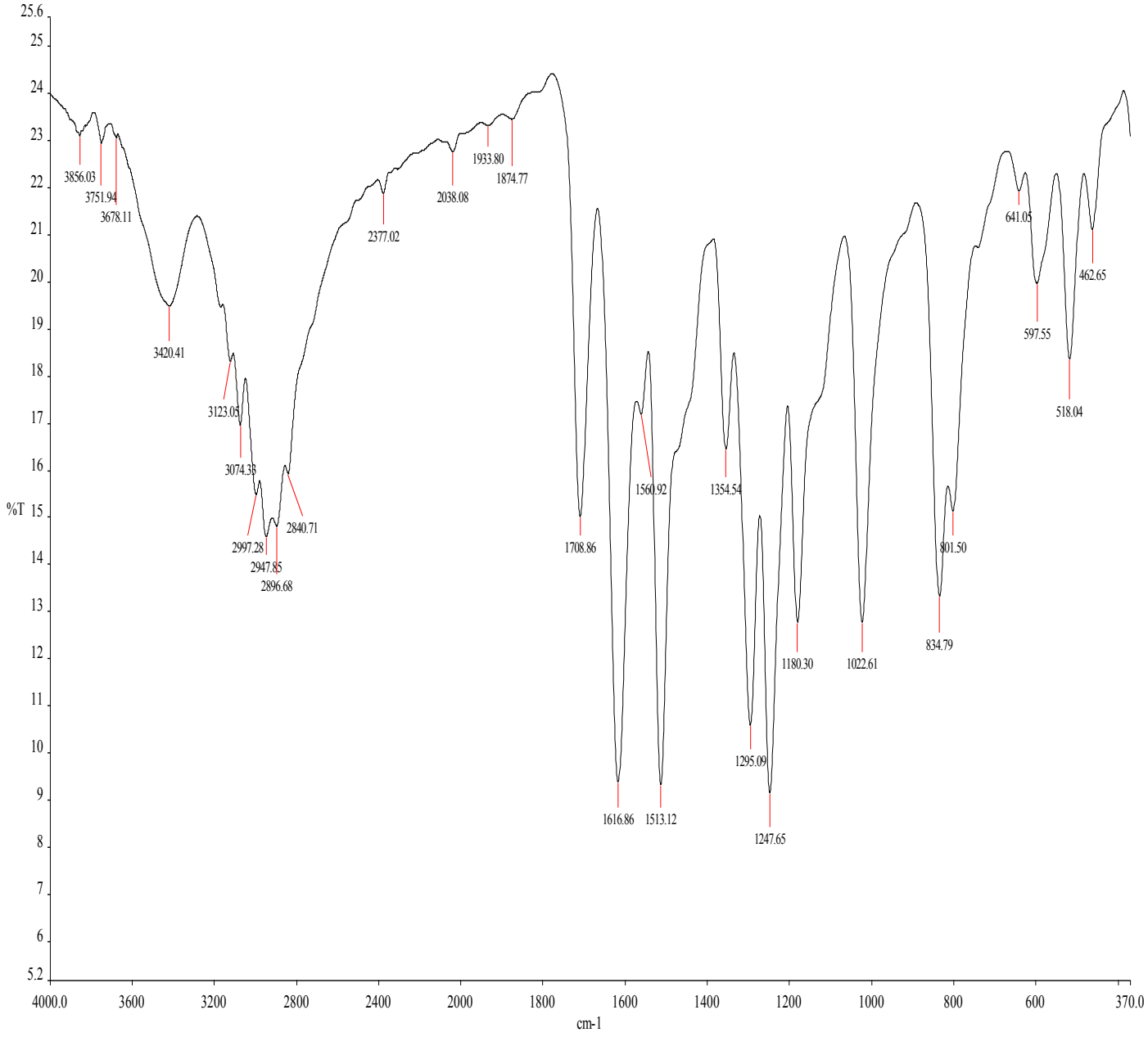

B. 1.2 Infrared spectrum of *N,N´-bis*(4-methylphenyl)imidazolinium chloride (L2)

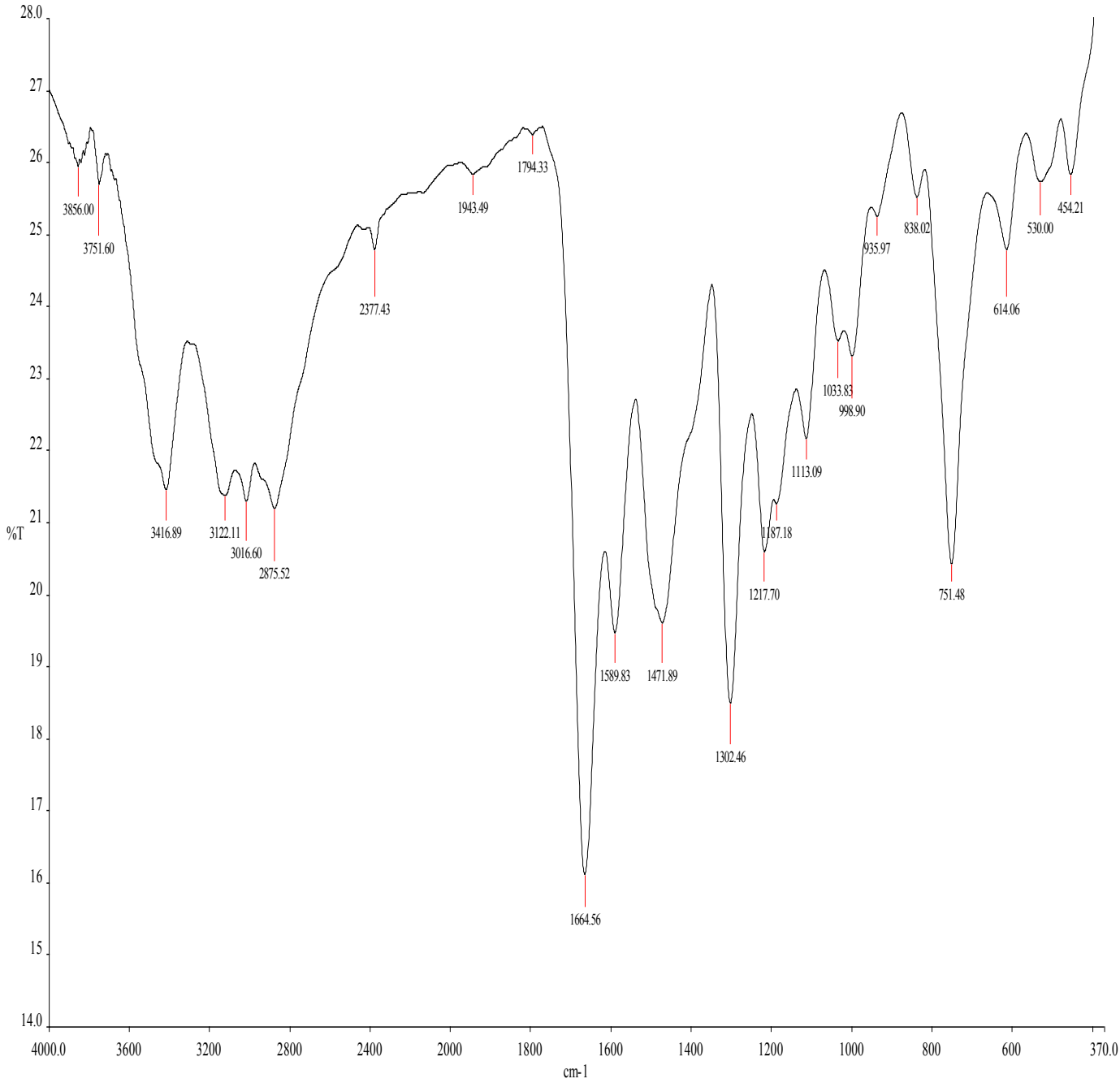

B 1.3 Infrared spectrum of *N,N´*-diphenylimidazolinium chloride (L3)

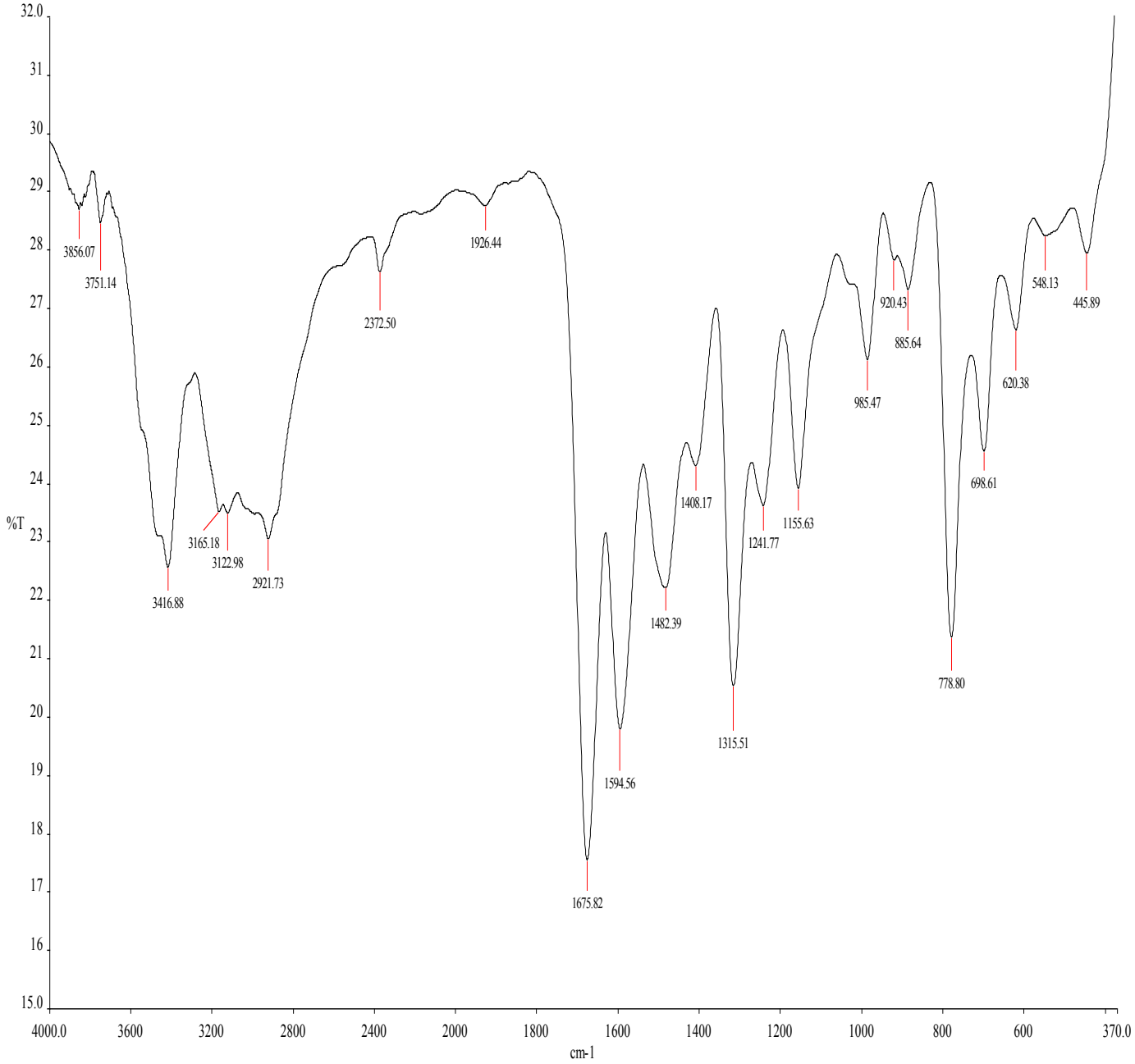

B. 1.4 Infrared spectrum of *N,N´-bis*(4-methoxyphenyl)imidazolinium chloride (L4)

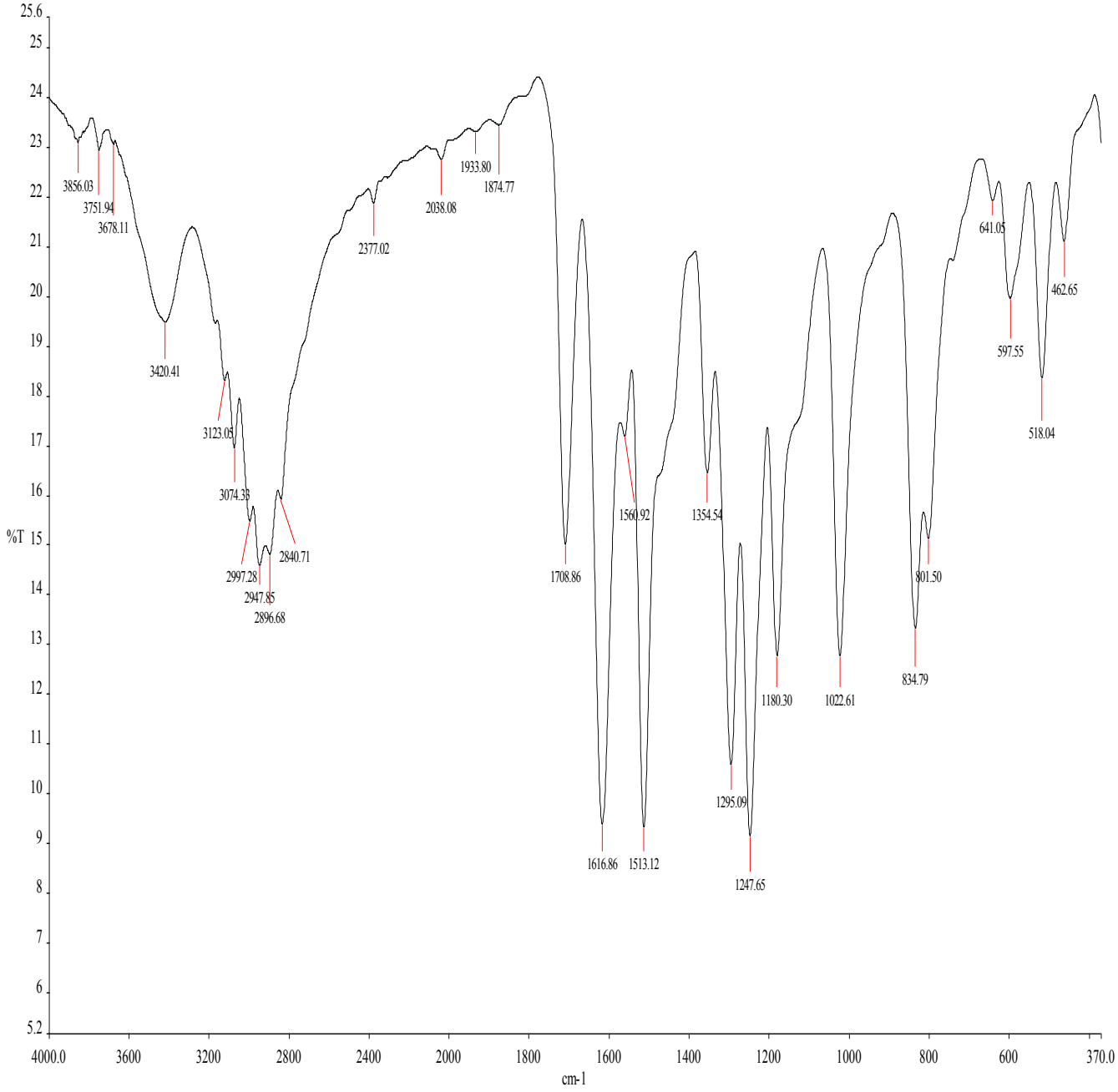

B. 1.5 Infrared spectrum of *N,N´-bis*(3-methylphenyl)imidazolinium chloride (L5)